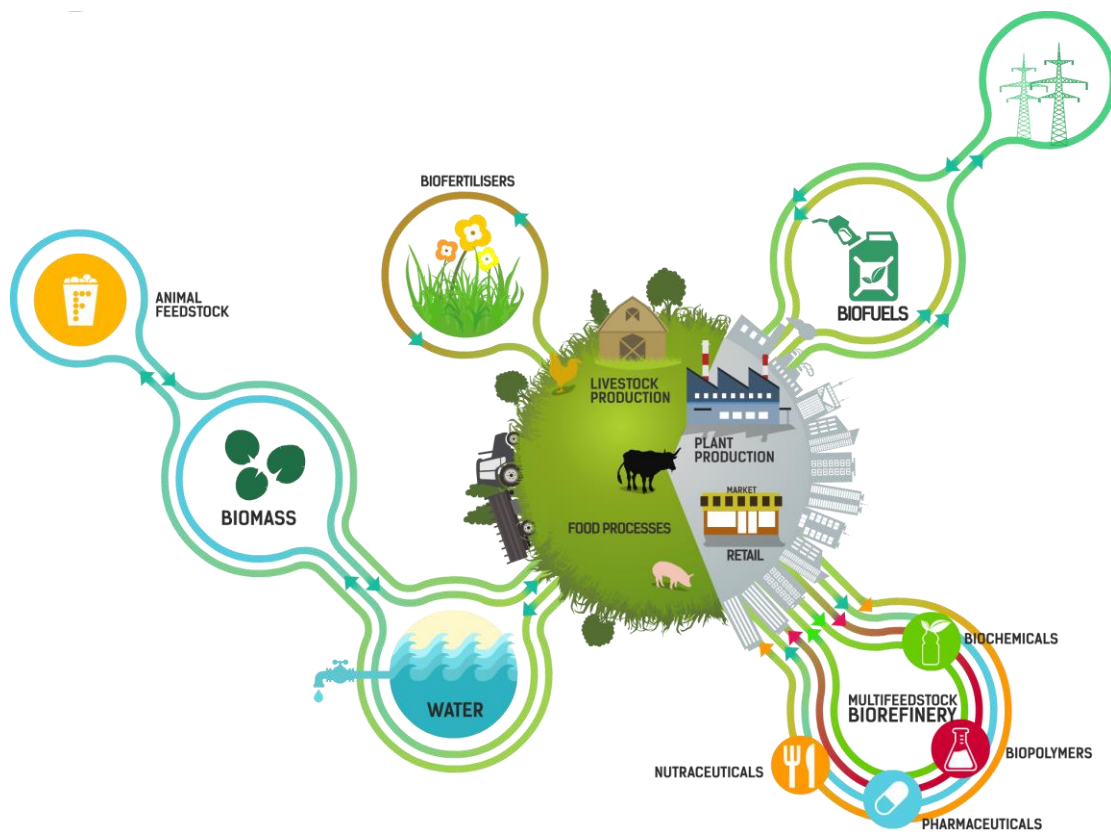


D2.6 Report of the Laboratory tests for Pyrolysis of forestry residues



DISCLAIMER

The opinion stated in this report reflects the opinion of the authors and not the opinion of the European Commission.

All intellectual property rights are owned by AgroCycle consortium members and are protected by the applicable laws. Reproduction is not authorised without prior written agreement.

The commercial use of any information contained in this document may require a license from the owner of that information.

ACKNOWLEDGEMENT

This project has received funding from the European Union's Horizon 2020 research and innovation programme under grant agreement Nº 690142.

Deliverable Document Sheet	
Project Acronym	AgroCycle
Project Title	Sustainable techno-economic solutions for the agricultural value chain
Grant Agreement number	690142
Call identifier	H2020-WASTE-2015-two-stage
Topic identifier	WASTE-7-2015 Ensuring sustainable use of agricultural waste, co-products and by-products
Funding Scheme	Research and Innovation Action
Project duration	36 months (June 2016 – May 2019)
Coordinator	NUID UCD – Professor Shane Ward
Website	www.AgroCycle.eu
Deliverable No.	D2.6
Deliverable title	Report of the Laboratory test for Pyrolysis of forestry residues
Description	Report will include experimental results for individual and/or combined pre-treatments. D2.6 covers the experimental results for the pyrolysis of three different forestry biomasses (conifers) as well as the biorefinery model proposed by means of virtual simulation
WP No.	2
Related task	Task 2.4
Lead Beneficiary	Exergy Ltd
Author(s)	Rocio Roldan
Contributor(s)	Eoin White – UCD
Type	Report
Dissemination Level	Confidential
Language	English – GB
Due Date	M24
Submission Date	

Date:	Action:	Version:	Ownership:
09/05/2018	Written	V.1	Rocio Roldan
10/05/2018	Reviewed/amended/approved	V.2	Eoin White
18/05/2018	Reviewed/amended/approved	V.3	Sotiris Patsios
23/05/2018	Amended	V.4	Rocio Roldan
25/05/2018	Submitted via Online Portal to Funding Agency	V.4	Tom Oldfield
18/10/2018	Re-submitted after minor corrections via Online Portal to Funding Agency	V.5	Anna Lesniak-Podsiadlo

Contents

Contents	4
Index of Tables.....	5
Index of Figures.....	5
1. Introduction	8
2. AgroCycle framework	10
3. Feedstocks.....	12
4. Reactors	19
5. Experimental preparation.....	23
5.1. Biomass preparation	23
5.2. Pyrolysis experiment	23
6. Pyrolysis results.....	26
6.1. Product yield	26
6.2. Determination of kinetic parameters of pyrolysis	30
6.3. Characterisation of the biomass and bio-oil	34
6.4. Other pyrolysis products – biochar and syngas.....	50
7. Simulations. Alternative process to upgrade bio-oil.....	52
7.1. Simulation specifications	53
7.2. Simulation Flowsheet	55
7.3. Section 10X. Pyrolysis.....	61
7.4. Section 20X. Bio-oil separation and upgrading	63
7.5. S-30X. Biochar valorisation	65
7.6. S-40X. Hydrocracking	67
7.7. Mass and energy balances. Electricity generated	68
7.8. Validation	76
8. Potential bio-oil applications in the AgroCycle context	78
9. Conclusions	80
10. References	81
11. Annex I. Tar composition	90

Index of Tables

Table 1. Lignocellulosic biomasses suitable for pyrolysis	12
Table 2. Advantages of the different pyrolysis reactor technologies	22
Table 3. Drawbacks of the different pyrolysis reactor technologies.	22
Table 4. Yields from Spruce wood pyrolysis	26
Table 5. Yields from pine wood pyrolysis	26
Table 6. Yields from larch wood pyrolysis.....	26
Table 7. Activation energy and pre-exponential factor during thermal decomposition of different biomass.....	31
Table 8. Proximate analysis of biomass (wt. %).....	35
Table 9. Elemental analysis of the biomass	38
Table 10. pH of pyrolysis bio-oil.....	39
Table 11. Density of pyrolysis bio-oil (kg/dm ³) @25 °C.....	40
Table 12. Viscosity of pyrolysis bio-oil (mm ² /s)	41
Table 13. The average specific heat capacity of pyrolysis bio-oil (J/g.K) for temperature range 25-100C.....	43
Table 14: CHNSO Elemental Analysis of the Bio-oils	48
Table 15. Determinants detected in pyrolysis bio-oil (mg/kg).....	49
Table 16. AgroCycle results comparison with literature review for bio-oil properties.....	49
Table 17. Aspen simulation component list.....	54
Table 18. Cyclones' parameters in pyrolysis section	62
Table 19. Absorption and desorption system in S-20X	65
Table 20. Biochar combustion reactors.....	66
Table 21. Cyclone system before turbine.....	66
Table 22. Hydrocracker calibrated model	67
Table 23. Properties of hydrocracking products	68
Table 24.Mass and energy balance of overall pyrolysis simulation	70

Index of Figures

Figure 1. Cellulose strand (fibre).....	14
Figure 2. Hemicellulose structure.....	15
Figure 3. Lignin structure	15
Figure 4. Map showing the distribution of Picea [81].....	16
Figure 5. Map showing distributions of Larix [87].....	17
Figure 6. Map showing distributions of Pinus [88].....	17
Figure 7. Bale production for bioenergy purposes (Courtesy of HAU/ Severn Carbon)	18
Figure 8. Samples of a) spruce wood, b) pine wood and c) larch wood used for the pyrolysis activity	23
Figure 9. Biomass before pyrolysis experiments.....	23
Figure 10. Diagram of fast pyrolysis system	24

Figure 11. Front view of the pyrolyser.....	25
Figure 12. Bio-oil recovery system.....	25
Figure 13. Pinus bio-oil. Left, particle size A; centre, particle size B; right, particle size C	27
Figure 14. Larch bio-oil. Left, particle size A; centre, particle size B; right, particle size C	27
Figure 15. Spruce bio-oil. Left, particle size A; centre, particle size B; right, particle size C	28
Figure 16. Biochar samples from the pyrolysis	28
Figure 17. Product yield from spruce pyrolysis	29
Figure 18. Product yield from pine pyrolysis	29
Figure 19. Product yield from larch pyrolysis	30
Figure 20. Mass loss curves during spruce decomposition at different heating rates.....	31
Figure 21. Arrhenius plot at constant conversion during spruce decomposition	32
Figure 22. Mass loss curves during pine decomposition at different heating rates.....	32
Figure 23. Arrhenius plot at constant conversion during decomposition of pine biomass	33
Figure 24. Mass loss curves during larch decomposition at different heating rates.....	33
Figure 25. Arrhenius plot at constant conversion during decomposition of larch biomass	34
Figure 26. Rate of decomposition of all biomass samples in the proximate analysis.....	36
Figure 27. Proximate analysis of spruce biomass.....	36
Figure 28. Proximate analysis of pine biomass.....	37
Figure 29. Proximate analysis of larch biomass.....	37
Figure 30. Density of pyrolysis bio-oil	40
Figure 31. Effect of temperature on viscosity of pyrolysis bio-oil	41
Figure 32. Water content in pyrolysis bio-oil	42
Figure 33. Density of pyrolysis oil as a function of water content.....	43
Figure 34. Heat flux of an empty specimen holder.....	44
Figure 35. Heat flow of standard sapphire relative to an empty specimen holder	44
Figure 36. Heat flow of spruce bio-oil.....	45
Figure 37. Heat flow of pine bio-oil.....	45
Figure 38. Heat flow of larch bio-oil.....	46
Figure 39. The Specific heat capacity of Spruce wood varying with temperature	46
Figure 40. The Specific heat capacity of pine wood varying with temperature	47
Figure 41. The Specific heat capacity of Larch wood varying with temperature	47
Figure 42. Pyrolysis stages when modelled [118]	53
Figure 43. Pyrolysis section in Aspen	56
Figure 44. Bio-oil separation and upgrading	57
Figure 45. Biochar valorization	58
Figure 46. Hydrocracking system (Aspen HYSYS)	59

Figure 47. Detailed hydrocracking system environment	59
Figure 48. Aspen Flowsheet for the pyrolysis of larch.....	60
Figure 49. Mass fraction of ethene in stream 207 as function of temperature in flash vessel	63
Figure 50. Mass fraction of ethene in stream 202 as function of temperature in flash vessel	64
Figure 51. Net Duty of flash vessel (energy requirements) as per the temperature	64
Figure 52. ASTM curve for bio-oil stream before final refining	67
Figure 53. Pyrolysis simulation mass balance	74
Figure 54. Pyrolysis simulation energy balance	75

1. Introduction

A huge interest has been drawn to the valorisation of agricultural and forestry wastes, co-products and by-products due to the increasing concerns over resource and energy scarcity. They are considered important sources of feedstocks to produce energy [1] and other derived bioproducts.

Several processes have been studied so far to produce energy from agroforest residues and by-products. The most exploited technologies for the conversion of lignocellulosic materials into energy are based on thermochemical processes, which include: combustion, pyrolysis, gasification and liquefaction at high pressure conditions [2], among others. The main differences among each process are detailed as follows:

- i) *Carbonisation.* It is a well-known process which has been used for millenniums to produce a solid fuel called charcoal. Charcoal was the first biofuel used by human beings and its different uses include: domestic cooking, metal refining applications and production of chemicals [3]. In terms of the forestry field, charcoal might be translated into a good opportunity for business in comparison to the traditional power generation which is usually decentralised.
- ii) *Pyrolysis.* It is considered one of the most attractive alternatives to produce renewable energies, due to its carbon negative feature. Pyrolysis consists of heating the selected biomass within an environment in absence of oxygen or any halogen. The outcomes from this process are a liquid product called bio-oil, a gas product or syngas (synthesis gas) and a solid by-product or bio-char. All these products are the result of the decomposition of the feedstock. The potential value of the products is relatively high in economic and environmental terms and no residues are generated, whereas bio-oil can be used to produce electricity or upgraded as a drop-in-biofuel, bio-char can be either burnt as an energy source or blended with fertilisers as a soil remediation. Bio-gas can be used either as an electricity source or recycled to the pyrolysis process [4] [5], as well as considered for the production of biochemicals in a biorefinery. Pyrolysis process is always the first step prior to any combustion and gasification processes.
- iii) *Gasification.* It is the conversion of carbonaceous material into a gaseous product by means of partial oxidation of the feedstock at high temperature and partial presence of oxygen. The main product is a mixture of permanent and non-condensable gases along with ash, tars and, char as a solid product. Biomass gasification is a relatively recent activity which is derived from the coal gasification as a well-established and well-known technology proved for more than a century. Nevertheless, both technologies are not comparable due to the chemical difference between feedstocks [6] [7]. Syngas product can be used as a source of energy by coupling a CHP or can be further upgrading through a syngas cleaning stage and use to produce chemicals and biofuels (synthetic hydrocarbons/methanol by Fischer-Tropsch route, DME, etc.).
- iv) *Liquefaction* (at relatively high conditions – high pressure and temperature). It is also known as hydrous pyrolysis [8]. It is carried out at high pressure and temperature and usually, in the presence of a solvent which enhances the

reactivity. It is considered a very flexible technology in terms of biomass which can be treated through this technology: woody biomass, industrial wastes, food wastes, manure, algae, etc. However, the costs associated to the use of this technology due to the high operating conditions (temperature and pressure) make the technology itself not economically feasible with most of the research to date have been on the development at small lab scale in batch experiments [9].

Pyrolysis and hydrothermal liquefaction of biomass are two technologies comparable in terms of the outcomes (products). These outcomes are intermediate products (biocrude, bio-oil) that can be refined into final products of interest. Nevertheless, there are significant differences like the previous pre-processing necessary for the treatment of the biomass since pyrolysis needs a lower water content in comparison to hydrothermal liquefaction. Other differences are found in the use of catalysts. In hydrothermal liquefaction is common the use of solvents as catalyst to promote the desired products, whereas in pyrolysis is not common to use catalysts. Differences also exist in the chemical composition of the products between pyrolysis and HTL, especially regarding the water and oxygen content as well as the heating value. On the other hand, operation at high pressure turns the liquefaction process less attractive from an economic perspective [10].

When the main product from lignocellulosic sources is a fuel, gasification is another alternative to be considered along with pyrolysis. The outputs of both technologies are the production of hydrogen and other fuels. In the case of pyrolysis, the gaseous effluent is mainly made up of H₂, CO₂, CO and other light hydrocarbons. Gasification however, produces a mixture of H₂, CO₂, CO (syngas) and N₂ when biomass is the feedstock. Some case studies involve the combination of gasification and pyrolysis in order to overcome some of the limitations reported so far [11] [12] [13].

Nevertheless, pyrolysis can be a suitable option when liquid fuels are sought, whereas gasification processes involve further conversion processes to turn the syngas product into ready-to-use products, such as liquid fuels through the Fischer-Tropsch process.

2. AgroCycle framework

Currently, Europe generates 1.3 billion tonnes of waste annually, of which 700 million tonnes are agricultural waste, accounting for one of the most produced bio-wastes worldwide. A projected one third increase in world population by 2050 will lead to increasing demands on the worlds agricultural resources. Compounding this, the impacts of climate change, particularly in more vulnerable areas of the world will drive desertification which is predicted to increase, and water shortages will become a major constraint on production. Implementation of innovative technologies and sustainable practices to maximise the value in existing agricultural resources is therefore of the upmost importance. A significant amount of existing food waste is avoidable and can be reduced by prevention measures at all level stages, from the production to the final consumption. Nevertheless, an unavoidable fraction of food waste remains and there is still a necessity to maximise its value through improved technological processes, practices and policies [14]. This necessity has led to the valorisation of all the fractions of this biowaste: proteins, lipids, carbohydrates and organic and inorganic fraction, by means of different biological and (thermo)chemical paths to produce biochemicals, commodities, and energy [15].

In this context, the AgroCycle project will perform an integral analysis of mechanisms to achieve a 10% increase in the recycling and valorisation of agricultural waste by 2020, maximizing the use of by-products and co-products via the creation of new sustainable value-chains. Agri-food wastes, coproducts and by-products (AWCB) are reported as having potential to replace current fossil-based (or non-renewable) energy and feedstocks. This shifting of current industrial practises to a new bio-based circular scheme can be developed by means of biorefineries, which are able to process the biomass or wastes into new bioproducts/energy [16]. However, there is a high dependence on different regional and seasonal factors which affect the actual economic potential of these schemes, such as supply of biomass, location, distance, technology for processing, pre-treatments, market, etc. In addition, other factors are relevant to determine the success of the technology and the feedstocks to evaluate whether it can help with climate change mitigation efforts [17].

The conversion of biomass to energy has primarily focused mainly on the necessary biochemical and thermochemical processes. From these processes, thermochemical processes can be subdivided into gasification, pyrolysis, carbonization, and direct liquefaction. Amongst the thermochemical processes, pyrolysis has received much more attention than others as its conditions could be optimized to produce high energy density pyrolytic oils as well as biochar and gas [18], which can be used in different industrial applications.

Pyrolysis is the thermochemical decomposition of organic material at high temperature, in the absence of oxygen or in an atmosphere of inert gases. Compared to combustion, pyrolysis has a lower process temperature and lower emissions of air pollutants such as polybrominated diphenylethers (PBDEs)

[19]. Additionally, the scale of pyrolysis plants is more flexible than incineration plants [20]. Nowadays, pyrolysis is gaining attention for the flexibility to generate a combination of solid, liquid and gaseous products in different proportions just by the variation of operating parameters such as temperature or heating rate. It also provides an opportunity of transforming materials of low-energy density into bio-fuels of high-energy density, at the same time recovering high value chemicals [21]. The products of thermochemical conversion can be categorized by their application. The specifications of the various products and their influence on the pyrolysis process are outlined below.

Char, a solid product of biomass pyrolysis, is a promising concept for climate change mitigation and adaptation, as it can sequester atmospheric CO₂ while improving quality of soil where it is stored [22] [23]. Its formation is favoured at low temperatures (225-300C) and long residence times. In nature, pyrolyzed bio-char particles fall to the ground surface and the black carbon is incorporated in the particulate phase of the smoke. In commercial bio-char pyrolysis systems, the process occurs in three steps: first, moisture and some volatiles are lost; second, unreacted residues are converted to volatiles, gasses and bio-char, and third, there is a slow chemical rearrangement of the bio-char [24].

Bio-oil is the liquid produced from the condensation of the pyrolysis vapor, and it is the main product of the fast pyrolysis (temperature range between 400-600C and short residence times). This product can be also formed by intermediate pyrolysis (300-500C) being able to reach up to 55% liquid yield conversion of the biomass. In that case the liquid product obtained has low tar yield and viscosity compared with the one from fast pyrolysis [25].

Non-condensable gases, they consist of a mixture of gases such as CO, CO₂, CH₄ and a few non-methane hydrocarbons, being CO₂ (~56%) and CO (~29%) the most abundant species in the pyrolysis products. Although, the composition depends on different chemical structures of biomass components [26]. Hemicellulose, with higher carboxyl content, account for a higher CO₂ yield. Cellulose displays a higher CO yield, mainly attributed to the thermal cracking of carbonyl and carboxyl. With a higher presence of aromatic rings and methoxyl functional groups, the pyrolysis of lignin releases much more H₂ and CH₄ [27].

One of the aims of the AgroCycle Project is to enhance the lignin rich agro-forestry waste into biofuels (syngas or liquid fuel) and soil amendments (biochar) based on pyrolysis process, this way the whole waste would be employed to produce valuable products. To this purpose, Task 2.4 in AgroCycle project aims at demonstrating the technical feasibility of the valorisation of forestry biomass into energetic products by means of pyrolysis.

This deliverable shows the outcomes from the experimental pyrolysis of three different conifers developed at lab scale by Exergy in Harpur Hill Laboratories in England (United Kingdom), as well as the proposition of a whole process for the valorisation of the products, especial focus on bio-oil and biochar, for energetic applications by means of virtual simulation.

3. Feedstocks

Table 1 gathers and lists some of the different lignocellulosic biomasses tested globally to produce bioenergy/bioproducts through thermochemical pyrolysis technology. This first revision has been focused on studies relevant to Europe, and specifically to the UK.

Table 1. Lignocellulosic biomasses suitable for pyrolysis

Biomass	Source	Availability in Europe – UK	Other data
Acacia wood	[28]	No	Available in Africa and Australia
Almond shell	[29] [30]	No	Available in Middle East, India and North Africa
Apple pulp	[31]	Yes	Crab apple grows in at the wet edge of forests, in farmland hedges or on very extreme, marginal sites (<i>Malus sylvestris</i>)
Apricot stones	[29]	No	Major production in Turkey, Iran and Uzbekistan
Arbutus Unedo	[32]	Yes	West Ireland. Strawberry tree
Argentinean hardwood species	[33]	No	South America
Aspidosperma Australae	[33]	No	South America
Aspidosperma Quebracho Blanco Schlecht	[33]	No	South America
Austrian pine	[34]	Yes	South England
Beech wood	[35]	Yes	<i>Fagus sylvatica</i> is found in South England
Silver birch	[36]	Yes	Scotland
Birch wood	[37]	Yes	Scotland
Cherry stones	[15]	Yes	Wild cherry is found throughout the UK except in the far north
Corn stover	[15]	Yes	Maize production in the West of England
Corn stalk	[38]	No	
Cotton cocoon shell	[39]	No	China, India and Pakistan are the major producers
Cotton gin waste	[40]	No	
Cotton stalk	[41]	No	
Cotton straw		No	
Cottonseed cake	[42]	No	
Cynara cardunculus L	[43]	No	South and western Europe and Australia
Eucalyptus wood	[44]	No	Eucaliptus is found in Australian, Nueva Guinea and Indonesia
Euphorbia rigida	[45]	No	South Europe
Extracted oil palm fibers	[46]	No	Palm oil tree is native from Africa
Forest wood	[47]	Yes	Different forests can be found across the UK
Grape residues	[48]	Yes	Sussex, Kent and other areas in the Southern England are suitable for

			grapes. Top grape producing countries are China, USA, Italy, France and Spain
Grape residue	[49]	Yes	
Grape seeds	[29]	Yes	
Grass	[50]	Yes	There are a wide range of grass types, in UK the most common are perennial types. Grass can be found worldwide
Ground nut shell	[51]	No	Different kind of groundnuts are found in Brazil, China and Africa
Hardwood (beech, chestnuts)	[52]	Yes	North and South England. Also found in continental Europe (Denmark, Norway and Sweden)
Hazelnuts (<i>Corylus avellans</i>) shells	[45]	Yes	It is found across Europe, including the British Islands
Lodgepole pine	[34]	No	Native from North America
Lucerne	[53]	Yes	It is available in the UK, but it grows in Mediterranean countries in Europe
Miscanthus pellet	[37]	Yes	<i>Miscanthus Sinensis</i> is found in Austria, Belgium, Czech Republic, France, Georgia, Germany, Hungary, Italy, Russia (native), Switzerland, Spain, the United Kingdom along with North America, Asia, Oceania and Chile
Oil palm shell	[54]	No	
Olive husk	[55]	Olive is produced at small scale in some regions of England	The major producers of olive are Spain, Italy, Greece, Turkey, Morocco and Syria. Portugal also produces olive
Olive stone	[56]		
Pine	[57]	Yes	Pine can be found in Scotland and a wide range of European countries as well as Asia and North America region
Pine sawdust	[58]	Yes	
Pinus insignis sawdust	[59]	Yes	
Ponderosa pine	[34]	No	North America
Rape seed	[60]	Yes (small production)	It is produced in China and Germany, France, Poland and Ukraine as main European countries
Rice husks	[61]	No	Rice is produced in Spain and Italy (Europe) and China
Safflower seed	[62]	No	It is not produced in Europe
Scotch pine	[34]	Yes	It is found in a small area of Scotland and the Northern Europe
Soft woods (Douglas fir, redwood, pine)	[63]	No	They are especially found in North America
Stalk of rape seed plant	[64]	Yes	
Straw	[65]	Yes	
Straw pellet	[37]	Yes	
Straw rape	[53]	Yes	
Straw stalk	[66]	Yes	
Sugar cane bagasse	[67]	No	It is produced in over 70 countries, top 5 cane sugar producers being Brazil, India, Thailand, China and Mexico.

Sunflower press oil cake	[68]	Yes	Sunflower grows in small areas in the south of England and Spain, Italy, Eastern Europe, Middle East and some regions in North and South America
Sunflower oil	[69]	Yes	
Switch grass	[53]	No	
Tobacco	[70]		
Tobacco dust	[71]		
Wheat straw	[72] [73]	Yes	The UK annual wheat straw yield has been estimated to be between 8 and 10 million tonnes.
Wood chips	[74]		

It is important to point out the increasing interest in the agroforest wastes for pyrolysis purposes in the last decade. In comparison to other biomasses, it requires smaller cultivation areas, and some parts of the crops become “wastes” after the cultivation process [75]. One of the main concerns related to the use of agricultural and forestry wastes as feedstock for pyrolysis is the Sustainability of biomass supply. Only farmers and landowners have total control of this area as well as of the knowledge about composition and transport due to the seasonal variability [76].

Lignocellulosic biomass is made up of three main components: cellulose (35-50%), hemicellulose (20-35%) and lignin (15-20%) along with other compounds such as ash (15-20%), shaping a woody structure [77]:

Cellulose ($C_6H_{10}O_5$)_a : It is the main compound and the most abundant organic polymer, which is found in the cell wall of the plants. It is made of D-glucose monomers. It is also considered a polysaccharide and it has a crystalline structure which makes it resistant to hydrolysis

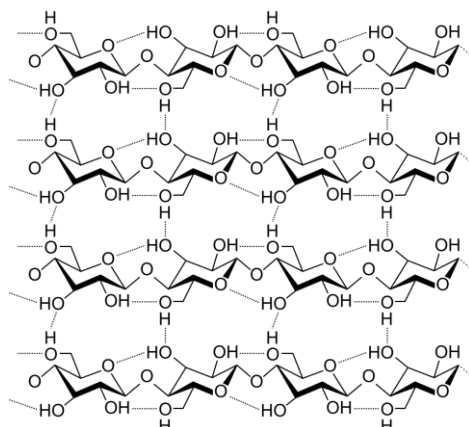


Figure 1. Cellulose strand (fibre)

Hemicellulose ($C_5H_{10}O_8$)_b: It is a branched polymer (polysaccharides) which is made up of some monomers such as glucose, galactose, mannose, xylose and arabinose, among others [78]. In opposition to cellulose, hemicellulose is amorphous, and it can be hydrolysed using acids, bases or specific enzymes.

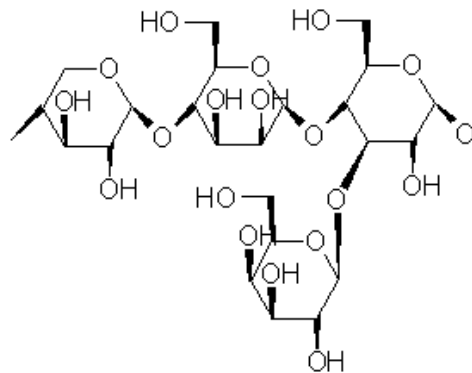


Figure 2. Hemicellulose structure

Lignin ($C_9H_{10O_3}(OCH_3)_{0.9-1.7}c$): is an aromatic phenol-based polymer. It is responsible for the rigid structure of the lignocellulosic biomass due to its three-dimensional structure. Lignin performs as a binding between hemicellulose and cellulose inside the plant cell wall. Lignin content has been reported up to 40% in lignocellulosic biomass [79] [80].

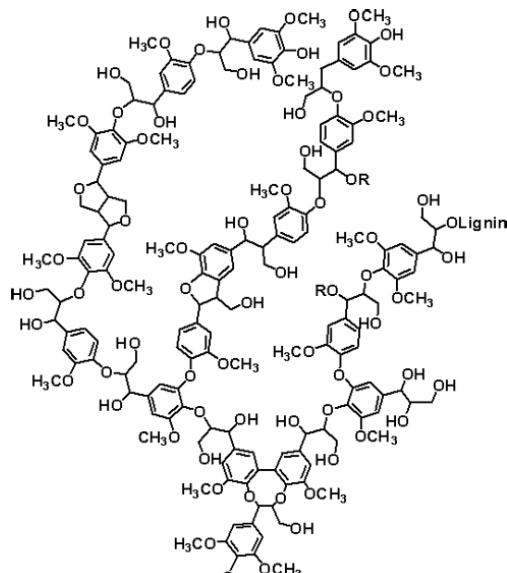


Figure 3. Lignin structure

After several discussions with the AgroCycle technical team and Harper Adams University (who offered to be a potential supplier of the biomass needed for the pyrolysis with the collaboration of Severn Carbon), three samples of conifer found in the UK were selected for the trials in Task 2.5:

- *Picea* or spruce. It is found in northern countries (boreal forest and subalpine areas of the Alps and Carpathian Mountains) in Europe, as shown in Figure 4. It has leaves with the shape of needles. Different species of *Picea* or *Picea abies* in Europe have been reported to be tested for pyrolysis, including the upgrading of bio-oil .

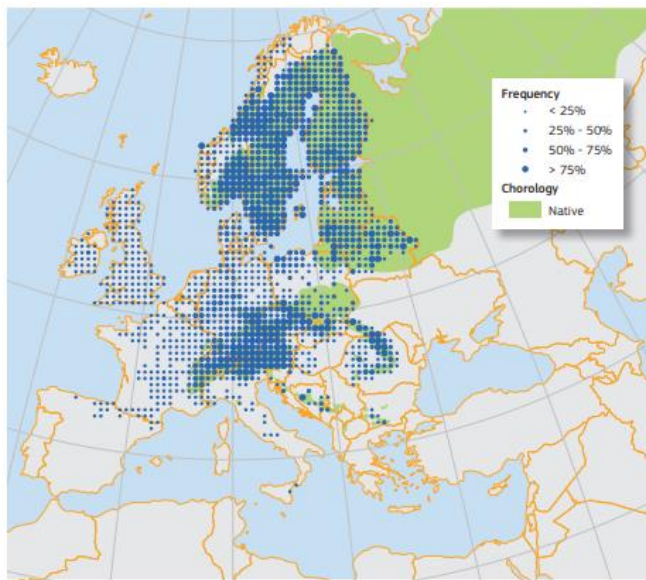


Figure 4. Map showing the distribution of *Picea* [81]

These kinds of trees can reach up to 200-300 years' life span [82]. Spruce wood is cheap and easy to find, depending on the grade sought and the final application of the wood, as an important timber tree in Europe. The wood has different applications, including construction, furniture, sound boards, pianos and other musical instruments (including Stradivarius violins) as well as for pulpwood applications. **In terms of sustainability, it is reported by the IUCN as one of the species of least concern** [83]. It is also known as "the Christmas Tree" in Europe, being a large conifer native across central and northern Europe. Outside Europe, it is also found in Northern American and Canada. This kind of conifer is one of which can tolerate warmer and humid summer weather conditions.

- *Larix* or larch, it is a sort of conifer found mainly in central Europe— From the Alps in eastern France to southern Poland, western Ukraine and northern Romania, passing across Carpathian and Slovenian Mountains [84]. It is grown mainly in dry places, as wet or chalky soils are not appropriate for its growth. Larch wood comes from strong and vigorous trees which are looking for light (sun hunters). They can reach up to 45 meters tall. It is the only conifer native to Central Europe (Alps and Carpathian Mountains), and it was introduced to the UK in the 17th century, where it has been widespread and naturalised. As *Picea*, **it is considered Least Concern at the global and EU28 member states level**, due to its wide availability (it is widespread) and range [85].

The wood from European larch has been valorised for multiple purposes: fences, gates, railway sleepers (before substitution by concrete and iron), as well as to build houses, especially in Alps and Carpathians mountains. The wood is also used for medicinal purposes, as the bark can be used as an astringent, balsamic, diuretic, expectorant, stimulant and to treat different wounds, eczema and psoriasis [86]. It is also possible to extract turpentine from the resin which can be used as a wood preservative.

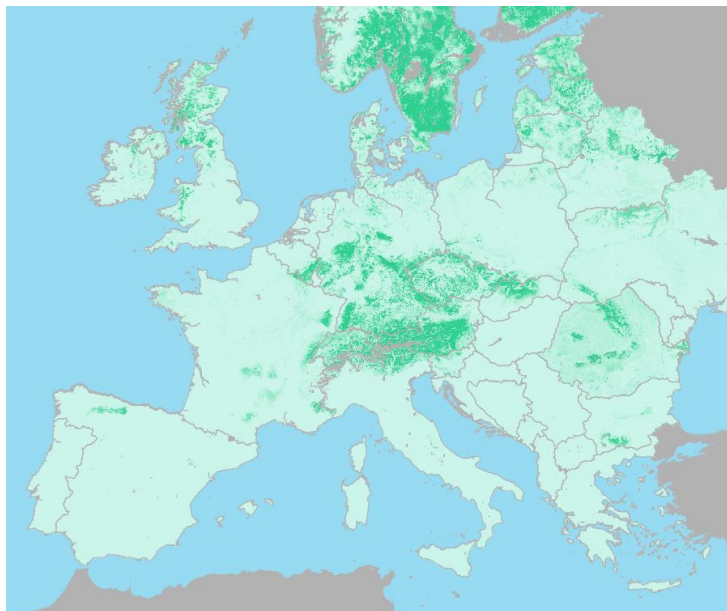


Figure 5. Map showing distributions of *Larix* [87]

- *Pinus* or pine, it is another species of conifer which can be found in northern hemisphere, although some species have been introduced in the southern hemisphere and subtropical regions of the planet. It has been also widely tested for pyrolysis seeking a potential suitable bio-oil, both in catalytic and non-catalytic conditions.

Pine is an important source for timber and for the pulp & paper industries. It was used in the past for construction and furniture, but currently these uses have been shifted to spruce (*Picea abies*), due to the lower content in resin and its smoother grain.



Figure 6. Map showing distributions of *Pinus* [88]

Conifers have been used for pyrolysis purposes, especially looking for potential agents to enhance soil properties from the biochar product. In Figure 7, the

bales of different conifers supplied for the pyrolysis activities in WP2 are shown. They were supplied by Harper Adams University (Newport, UK) in early 2017.



Figure 7. Bale production for bioenergy purposes (Courtesy of HAU/ Severn Carbon)

4. Reactors

The choice of a pyrolysis technology will often depend on final products targeted (biochar, bio-oil or syngas). Also, the type of reactor employed for the pyrolysis of the waste must be given great importance because of the large amount of heat to be transferred across the reactor wall to ensure the degradation of the material. Usually the pyrolysis process is performed under atmospheric pressure, however vacuum pyrolysis (which can be about 5 kPa) has some advantages such as its short residence time and the low decomposition temperature which reduces the occurrence and intensity of secondary reactions. This type of pyrolysis is used in different types of feedstock, including wood. However, it is difficult to achieve in practice at an industrial scale [89].

Fixed bed reactor

Fixed bed reactor is the simplest solution, due to its easy design. In this type of reactor, the feedstock is placed in the reactor, which is heated externally. Before the experiment starts the reactor is flushed by an inert gas, and the gas flow is maintained to provide an anaerobic atmosphere. The gases and vapours obtained are discharged from the reactor during the pyrolysis, but char is usually removed after the process. The fixed bed reactor is characterized by a low heating rate [90]. This type of reactor could be used at a larger scale provided that the technology used enables better heat transfer, and it is a good option to provide experimental information on the pyrolysis parameters and its product. The reactor used in the AgroCycle project is a fixed bed reactor.

Fluidized bed reactor

This type of reactor consists of a vessel containing a mass of heated particles (inert sand or catalyst particles), that are fluidized by passing inert gas or recycled product gas through the particle bed. The biomass is injected into or above the hot particles by a solid feeder such as a screw feeder or intermittent solid slug feeder. These reactors are characterized by a high heating rate and a good blending of the feedstock. However, there are important difficulties in its use as the feedstock must be tiny to be introduced in the reactor and float in the fluid. There are difficulties to separate the char from the bed material. This, along with the difficulty of scale-up, means that this reactor is rarely used in large-scale projects [91]. Fluidized bed reactors can be further broken down into the following configurations:

a. **Bubbling Fluidized Bed (BFB) reactor**

BFB reactors utilize fluidized bed reactors with gas passing through the reactor so the solid fluidization is in the ‘bubbling’ regime, it means that the bed has fully expanded and is bubbling aggressively but without reaching the turbulent flow regime. Typically, vapour residence times in BFB reactors are between 0.2-5 s, depending on the reactor size [92].

b. **Circulating Fluidized Bed (CFB) reactor**

CFB reactors have also high heat transfer rates and short vapour residence times, among 0.5-1 s. The heat transfer medium in this reactor is the bed of

particles, which is circulated using high flowrates of gas from the reactor vessel into a burner. In the burner, the particles are exposed to oxygen and recycled product gas or solid reaction products are burned to heat the particles and then they are circulated back. As a result, the solid residence time is approximately the same as the vapour residence time, and the reactor operates at high superficial gas velocities (in transport conditions). As a result of these high flowrates, solids separation and bio-oil vapour condensation can become more challenging. CFB reactors can be either up flow (more traditionally) or downflow (used for plug flow control of short residence times) [92].

Batch and Semi-batch reactor

Batch reactors are a closed system with no input or output of reactants or products while the reaction is occurring resulting in high conversion.

Semi-batch reactors allow the addition of reactants and the removal of products, while the process is performing. Although products are not uniform from batch to batch and increasing the scale is problematic. Another additional disadvantage is the long solid residence time and the difficulty of removing char [93].

Rotatory Kiln reactor

It is commonly used in slow pyrolysis, operating at temperatures around 500°C with a residence time of about 1 hour, and it is traditionally used for biochar production [94]. This type of reactor has been implemented as a practical industrial solution at various scales so far, it offers better heat transfer to the feedstock than the fixed beds and it is less complicated than the fluidized beds [95].

Furthermore, a rotary kiln pyrolyser has many advantages over other types of reactors. For example, the slow rotation of an inclined kiln enables a good mixing of wastes, thus it is possible to obtain more uniform pyrolytic products [96]. However, the conditions for the exchange of matter and heat between the solid and the gas are not very effective, and then, the residence time (reaction volumes) is higher than those with the other pyrolysis technologies [97].

Microwave assisted reactor.

It is a relatively novel process which was developed initially by Tech-En Ltd, in the UK [98]. This process consists of a mixture of the feedstock material with a microwave-absorbent material, such as particulate carbon, which can absorb the microwave energy (electromagnetic wave) to produce sufficient thermal energy to achieve the temperature conditions for pyrolysis process. The microwave heating cracks the feedstock material into smaller particles in the absence of oxygen. As any other pyrolysis process, the volatile components are either condensed as bio-oil or collected in the incondensable mixture (pyrolysis gases) [99]. Microwave heating can be better than conventional heating because of various advantages. Hot spots, which form under microwave irradiation would have significant influence on the yield and characteristics of microwave processing products. The solid products of microwave pyrolysis at proper microwave power levels can have high heating values and specific surface areas with higher gas and solid yields but lower liquid yield than conventional pyrolysis [100]. One of the main advantages is the possibility to pyrolyse large particle materials, thus previous energy-

intensive grinding pre-treatments can be avoided [101]. This technology is reported also more tolerant to water content in comparison to other conventionally established pyrolysis technologies, where the water content must be below 10 wt%, therefore a previous drying step can be also skipped [102].

Ablative reactors

The ablative reactor is composed of a chamber, which contains a spinning bowl where the biomass can be placed, and a hot plate at the top that can move down and apply pressure against biomass. This type of reactor can be used for bio-oil production through fast pyrolysis. Fast pyrolysis initiates as the hot plate contacts the biomass, and a high flow rate of inert gas rapidly sweeps the generated vapours out of the chamber for condensation [103].

One of the advantages to use this reactor, it is that as reaction rates are not limited by heat transfer through the biomass, large particles can be used, and in principle there is no upper limit to the size that can be processed. The process in fact is limited by the rate of heat supply to the reactor rather than the rate of heat absorption by the pyrolysing biomass as in other reactors. There is no requirement for inert gas, so the processing equipment is smaller, and the reaction system is thus more intensive. However, the process is surface area controlled so scaling is tough and the reactor is mechanically driven so is thus more complex [104].

Auger reactor

In this type of reactor biomass is mixed with a dense heat carrier. By using high thermal conductivity heat carriers, the energy required for fast pyrolysis is rapidly transferred to the biomass. The vapours generated are quickly diverted to a condensation train to minimize reaction time and the char produced is separated from the heat carrier independent of the pyrolysis reactions and into a char storage system [92].

Table 2 summarises the advantages of each of the reactors mentioned above with Table 3 highlighting the main disadvantages of the reactors.

The reactor selected is a fixed bed reactor (as shown in section 5.2 Pyrolysis experiment), externally heated by means of 15.8 kW radiant heater, in the presence of nitrogen as the inert gas. The selection of a fixed bed, as stated above, was due to the simplicity in its use and design, as well as its potential scalability for the subsequent application of the results in a model (by simulation) to demonstrate the feasibility of the solution at larger scale. Its potential to obtain experimental parameters also makes this selection more attractive for the use different feedstocks. On the other hand, better heat and matter transfers, in comparison to other reactors, also lead to the use of this reactor for obtaining more accurate kinetic parameters.

Table 2. Advantages of the different pyrolysis reactor technologies

Fixed bed	Fluidized bed reactor		Batch and Semi-batch reactor	Microwave reactor	Ablative reactor	Rotating reactor	Kiln	Auger reactor
<ul style="list-style-type: none"> Simple Scalable Good heat transfer Useful for experimental parameters Applicable for fast and slow pyrolysis 	BFB <ul style="list-style-type: none"> Good temperature control and mixing. Easy to scale up. Well-established technology. Intense heat and mass transfer 	CFB <ul style="list-style-type: none"> Well-established technology 	<ul style="list-style-type: none"> Good heat and mass transfer. Controllable residence time. Very large processing capacity. 	<ul style="list-style-type: none"> Good temperature control. Capability of minimising unwanted reactions. 	<ul style="list-style-type: none"> Uniform heating. Large size piece of wood can be fed. Rapid reaction process. Produce chars with large specific surface areas. 	<ul style="list-style-type: none"> Good heat transfer. Large particle size can be used. Inert gas is not required. Controllable residence time. System is more intensive. 	<ul style="list-style-type: none"> Centrifugal forces move heated sand and biomass. No carrier gas needed. Easy quenching. 	<ul style="list-style-type: none"> Low pyrolysis temperature (400C). Compact and flexible design. No carrier gasses. Quality bio-char produced

Table 3. Drawbacks of the different pyrolysis reactor technologies.

Fixed bed	Fluidized bed reactor		Batch and Semi-batch reactor	Microwave reactor	Ablative reactor	Rotating Kiln reactor	Auger reactor
<ul style="list-style-type: none"> Low heating rate Higher residency times Not uniform product distribution 	BFB <ul style="list-style-type: none"> Product dilution from fluidization gas. Condensation train and separation challenges. Particle size restricted. 	CFB <ul style="list-style-type: none"> Challenging operate/condensation/separation. Smaller biomass particle required. High gas flow and product dilution. High separation and quenching requirements. 	<ul style="list-style-type: none"> Difficult scale up. Not uniform product production. Long solid residence time. Difficulty of removing bio-char from the reactor. 	<ul style="list-style-type: none"> Relatively new technology. Produce low liquid yields (less than 30%). 	<ul style="list-style-type: none"> Reaction rates limited by heat transfer to reactor. Process is surface area controlled, high cost to scale up. High gas flow and product dilution. 	<ul style="list-style-type: none"> Complex process. Difficult to scale up. High capital costs. Small particle size needed. 	<ul style="list-style-type: none"> Plugging risk. Low bio-oil yield. Moving parts in the hot zone. Heat transfer limitations at large scale.

5. Experimental preparation

5.1. Biomass preparation

A series of biomass pyrolysis trials on forestry residues were conducted to obtain the mass yields and distribution of bio-oil, bio-char and gases in the product. The aim of the experiments was to analyse the effect of the nature of the biomass, the particle size and pyrolysis temperature on pyrolysis yields, and the product distributions. In this study, three types of wood were analysed: pine wood, spruce wood and larch wood. Figure 8 a), b) and c) shows the spruce, pine and larch wood, respectively. They were initially classified into different particle sizes using Retsch AS200 sieving machine and test sieves. They were grouped according to mesh sizes; 1 - 3mm (A), 4- 6.6mm (B) , and 6.7- 20mm (C) with total length between 1-50mm.

The type and the capacity of the reactor, pyrolysis temperature, solid residence time, carrier gas flowrate, vapour residence time, and biomass feedstock type and size were identified as the parameters having the most influence on product yields and their properties [94].

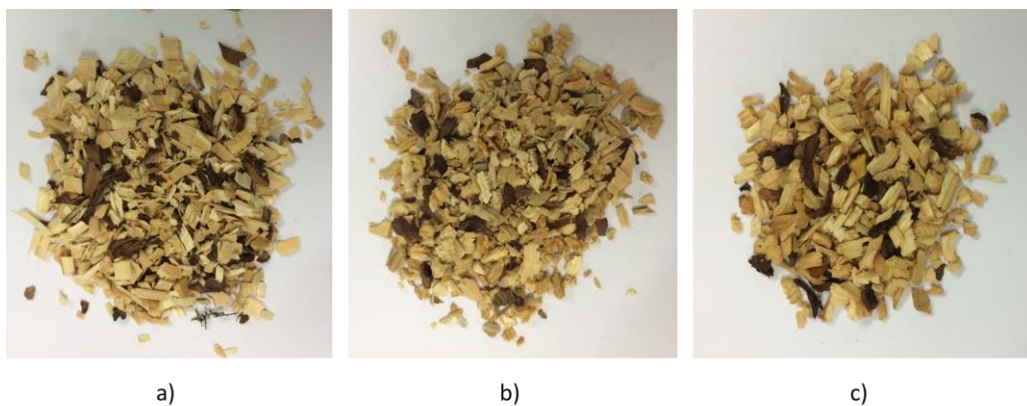


Figure 8. Samples of a) spruce wood, b) pine wood and c) larch wood used for the pyrolysis activity



Figure 9. Biomass before pyrolysis experiments

5.2. Pyrolysis experiment

There are three different types of pyrolysis processes: fast pyrolysis, intermediate pyrolysis (torrefaction) and slow pyrolysis – microwave pyrolysis is not considered. In this study the experiments were carried out at the reaction

temperature of 300, 400 and 500 C. Usually the pyrolysis conditions are optimized in order to maximize the liquid and gas products, however, there is always a fraction of biochar, that in this case would be also valorised as a product in other activities in the AgroCycle project – notably Task 2.5, which used biochar as a catalyser in the microbial fuel cell (MFC) experiments, and to WP4 to be tested as adsorbent in wastewater treatment purposes,. Its use for soil enhancement was discarded in early conversations with researchers working on WP3. The samples were classified as function of their particle size, that were in the ranges of 1-3 mm, 4-6.6 mm and 6.7-20 mm. The experiments were performed at Harpur Hill Laboratory in Buxton (University of Sheffield, Sheffield, UK).

The equipment employed for this study was a cylindrical fixed bed reactor externally heated using 15.8 kW radiant heater. The reactor was initially warmed up from ambient until it reached the desired reaction temperature. The temperature was maintained by a control unit connected to K-type thermocouple (Al-Cr) fitted below the pyrolysis chamber. An inert atmosphere was maintained by a continuous flow at 4 LPM of N₂ flow rate. Figure 10 presents a schematic of the equipment used for the pyrolysis process.

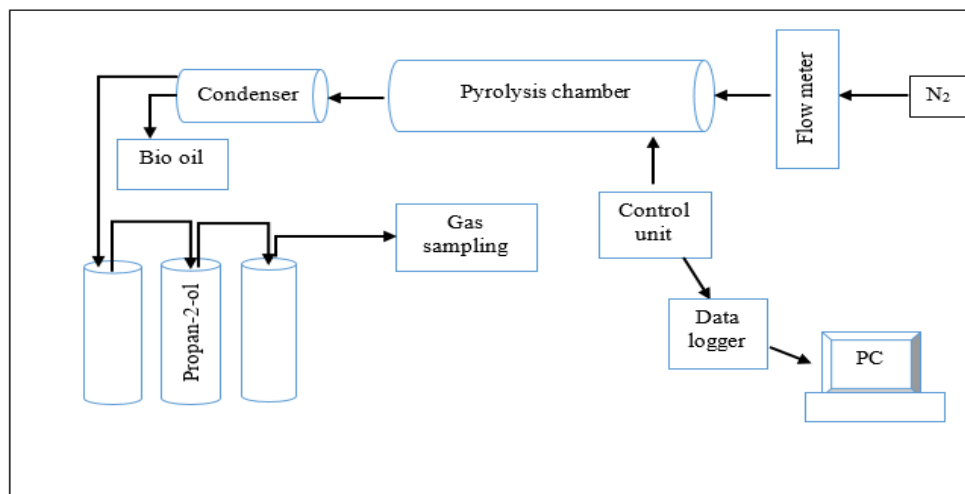


Figure 10. Diagram of fast pyrolysis system

Once the reactor has reached the optimum operation conditions, 60 g of biomass are fed into the central heating zone of the pyrolyser (Figure 11).

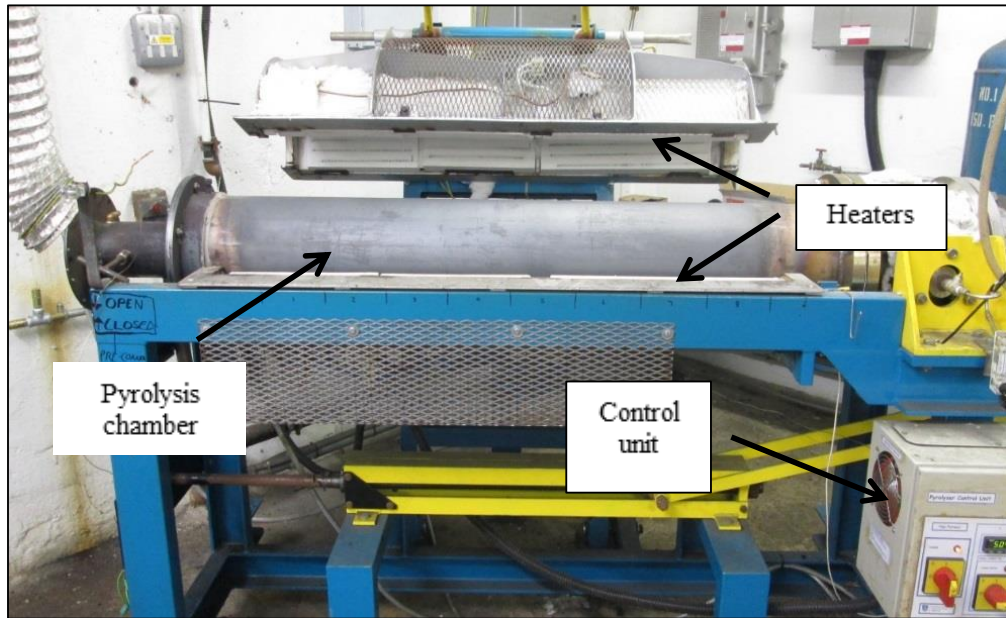


Figure 11. Front view of the pyrolyser

The biomass pyrolyses for 45 minutes producing char and gases. The hot volatiles are suppressed by a water condenser for the bio-oil recovery (Figure 12), and the non-condensable gases are drawn-out by an extractor fan. Char and bio-oil are collected at the end of the experiment for mass balance analysis, and gas yield is calculated by difference (1).

$$G = M - \sum(C + O) \quad (1)$$

Where 'G' (g) is the mass of gas obtained in the pyrolysis, 'M' (g) the initial weight of biomass employed in the experiment and 'C' (g) and 'O' (g) are respectively, the weight of bio char and bio-oil obtained as products of the pyrolysis.

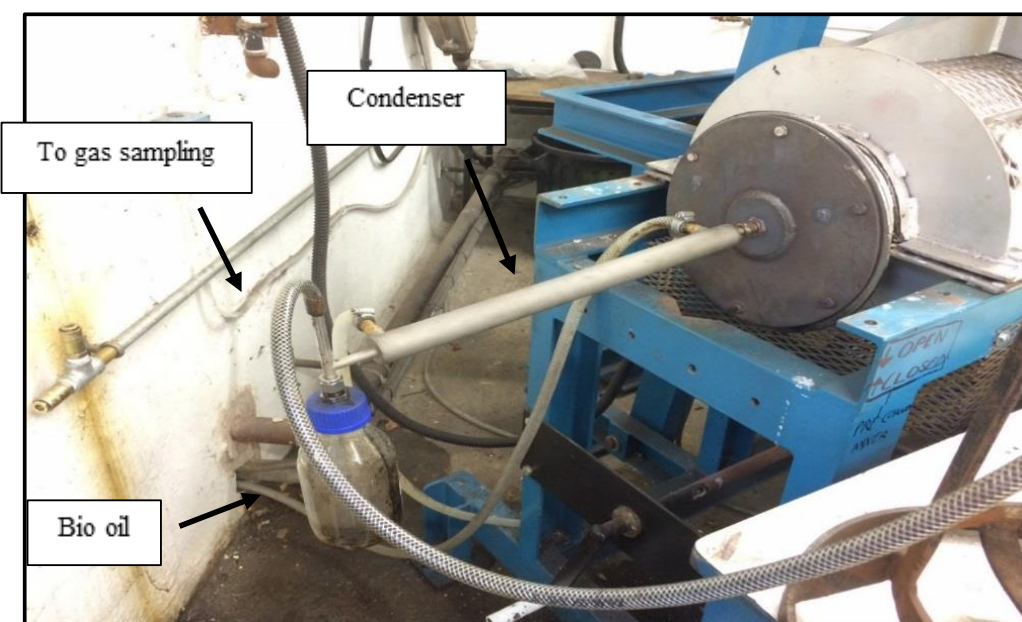


Figure 12. Bio-oil recovery system

6. Pyrolysis results

6.1. Product yield

The aim of the experiments is to investigate the effect of particle sizes and temperatures on pyrolysis yield and product distributions. Equation 2 was used to determine the yield of the pyrolysis products (char, bio-oil or gas), establishing a relation between the mass of pyrolysis product obtained and initial weight of the biomass employed in the experiment:

$$Y_i = \frac{M_i}{M} \times 100 \quad (2)$$

Where 'Y_i' (%) is the yield of the pyrolysis product, 'M_i' (g) the mass of pyrolysis product and 'M' (g) the initial weight of biomass.

The yields and products distributions of the pyrolysis are summarized in Table 4 to Table 6, regarding the type of wood.

Table 4. Yields from Spruce wood pyrolysis

Temperature	300C			400C			500C		
Particle size (mm)	1-3.0	4-6.6	6.7-20.0	1-3.0	4-6.6	6.7-20.0	1-3.0	4-6.6	6.7-20.0
Char (wt%)	35	35	33	27	26	26	23	22	21
Bio-oil (wt%)	27	25	27	27	28	26	21	20	20
Gas (wt%)	38	40	40	46	46	48	56	58	59

Table 5. Yields from pine wood pyrolysis

Temperature	300C			400C			500C		
Particle size (mm)	1-3.0	4-6.6	6.7-20.0	1-3.0	4-6.6	6.7-20.0	1-3.0	4-6.6	6.7-20.0
Char (wt%)	28	28	28	22	22	22	20	20	20
Bio-oil (wt%)	30	27	28	25	23	23	20	18	20
Gas (wt%)	42	45	43	53	55	55	60	62	60

Table 6. Yields from larch wood pyrolysis

Temperature	300C			400C			500C		
Particle size (mm)	1-3.0	4-6.6	6.7-20.0	1-3.0	4-6.6	6.7-20.0	1-3.0	4-6.6	6.7-20.0
Char (wt%)	33	33	33	25	25	25	22	21	22
Bio-oil (wt%)	28	27	27	25	25	23	20	19	18
Gas (wt%)	38	40	40	50	50	52	58	60	60

Tables 4-6 highlight that the pyrolysis of the pine wood provides the product with richer fraction of gas, followed by the pyrolysis of the larch wood. This fraction increases with the temperature and size of the particles, and in the case of the pine wood goes from 42 to 60%. Compared with another study carried out in the same type of reactor [105],

the product obtained in the pine wood pyrolysis is composed mainly of bio-oil at high temperatures (50-60 wt% at 400-600°C) and bio char at low temperatures (65 wt% at 300°C). The fractions of bio-oil and gas increase with the temperature increasing, as in the present experiments.

As it has been exposed in another study of pyrolysis of agro-forestry waste, the lower the temperature at which pyrolysis occurs, the higher the carbon recovery of the original biomass [106]. If the feedstock is dry and the bio-char yield is high, the heat produced can warm the incoming feedstock sufficiently to initiate the pyrolyzing reactions to sustain the process [107]. The production of bio-char is favoured when there are low temperatures and low oxygen levels inside a pyrolysis chamber.

Analysing the products distribution, it is shown that independently to the nature of the agro-forestry waste, the production of bio-oil is the least favoured option, and its formation decreases gradually with the increment on the temperature and particle size. However, the production of char and bio-oils at low temperatures is similar, with the production of non-condensable gases being the most favourable option in all cases.

The difference in the distribution of the products increase rapidly with the temperature and particle size, as the char production is favoured at low temperature and small particle size, contrary to the production of lighter products such as the bio-oil and gases. This difference is bigger in the pine wood, with a rate among 7 and 40%. In all the cases, the production of bio-oil and char is less favoured than the formation of the gases. Regarding different studies [108], for pyrolysis, generally, temperature can be adjusted within the range of 400-600C to maximize the production of bio-oil. In this temperature range, more than 45 wt% oil can be produced. As it can be seen in the tables above, the production of bio-oil is higher when the pyrolysis temperature is lower regardless of the type of wood studied, contrary to what has been found in previous studies. This may be related with time of residence, as it is normal to perform fast pyrolysis to enhance the production of the liquid fraction applying shorter times of residence (magnitude in the order of seconds) [109].



Figure 13. Pinus bio-oil. Left, particle size A; centre, particle size B; right, particle size C



Figure 14. Larch bio-oil. Left, particle size A; centre, particle size B; right, particle size C



Figure 15. Spruce bio-oil. Left, particle size A; centre, particle size B; right, particle size C



Figure 16. Biochar samples from the pyrolysis

6.1.1. Effect of Particle size:

At similar reaction temperature, it can be observed that particle size exerts little influence on product yield. Char yield is similar across all particle sizes, with a slightly higher oil yield obtained from small particles pyrolysis. However, the differences are very small, around 1-3 % as in the case of pine pyrolysis. The same can be said about gas production. Higher bio-oil is expected when pyrolysing small particles, however this is not in fact the case. Long reaction time in the reactor, (~45 minutes) coupled with volatiles residence time (~1s) might induce thermal cracking of volatiles into permanent gases.

6.1.2. Effect of pyrolysis temperature:

Temperature exerts a significant influence on product yield. In general, a decrease in total char and bio-oil is observed when reaction temperature is increased. This however, results in greater gas production with temperature. Pyrolysis of pine wood at 300 C produces the highest amount of char at around 35%, followed by larch and spruce at 33.33% and 28.33%, respectively. In contrast, pyrolysis of larch wood at the same reaction temperature produces the highest amount of bio-oil at 30%, owing to its higher volatiles content. Meanwhile, bio-oil obtained from spruce and pine pyrolysis ranges between 28 to 33% at 300C and decreases further to 20% at 500C.

Notable decreases in char yield with reaction temperature is observed across all samples. For example, char obtained from larch pyrolysis decreases by about 12% to 28.33 % as the reaction temperature is increased from 300 to 500C. Similarly, it has resulted in 10% decrease in bio-oil production. This can be explained by greater primary decomposition and enhanced secondary reactions which favour conversion into gases. Gas production ranges between 36-60% during pyrolysis of biomass, with higher amount emitted at high temperature.

6.1.2.1. Bio-Oil Yield:

Bio-oil production is predominantly influenced by the pyrolysis temperature. The highest bio-oil yield was at 300C, and lowest bio-oil yield at 500C for the three biomasses tested. This contributed to the release of volatile matter into the gas at high temperature.

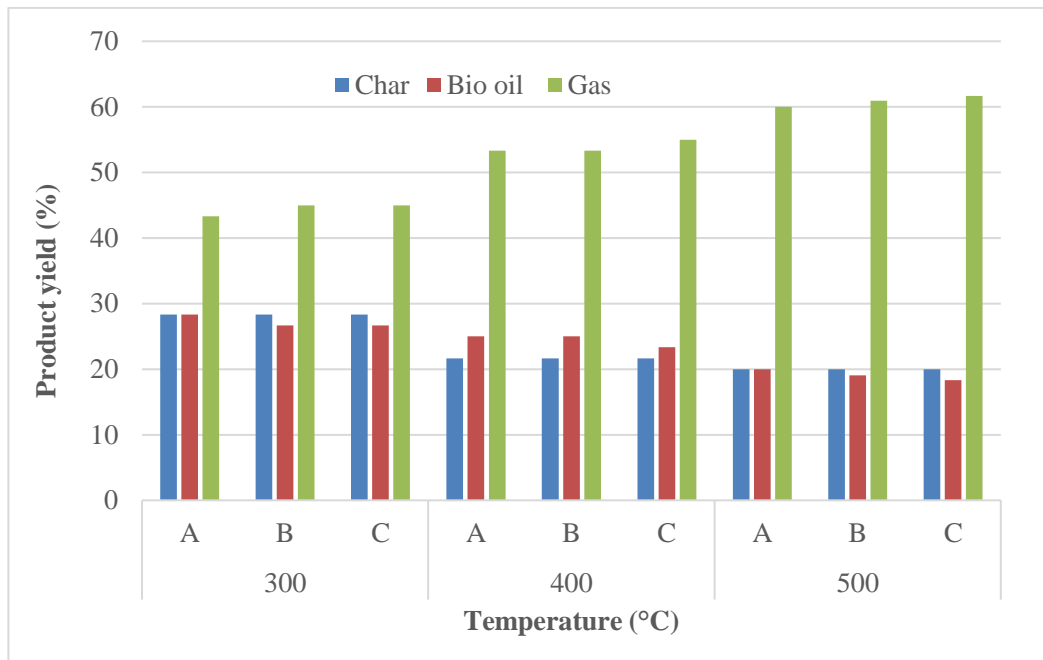


Figure 17. Product yield from spruce pyrolysis

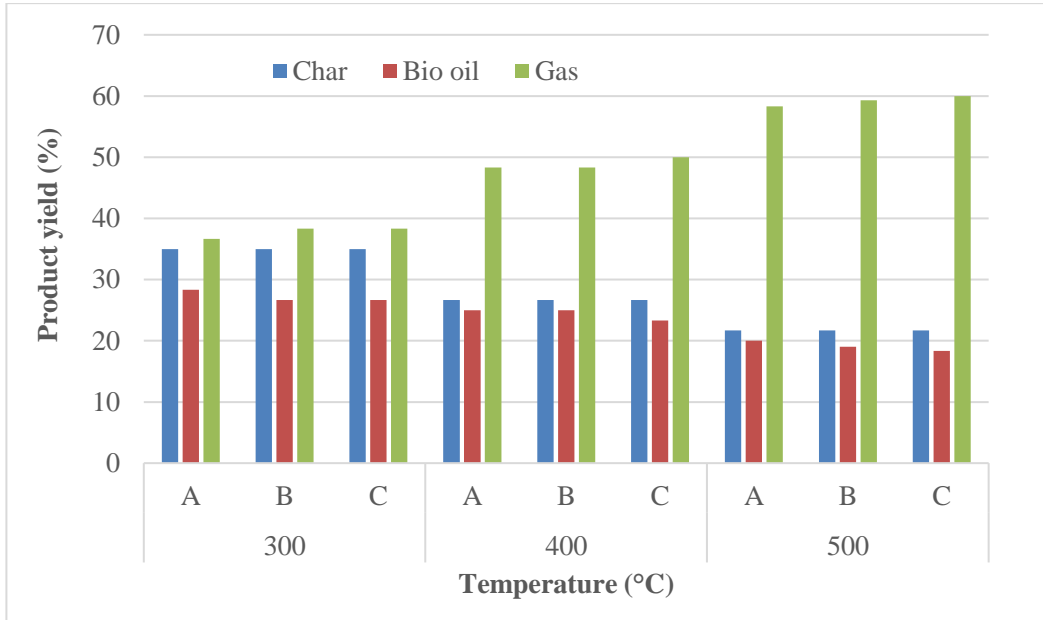


Figure 18. Product yield from pine pyrolysis

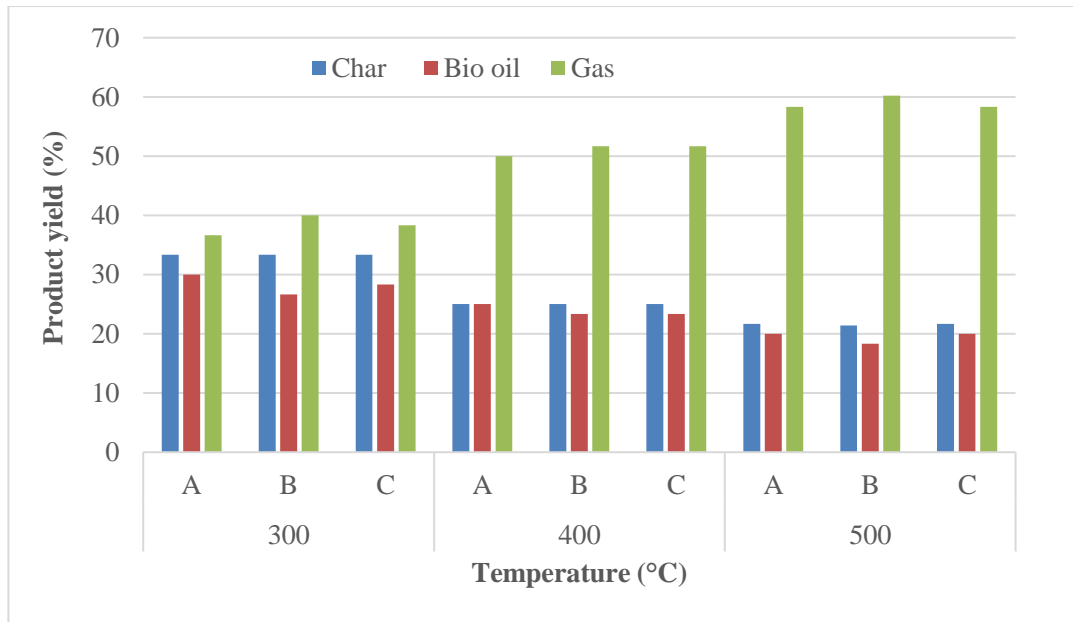


Figure 19. Product yield from larch pyrolysis

6.2. Determination of kinetic parameters of pyrolysis

Kinetic study for kinetics' parameters determination is a key step to understand the decomposition rate of the biomass into the new products. These parameters – energy of activation, pre-exponential factor and conversion factor, are necessary for the process conditions study, the modelling of the reactor and a potential CFD modelling.

For kinetics parameter determination, four heating rates were selected. Approx. 10 ± 1 mg biomass was heated from 30-600C at 5, 10, 20 and 40 C/min. This procedure follows ASTM E1641 for the determination of kinetics parameters including Arrhenius activation energy, E (J/mol) and pre-exponential factor, A (min^{-1}) based on the assumption that the decomposition obeys first-order kinetics using Flynn/Wall/Ozawa (FWO) is conventional method. N_2 was set at 40 mL/min throughout the temperature program.

$$\frac{\partial \alpha}{\partial t} = A (1 - \alpha) \exp \left[\frac{-E}{RT} \right] \quad (3)$$

Where ' α ' is the conversion factor, ' A ' the pre-exponential factor (min^{-1}), ' β ' the heating rate (K/min), ' E ' the activation energy (J/mol), ' R ' the gas constant (J/mol·K) and ' T ' the absolute temperature (K).

To obtain the parameter of the Arrhenius expression, equations (4) and (5) were employed to determine activation energy and the pre-exponential factor, respectively.

$$E = \left(\frac{R}{b} \right) \frac{\Delta \log \beta}{\Delta 1/T} \quad (4)$$

$$A = \left(\frac{-\beta \cdot R}{E} \right) (\ln [1 - \alpha]) 10^a \quad (5)$$

The parameters represented in the equation (4) 'E', 'R', ' β ' and 'T' are the same as in the equation (5), 'b' is the logarithm of the approximation derivate or Doyle approximation (K/min) and 'a' is the logarithm of the approximation integral.

To carry out the study of the kinetic parameters of the pyrolysis, an initial mass is taken in the region of equilibrium temperature where no mass loss was recorded, while final mass is taken once the plateau has been reached at the end of weight loss. Conversion factor (α) is chosen at 5, 10, 15, and 20% of total mass loss. This is to ensure low variation in the calculated activation energy (E) during the initial stage of biomass decomposition. In Table 7, the Arrhenius results obtained as a function of the conversion of the biomass for each type of wood are shown.

Table 7. Activation energy and pre-exponential factor during thermal decomposition of different biomass

Biomass	Spruce	Pine	Larch			
Conversion (α)	E (kJ/mol)	In A (min $^{-1}$)	E (kJ/mol)	In A (min $^{-1}$)	E (kJ/mol)	In A (min $^{-1}$)
0.05	165.64	14.94	161.57	14.95	159.08	14.96
0.10	162.03	14.35	165.54	14.79	157.74	14.36
0.15	164.13	14.07	166.67	14.52	159.92	14.08
0.20	163.19	14.21	167.5	14.66	160.23	13.76

In Figure 20, Figure 22 and Figure 24, the mass loss curves during biomass decomposition at different heating rates are presented, for the spruce, pine and larch wood. Figure 21, Figure 23 and Figure 25 show the Arrhenius plot at constant conversion during biomass decomposition for the three types of wood studied.

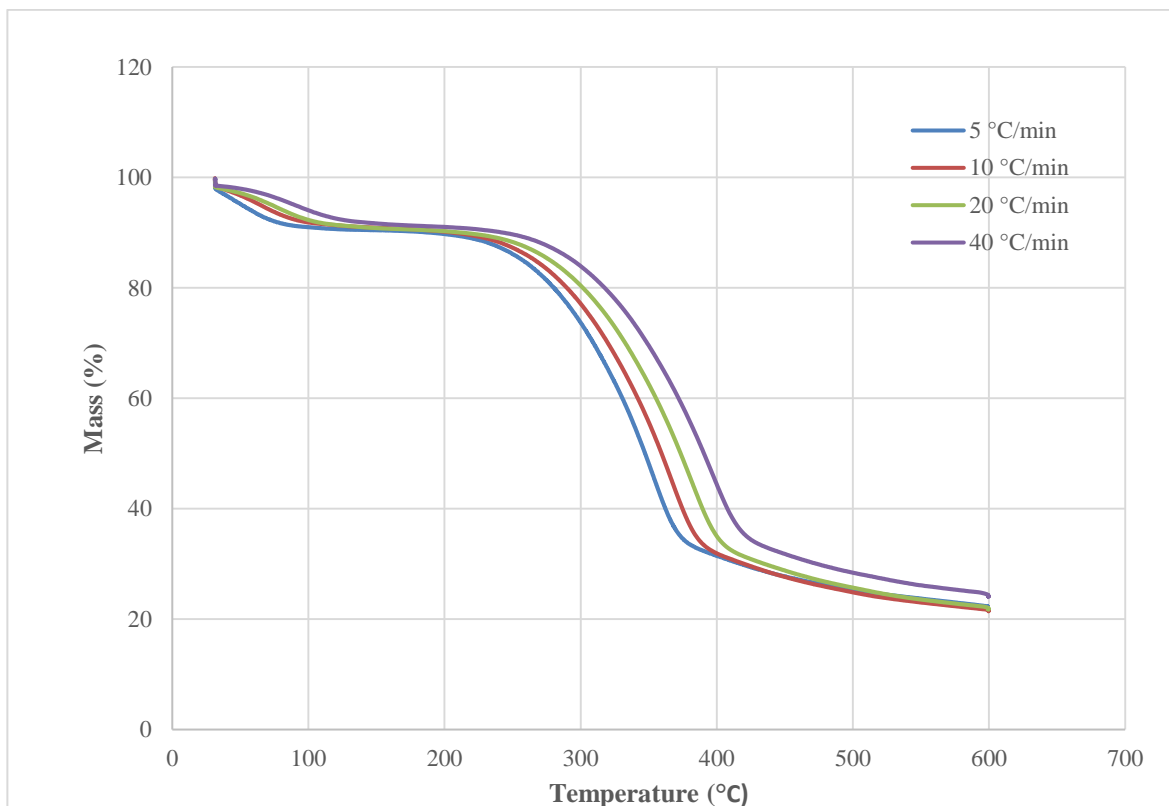


Figure 20. Mass loss curves during spruce decomposition at different heating rates

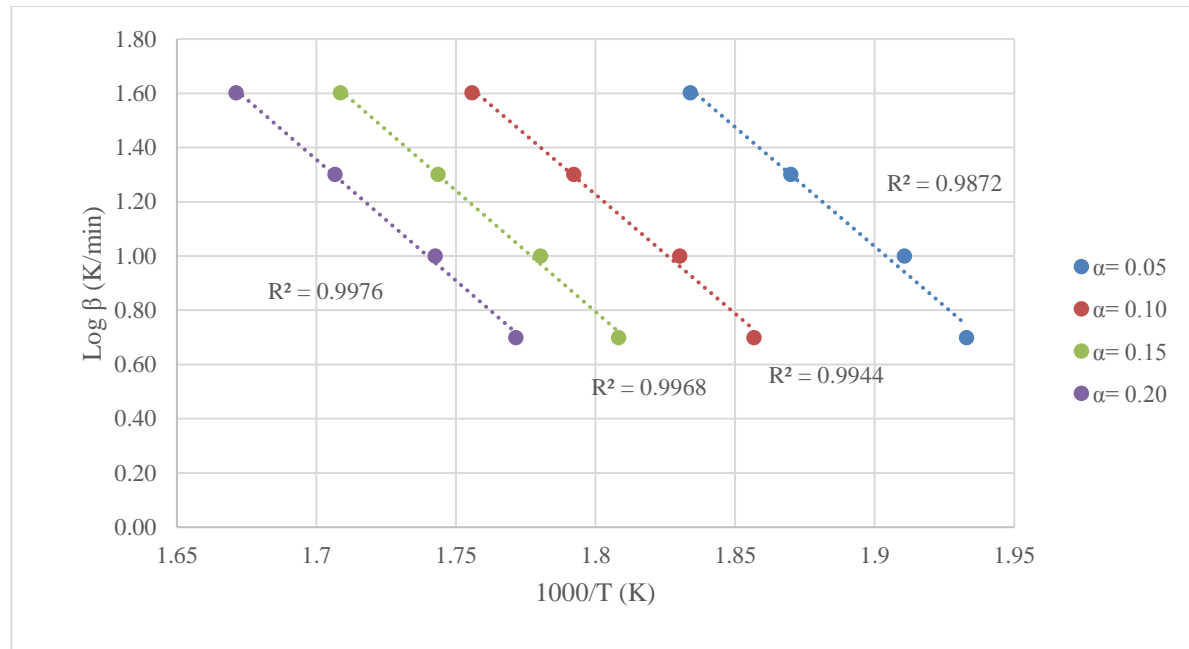


Figure 21. Arrhenius plot at constant conversion during spruce decomposition

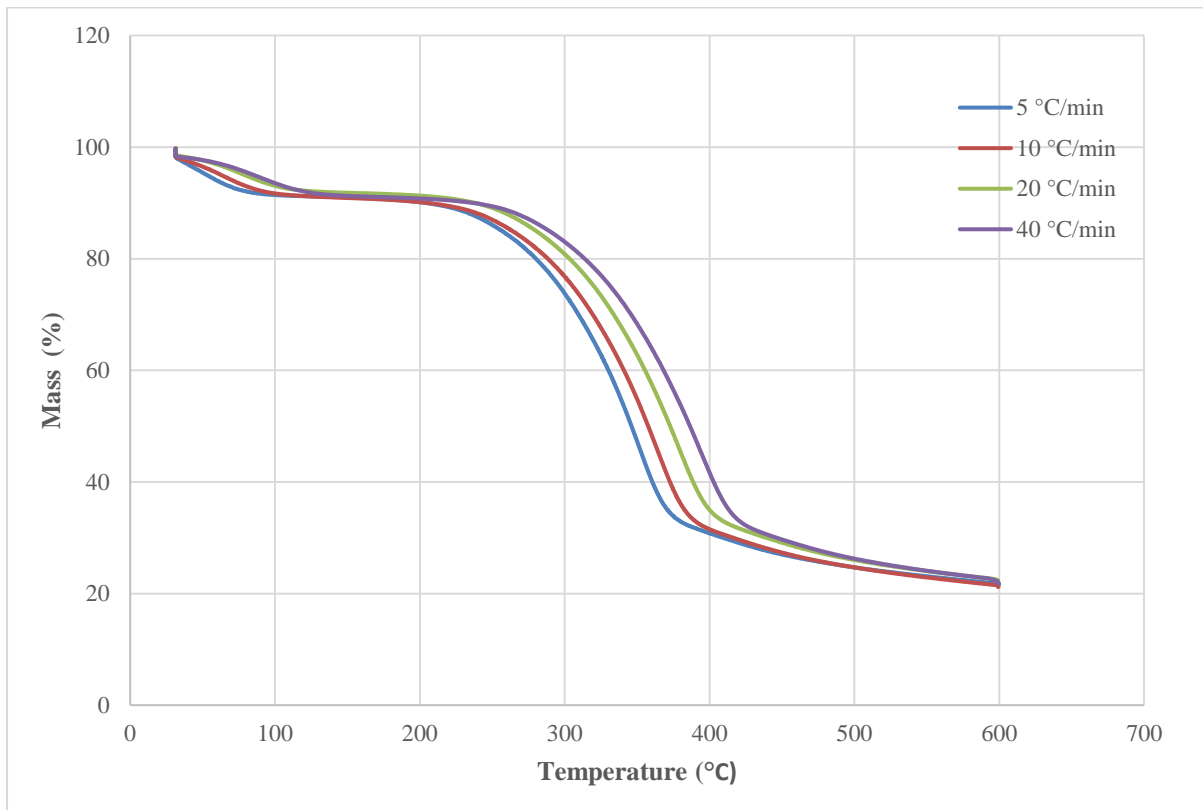


Figure 22. Mass loss curves during pine decomposition at different heating rates

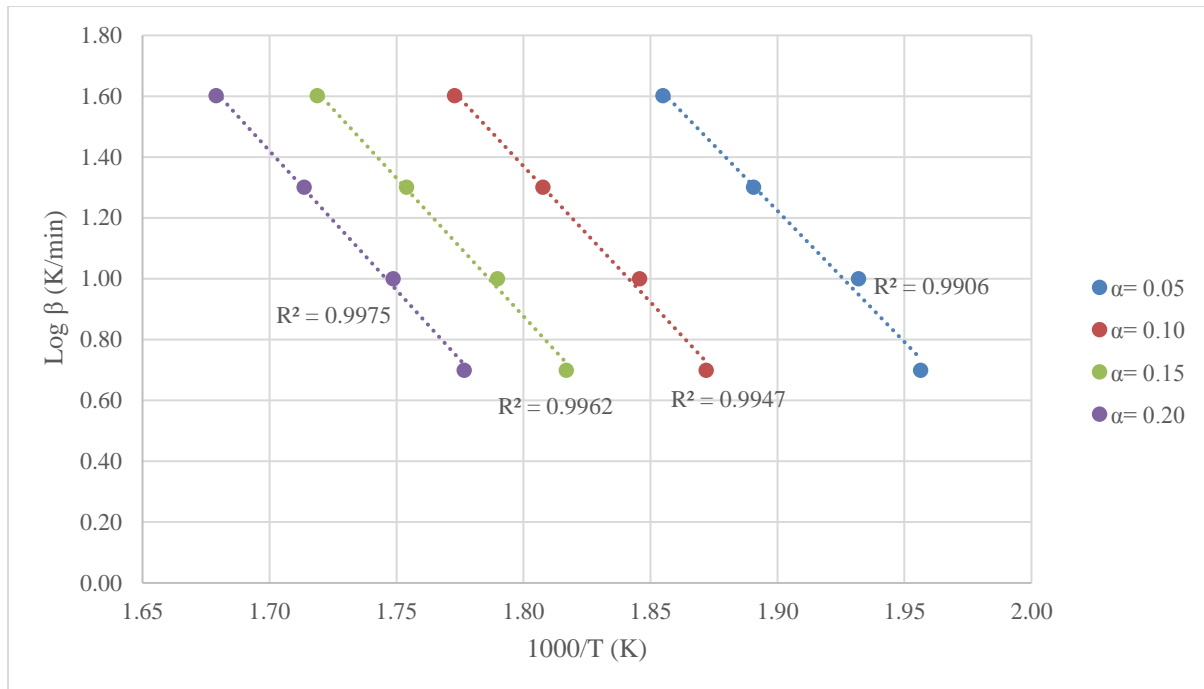


Figure 23. Arrhenius plot at constant conversion during decomposition of pine biomass

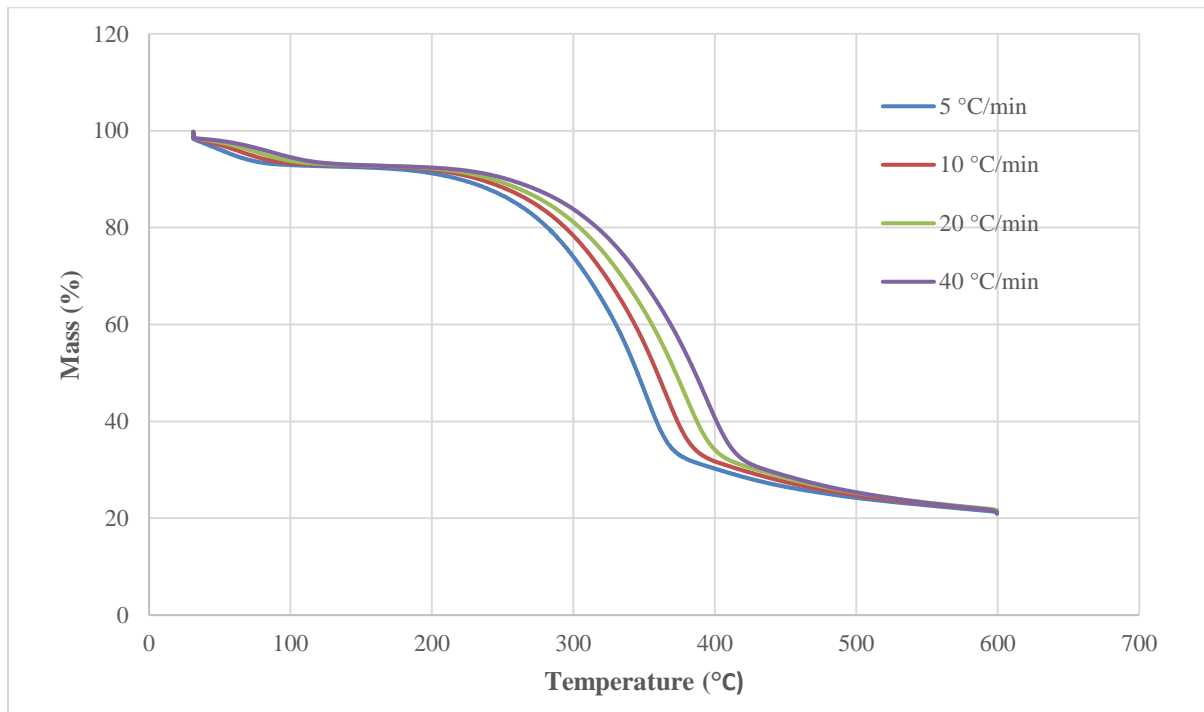


Figure 24. Mass loss curves during larch decomposition at different heating rates

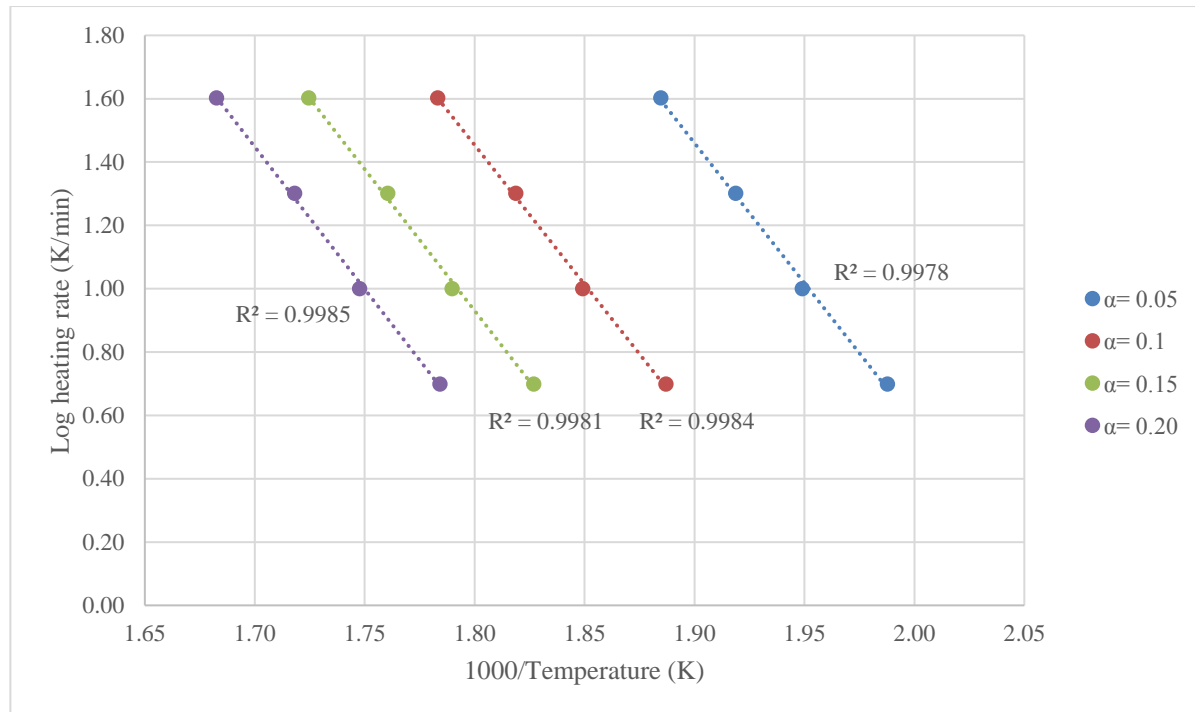


Figure 25. Arrhenius plot at constant conversion during decomposition of larch biomass

6.3. Characterisation of the biomass and bio-oil

6.3.1. Biomass

Analysis and characterization of the different biomasses is an essential step to analyse, assess and determine the behaviour of the biomass, and then the subsequent products, to link properties to the product after conversion (biofuels), to conclude the reaction conditions, and to study the value of the biomass.

6.3.1.1. Proximate analysis

To have a complete characterisation of the biomass employed in the pyrolysis, an analysis to determine the biomass composition in terms of moisture, volatiles, fixed carbon and ashes as percentage of total weight (wt.%) were conducted. The instrument employed was the thermogravimetric analyser Perkin Elmer TGA 4000. These analyses are very important to link the further properties of the bio-oil with the kind of biomass employed in the pyrolysis as well as to model the feedstock in commercial software.

The proximate analysis is the simplest analysis and it is the most commonly used for biomass analysis. The higher the volatile matter, the higher the biomass conversion in comparison to biomasses with higher fixed carbon content. It is also linked to the future production of bio-oil, which increases according to the volatile matter as well as the biochar is reported higher for biomasses with high fixed carbon.

Around 13 ± 1 mg of powdered biomass (size $< 200 \mu\text{m}$) was used, with N_2 and O_2 as purge gas at 40 and 20 mL/min, respectively. The instrument was programmed to heat the samples from 30-600C under N_2 at 20 C/min to release moisture and volatiles. The temperature was then ramped from 600 to 650C at 25C/min under O_2 to ensure

complete oxidation of the remaining fixed carbon. Ash content was computed by difference (6):

$$\text{Ash} = M - (\sum \text{moisture} + \text{volatiles} + \text{fixed carbon}) \quad (6)$$

The proximate analyses of spruce, pine, and larch biomass are presented in Table 8. Small mass loses (< 8 wt.%) occur when the biomass was heated from 30 to 100C, which corresponds to the removal of loosely-bound water. Within this context, spruce contains the highest moisture at around 7.9 wt.%, followed by pine and larch biomass. No further mass loss is recorded at this stage until the start of decomposition temperature, which occurs at around 180C for larch biomass. Meanwhile, pine and spruce decomposition starts at around 200 and 220C, respectively. Thermal decomposition at this stage corresponds to the amount of volatiles within biomass. In general, woody biomass has volatiles content at around 70 wt.%, which made it ideal for pyrolysis process. For instance, larch wood has the highest volatile matter at around 71.3 wt.%, followed closely by pine wood and spruce wood. Removal of volatiles leaves behind fixed carbon, which is oxidised upon contact with oxygen. Pine wood recorded the highest amount of fixed carbon at 23.5 wt.%, followed by larch (22.7 wt.%) and spruce wood (22 wt.%). Unlike agricultural residues, woody biomass in this study has low amount of ash, below 2 wt. %.

Table 8. Proximate analysis of biomass (wt. %)

Biomass	Spruce	Pine	Larch
Moisture, %	7.85 ± 1.15	5.92 ± 0.62	5.15 ± 0.53
Volatile, %	68.34 ± 0.87	69.73 ± 0.16	71.25 ± 0.89
Fixed carbon, %	22.01 ± 0.25	23.51 ± 0.20	22.74 ± 0.27
Ash, %	1.80 ± 0.28	0.83 ± 0.58	0.86 ± 0.26

According to Table 8, larch contains the highest volatiles content and spruce the least. It means that, theoretically, spruce will be able to produce a higher amount of bio-oil whilst pine would lead to the highest amount of bio-char.

Figure 26 - Figure 29 present the rate of decomposition of all three biomass samples (derivative weight loss rate – %/min), which is the proximate analysis of spruce, pine and larch biomass, respectively.

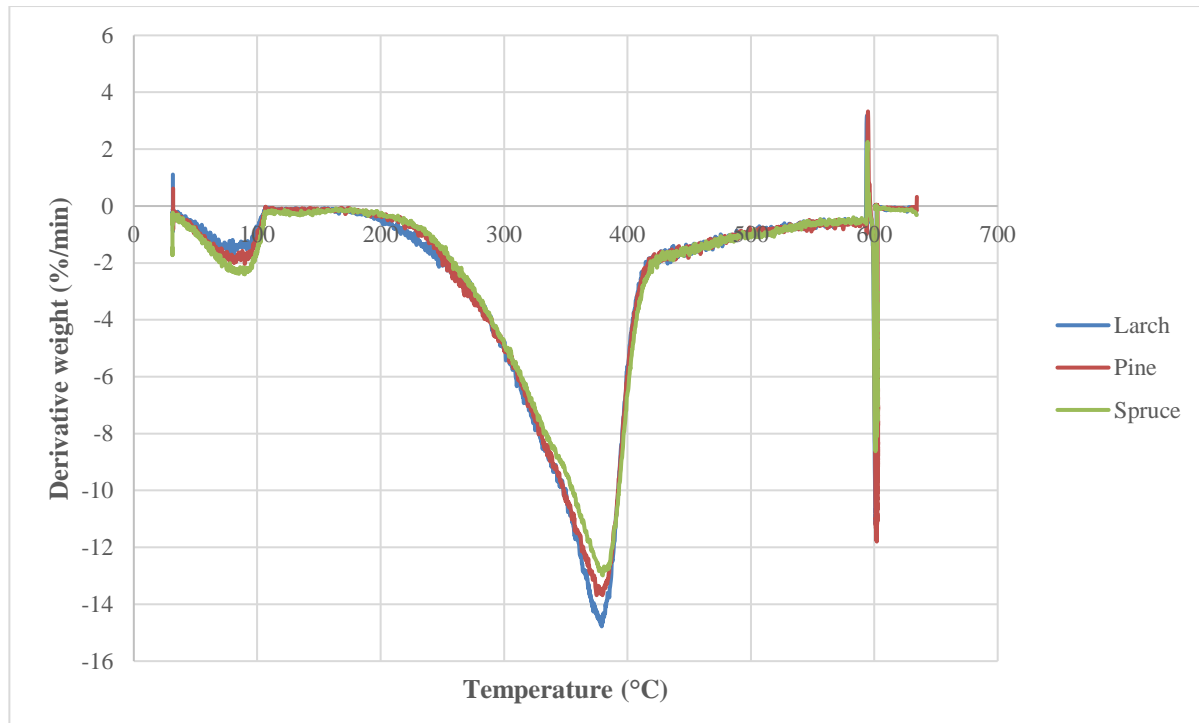


Figure 26. Rate of decomposition of all biomass samples in the proximate analysis

The first peak on the rate of decomposition of the biomass in the proximate analysis contributes to the release of the moisture; the second peak is mainly due to the release of volatile matter. Figure 26 showed that all biomasses have released most of volatiles before the temperature of 400C. Larch has the highest volatile matter.

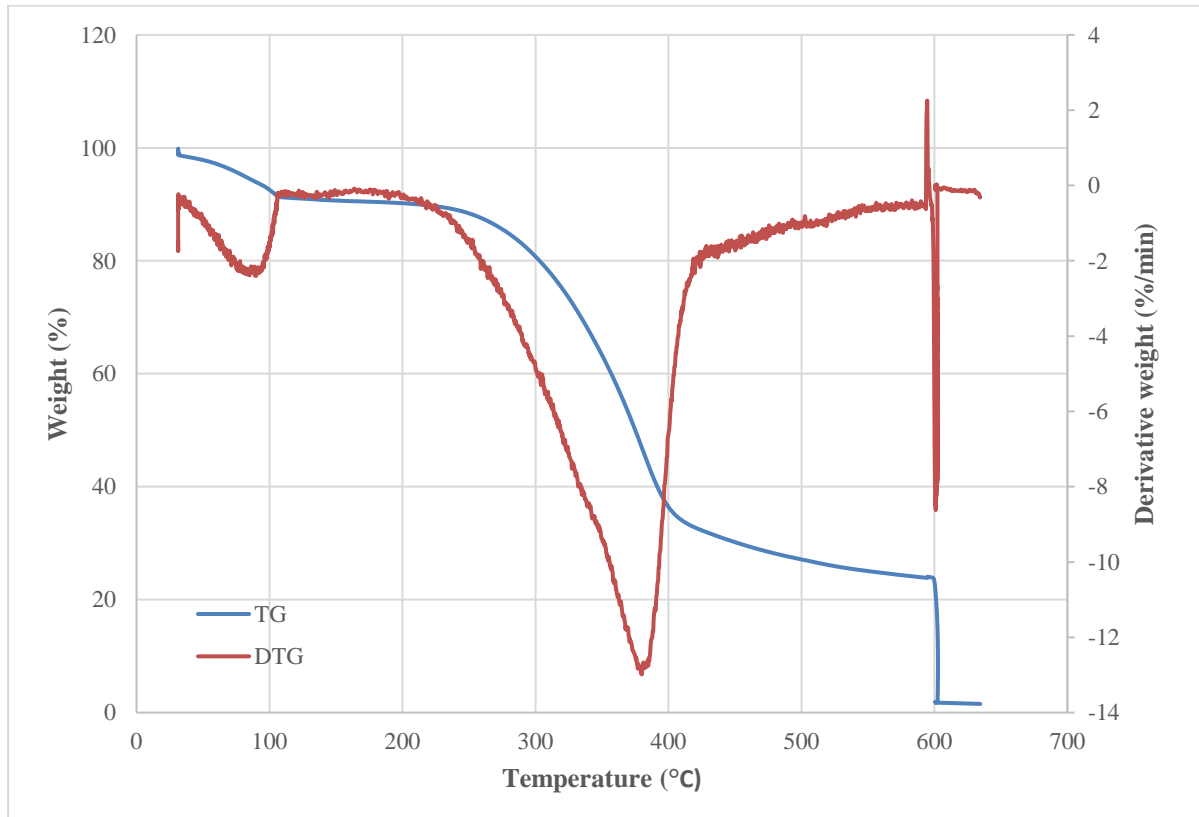


Figure 27. Proximate analysis of spruce biomass

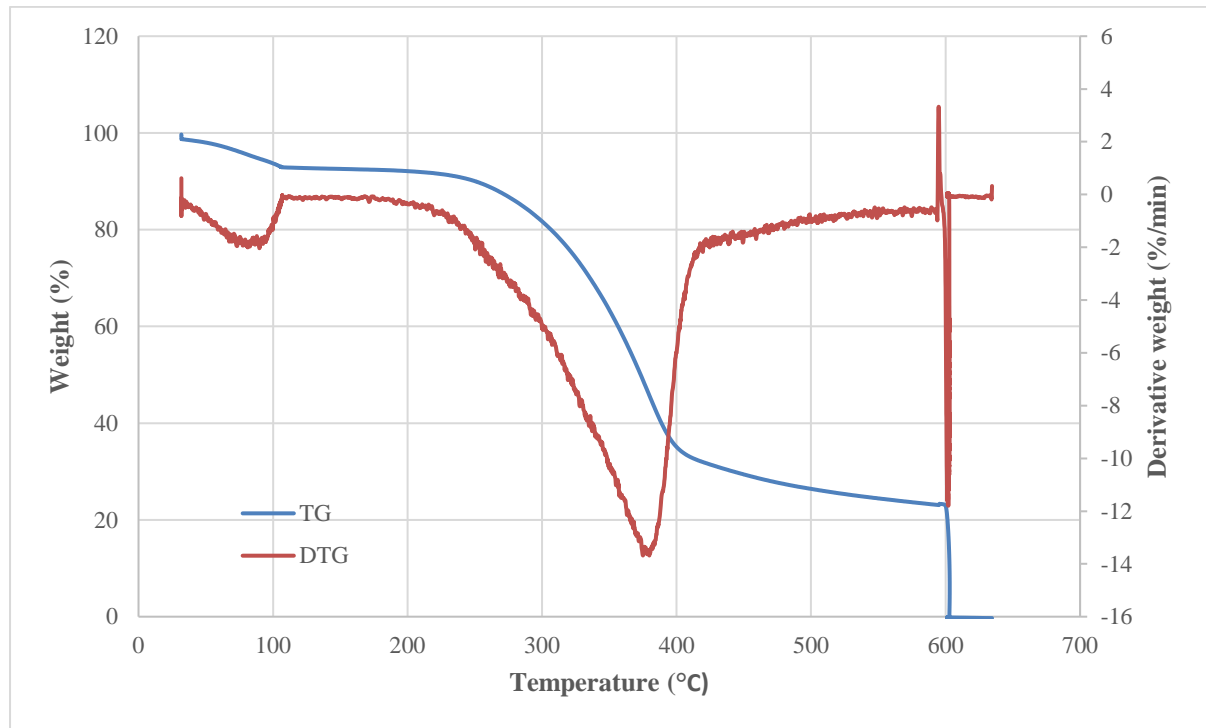


Figure 28. Proximate analysis of pine biomass

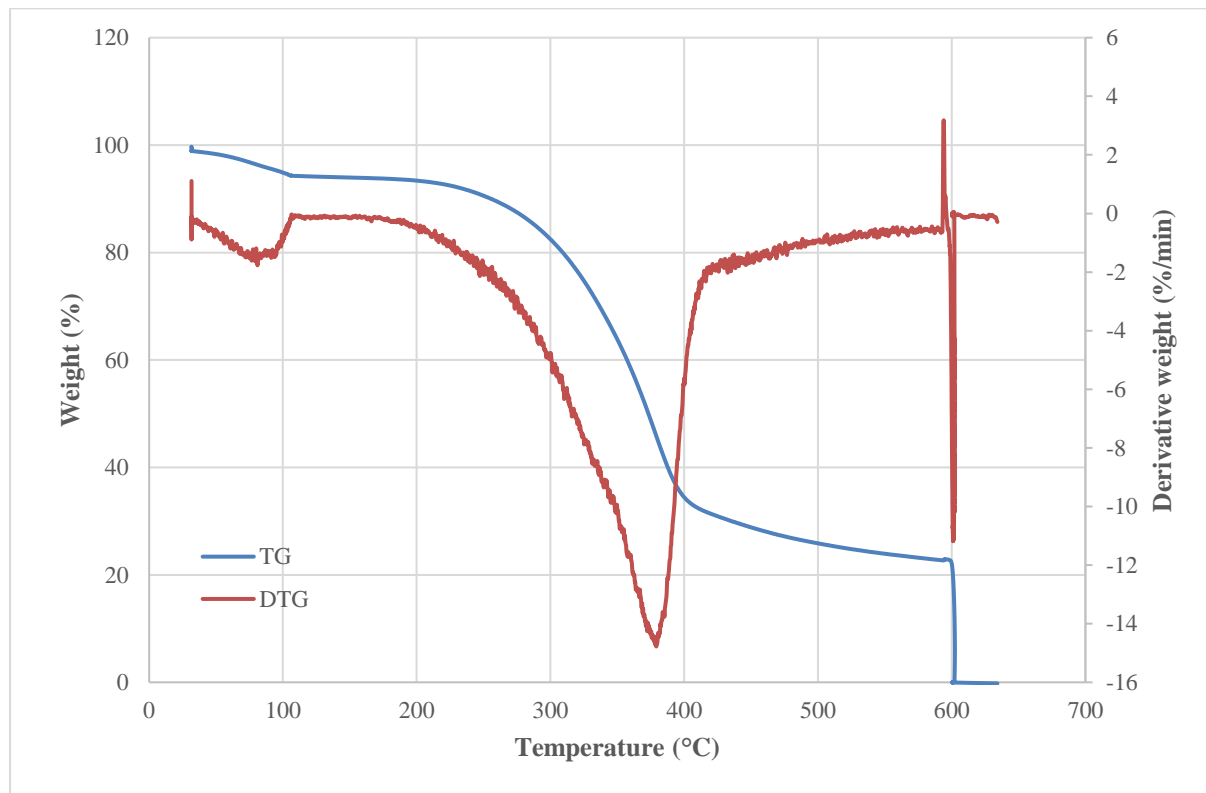


Figure 29. Proximate analysis of larch biomass

6.3.1.2. Ultimate analysis

Ultimate analysis of the biomass (also known as elemental analysis) was also carried out for the three samples. This analysis is more thorough than the proximate analysis and provides information about the composition of the feedstock such as the carbon, hydrogen, nitrogen, sulphur, and oxygen (by difference) content in the sample. Each element is determined by means of chemical analysis. The ultimate analysis was performed using Thermo Scientific Flash 2000 organic elemental analyser. The analysis conducted according to ASTM D3176. Results are shown in Table 9.

Table 9. Elemental analysis of the biomass

Properties	Spruce	Pine	Larch
C	46.69 ± 0.36	47.11 ± 0.74	46.99 ± 0.01
H	6.26 ± 0.11	6.22 ± 0.09	6.22 ± 0.06
N	0.29 ± 0.01	0.33 ± 0.01	0.32 ± 0.02
S	0.14 ± 0.01	0.05 ± 0.05	0.14 ± 0.03
O*	46.62	45.55	46.33
H/C	1.61	1.58	1.59
O/C	0.75	0.73	0.74
Empirical formula	CH _{1.61} O _{0.75}	CH _{1.58} O _{0.73}	CH _{1.59} O _{0.74}
Calorific value	19.15 ± 0.05	19.22 ± 0.05	19.20 ± 0.05

6.3.2. Bio-oil

Bio-oil is the denomination of the liquid phase obtained from the pyrolysis process. It is characterized as dark flowing liquid produced after the quenching of the gaseous products. Secondary reactions during the pyrolysis process produce water, so bio-oil represents two liquid phases, an organic phase and an aqueous phase. The organic one is the main target of this AgroCycle activity as it can be used directly or after an upgrading stage as a potential biofuel. Aqueous phase cannot be used directly as a biofuel, it needs to be upgraded due to the presence of components such as organic acids and phenols [110].

Pyrolysis bio-oils were characterised for pH, elemental analysis, water content, Gas Chromatography/ Mass Spectrometry (GC/MS), and specific heat capacity. From yield computation, it can be seen that particle size exerts little influence on product yield compared to temperature. For this reason, bio-oil characterisation was conducted on samples obtained from particle size A to determine the influence of temperature on bio-oil properties. Bio-oils obtained from pyrolysis of biomass (particle size A) are chosen for analysis.

6.3.2.1. pH of bio-oil

Acidity is an important parameter to determine. The presence of acid components, such as phenols or organic acids, characterises bio-oil as an acid and corrosive mixture which may affect the bio-oil handling the equipment used.

To determinate the pH of the bio-oil, the pH tester HI 91803 (Hanna Instrument) was first calibrated with two points calibration using buffer pH 7 and pH 4 buffer solutions at 25C. The pH values of the bio-oil samples are presented in Table 10.

Table 10. pH of pyrolysis bio-oil

Temperature	300C			400C			500C		
	A	B	C	A	B	C	A	B	C
Spruce	3.23	3.18	3.11	3.26	3.22	3.37	3.20	3.51	3.40
Pine	2.27	3.01	2.70	3.18	2.46	2.82	3.03	3.47	3.49
Larch	2.26	3.19	3.22	3.08	3.27	2.91	2.54	3.55	3.08

It is shown that the pH of the bio-oil obtained from pine has the trend to be lower than the bio-oil obtained from the other types of wood. In general, the pH of the bio-oil is mainly acid, and this acidity decrease with the increment of the pyrolysis temperature. The particle size exerts some influence on the pH as observed within the same temperature, e.g. in larch the pH varies at the same temperature conditions according to the particle size, showing lower pH as per the particle size decreases.

Usually the pH of the bio-oil is reported between 2-3 due to the presence of organic acids (carboxylic).

6.3.2.2. Elementary analysis of bio-oil

For the elemental analysis the Vario MICRO cube (Elementar) for CHN determination was employed. Around 2-4 mg oil sample was placed into tin capsules with the addition of Chromosorb W 30-60 Mesh as absorbent for nitrogen determination. The sample was oxidised at 900°C, where combustion gas flow through Gas Chromatography - Temperature Programmed Desorption (GC-TPD) column to determine the composition of organic element as a percentage of total weight (wt.%). The remaining composition such as oxygen (O) and sulphur (S) was computed by difference (7). The analysis was run in triplicate to ensure consistency. The procedure follows ASTM D3176, which is the Standard Practice for Ultimate Analysis of Coal and Coke.

$$O + S = 100 - \sum(C + H + N) \quad (7)$$

6.3.2.3. Density of bio-oil

The density of pyrolysis bio-oil is determined using 5 mL Gay Lussac density bottle. It comes with a close-fitting ground glass stopper with a capillary hole, which allows the release of spare liquid and air bubble. This gives a precise weight of liquid at known volume. Initially, a clean and dry pycnometer is filled with liquid of well-known density, in this case distilled water at 25C, $\rho = 0.99705 \text{ g/cm}^3$, and the weight is recorded. The procedure is repeated with liquid of unknown density (bio-oil). This yields a relation that provides the density of bio-oil.

$$\rho_L = \frac{m_L}{m_{H_2O}} \times \rho_{H_2O} \quad (8)$$

The density of the pyrolysis bio-oil samples measured at 25C are presented in Table 11.

Density of pyrolysis bio-oil is about 1.2 kg/dm³ at 25C. Density of bio-oil decreases with an increase in reaction temperature. For example, the density of pine bio-oil

decreases from 1.214 kg/dm³ to 1.1.95 kg/dm³ as the reaction temperature is increased from 300 to 500C. Similar results are observed in the bio-oil obtained from spruce and larch decomposition.

Table 11. Density of pyrolysis bio-oil (kg/dm³) @25 °C

Temperature	300C	400C	500C
Spruce	1.250	1.228	1.198
Pine	1.214	1.206	1.195
Larch	1.227	1.204	1.205

In Figure 30, the densities of the bio-oils obtained in the pyrolysis of the different types of wood are represented as a function of the pyrolysis temperature. It is clear to see that when the temperature of the thermal treatment increases, the density of the liquid product obtained is lower.

Literature research reports values for bio-oil density at temperatures between 15-25C within a range of 1.10-1.30 kg/dm³. The density of the different bio-oils is reported within the range at 300, 400 and 500C for the three biomasses analysed.

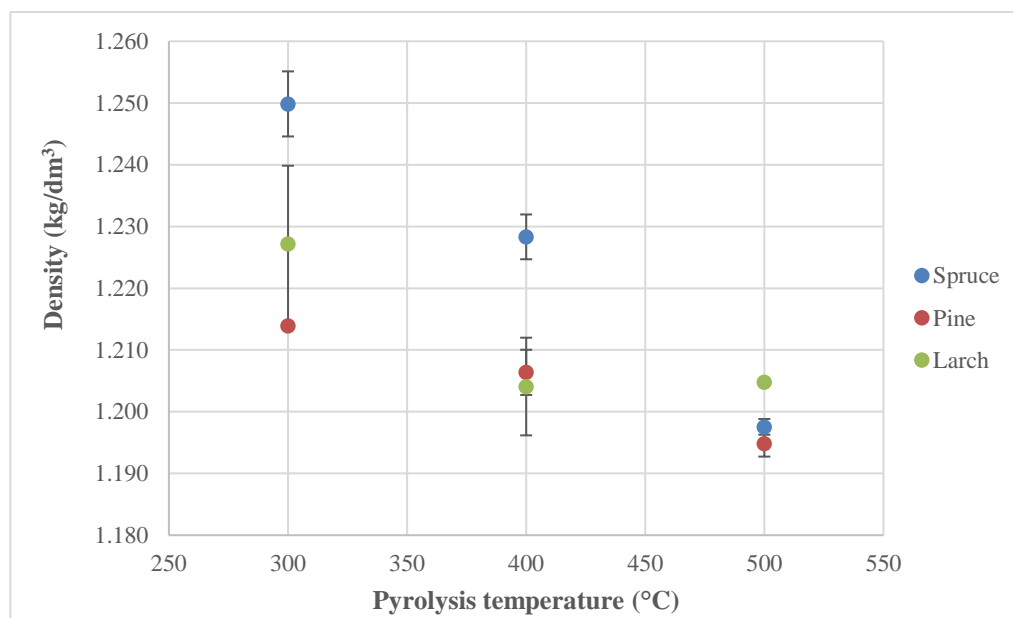


Figure 30. Density of pyrolysis bio-oil

6.3.2.4. Viscosity of bio-oil

Viscosity is strongly dependent of the selected feedstock, the pyrolysis technology, the pre-treatment of the biomass and the conditions applied, among others. It is reported between 15-35 cSt at 40C, but the density could be altered as per the storage time due to secondary degradation reactions among bio-oil components [111].

Meanwhile, the viscosity of bio-oil was measured using a calibrated routine Cannon-Fenske viscometer size 150 (C = 0.034). The viscometer was submerged in a temperature-controlled water bath. Around 8 mL oil was pipetted into the access tube. Suction is applied to draw the bio-oil above meniscus level 'C' and onto an overfill reservoir. The liquid is retained at this position for 10 minutes to reach equilibrium with bath temperature. The pressure was relieved at this point, allowing the oil to flow freely

under gravity. The efflux time between mark 'C' and 'E' is recorded to the nearest ± 0.01 s using stopwatch. The kinematic viscosity (v) is calculated by multiplying the efflux time (t) with viscometer constant, C , with the equation (9). The viscosity of bio-oil is determined over temperature range of 30-50°C. The procedure is conducted following ASTM D445, which is the Standard Test Method for Transparent and Opaque Liquids.

$$v \left(\frac{mm^2}{s} \right) = C \left(\frac{mm^2}{s^2} \right) \cdot t (s) \quad (9)$$

Table 12 shows the kinematic viscosity of pyrolysis bio-oil as a function of temperature. The viscosity ranges between 7-9 mm²/s across all samples. Larch bio-oil recorded a viscosity of approx. 9.3 cSt at 30C, which decreases to 8.4 cSt at 50C. The effect of temperature on viscosity of pyrolysis bio-oil is shown in Figure 31.

Table 12. Viscosity of pyrolysis bio-oil (mm²/s)

Temperature	30C	40C	50C
Spruce @ 300C	8.433	8.174	7.975
Spruce @ 400C	8.435	8.148	7.974
Spruce @ 500C	8.081	7.885	7.770
Pine @ 300C	8.181	8.002	7.834
Pine @ 400C	8.119	7.947	7.805
Pine @ 500C	8.102	7.930	7.784
Larch @ 300C	9.219	8.742	8.367
Larch @ 400C	8.513	8.307	8.068
Larch @ 500C	8.101	7.895	7.784

The density of the analysed bio-oils is reported below the literature values (circa half of the minimum value of the range).

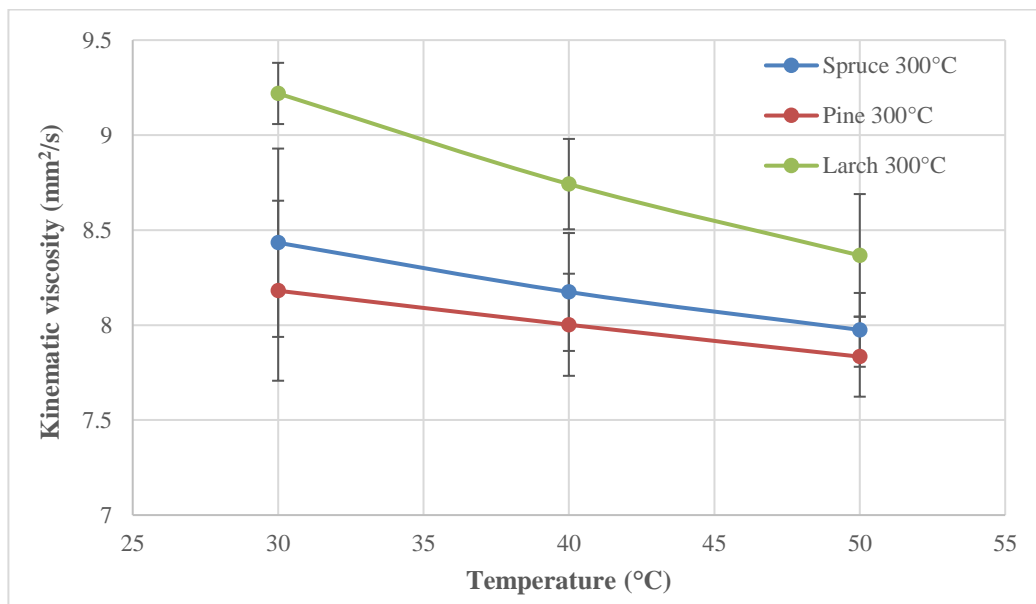


Figure 31. Effect of temperature on viscosity of pyrolysis bio-oil

6.3.2.5. Moisture (water) content of bio-oil

Bio-oil moisture (water content) is reported as the most abundant single compound. It is usually reported between 15-30% in literature [112], although depending on the biomass composition and source, values up to 40-60 % can be achieved as the Su et al. (2010) work shows (based on sawdust furniture pyrolysis) [113]. The moisture content increases according to the storage time for the bio-oil, due to secondary reactions of etherification and esterification between bio-oil components.

Bio-oil was sent to Quality Context Ltd for the determination of moisture content in bio-oil using volumetric Karl-Fischer (KF) titration. Methanol and Karl Fischer Aqualine Complete 5 are used as solvent and working reagent, respectively. It works by measuring the voltage signal corresponds to the reaction between water and iodine until it reaches potentiometric endpoint. This signal corresponds to water content in the solution (%). The sample is shaken to ensure homogenisation prior to analysis. An aliquot (1 mL) is taken for KF titration. The water content in pyrolysis bio-oil as a function of pyrolysis temperature are presented in Figure 32. The density of the pyrolysis oil as a function of water content was analysed in Figure 33.

As shown in Figure 32, in general, bio-oil has moisture content of more than 20%, with an increasing trend with pyrolysis temperature. For example, water content in spruce bio-oil increases from 20.58 % to 59.55 % when the pyrolysis temperature is raised from 300C to 500C. Intense thermal decomposition at around 200C causes chemical reactions and phase changes that release volatiles in the form of water-soluble compounds upon condensation.

High water content could affect bio-oil stability by inducing phase separation. Density is a function of water content, where its value decreases with an increase in water content.

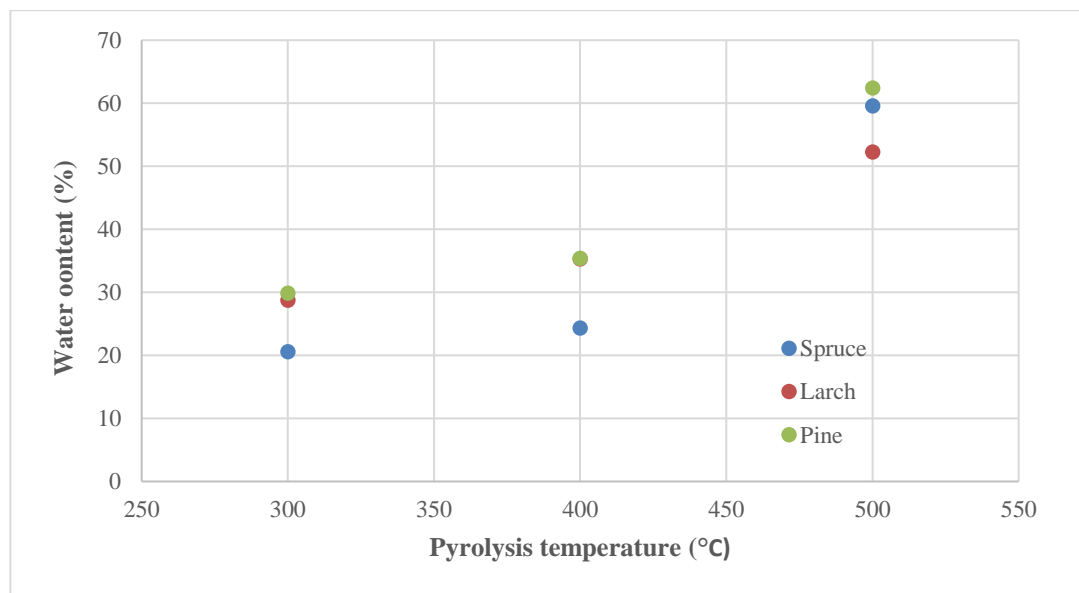


Figure 32. Water content in pyrolysis bio-oil

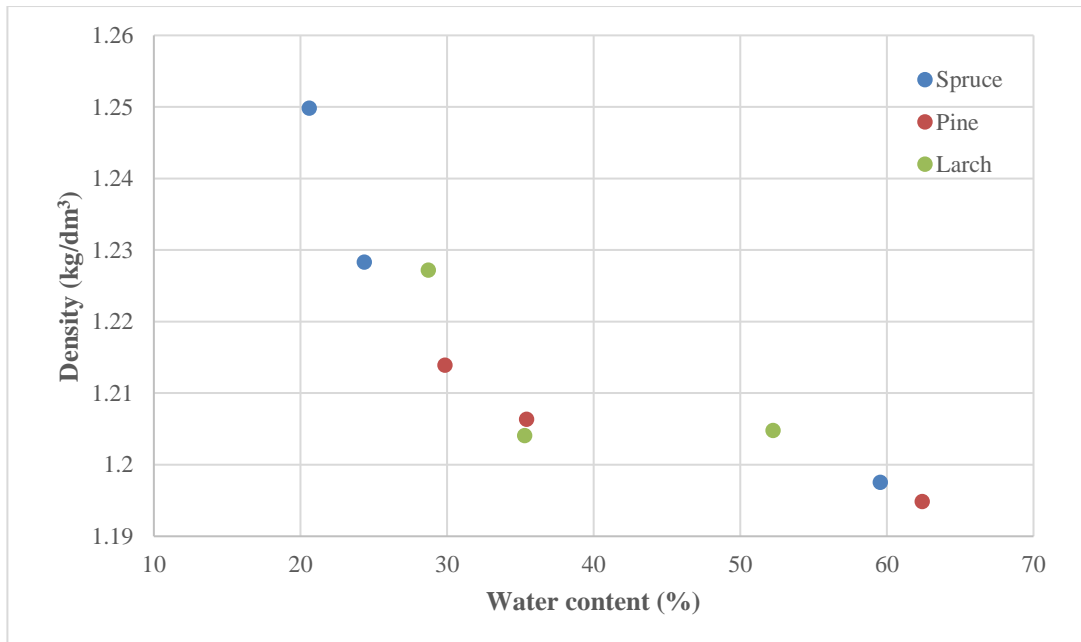


Figure 33. Density of pyrolysis oil as a function of water content

6.3.2.6. Specific heat capacity of bio-oil

Specific heat capacity of bio-oil is determined using Perkin Elmer Pyris 1 Differential Scanning Calorimeter (DSC), following ASTM E1269. Initially, a steady-state isothermal baseline is determined using an empty specimen holder (aluminium), followed by standard material, *i.e.*: synthetic sapphire disk. The test specimen is held at an initial temperature for 4 minutes, before being heated from 25 to 100C at a rate of 20 °C/min. N₂ flow was kept at 50 mL/min throughout the experiment. The procedure is repeated for unknown specimens. The measured output signal, ϕ_m (mW), m=measured is translated as the heat flow required to increase the temperature of the specimen. A baseline correction is performed to eliminate the heat transfer to specimen holder, thus giving the true heat flow of unknown specimen during DSC analysis. The specific heat capacity (C_p) is determined from the following:

$$Q_r = Q_{true} = K_Q \cdot \int \phi_m - \phi_{bl}$$

$$Q = m \cdot C_p \cdot \Delta T$$

The specific heat capacity over the temperature 25-100C was measured for all bio-oil samples and the three biomasses at pyrolysis temperature 300, 400 and 500C. The heat flow measurements of the three biomasses are presented from Figure 34 to Figure 38. The Specific heat capacity varying with temperature is presented in Figure 39 for Spruce, in Figure 40 for Pine and in Figure 41 for Larch. Finally, Table 13 presents the average specific heat capacity of pyrolysis bio-oil (J/g·K) for temperature range 25-100C.

Table 13. The average specific heat capacity of pyrolysis bio-oil (J/g·K) for temperature range 25-100C

Temperature (C)	300	400	500
Spruce	1,603.52	1,528.01	1,724.02
Pine	1,883.59	1,943.27	2,084.24
Larch	1,190.67	1,291.66	1,485.25

Figure 34. Heat flux of an empty specimen holder

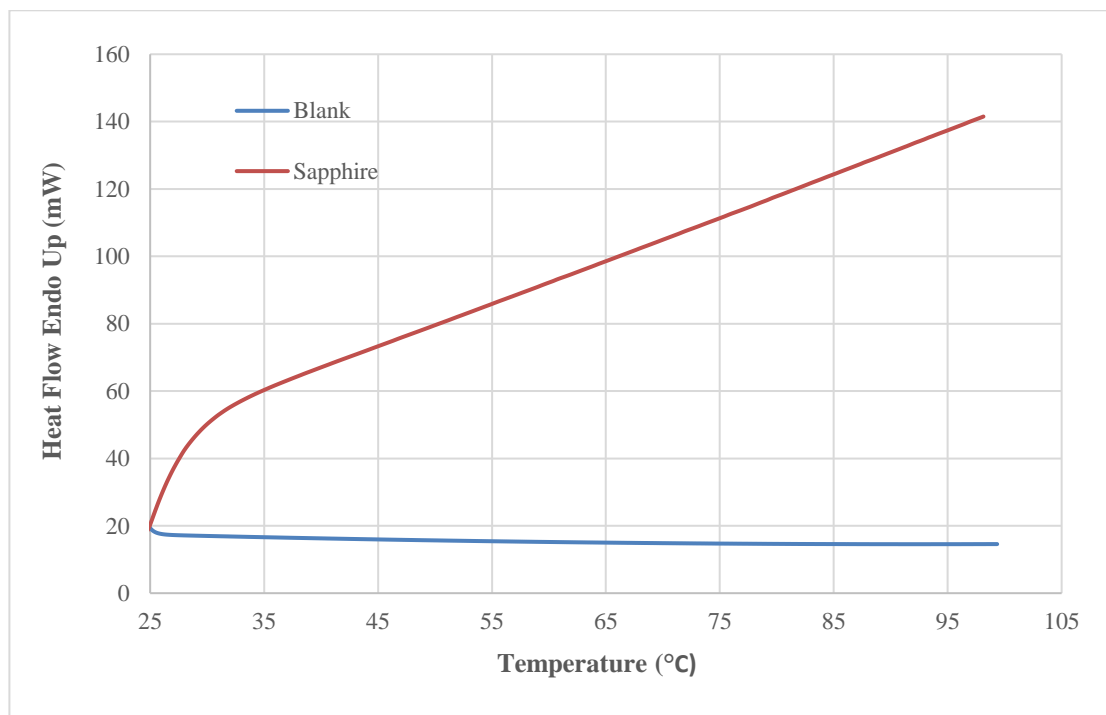
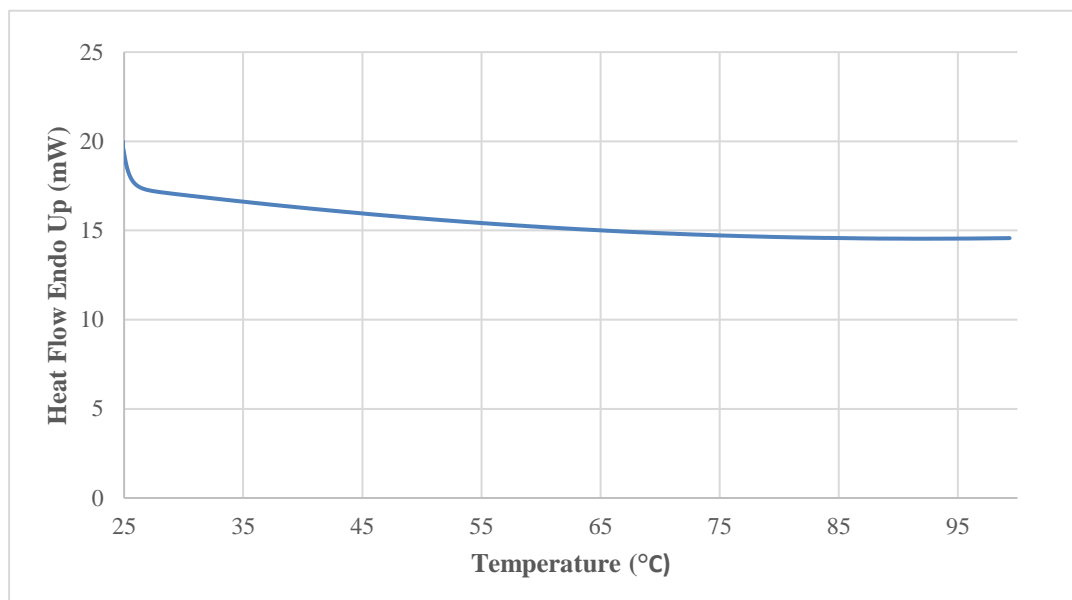


Figure 35. Heat flow of standard sapphire relative to an empty specimen holder

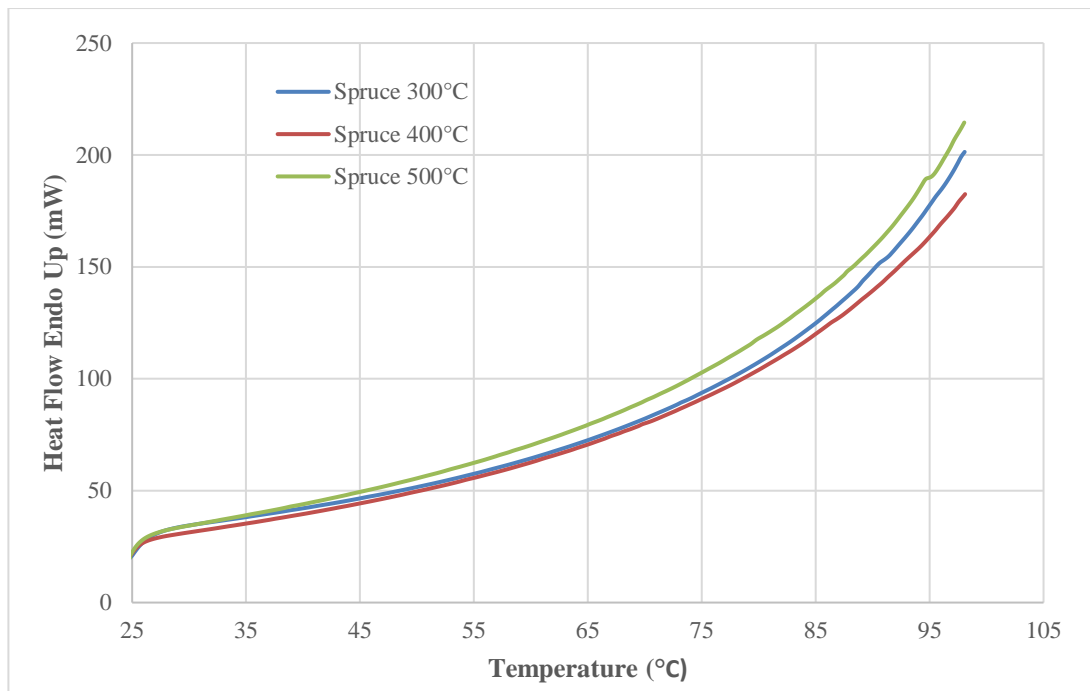


Figure 36. Heat flow of spruce bio-oil

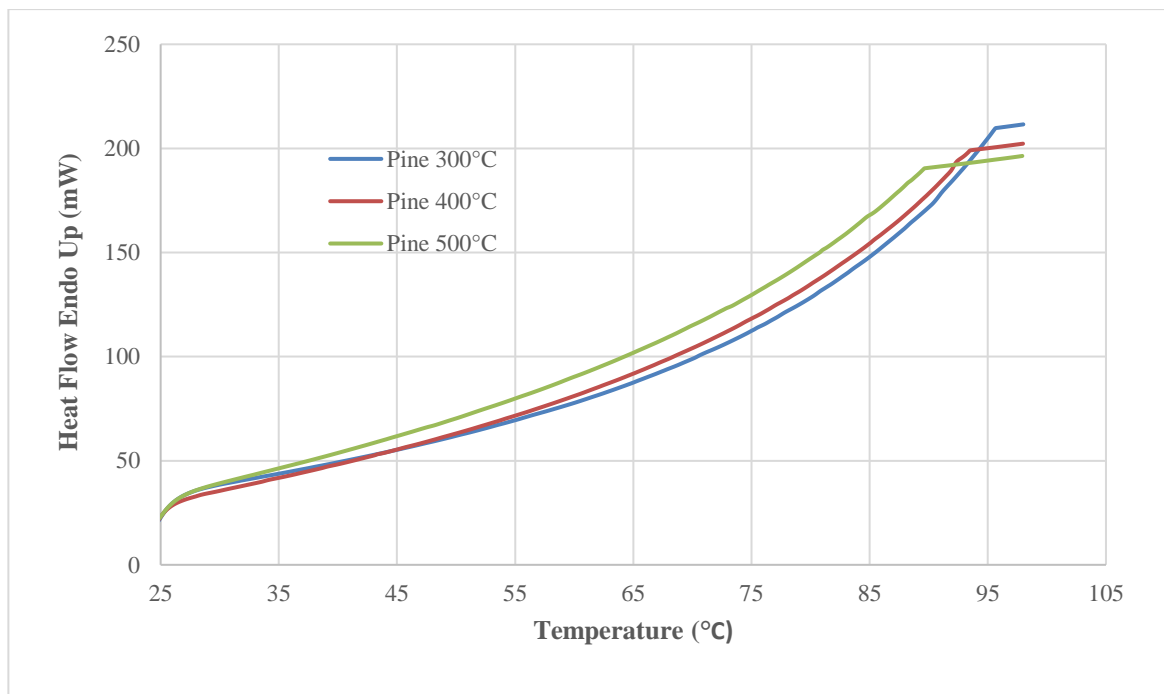


Figure 37. Heat flow of pine bio-oil

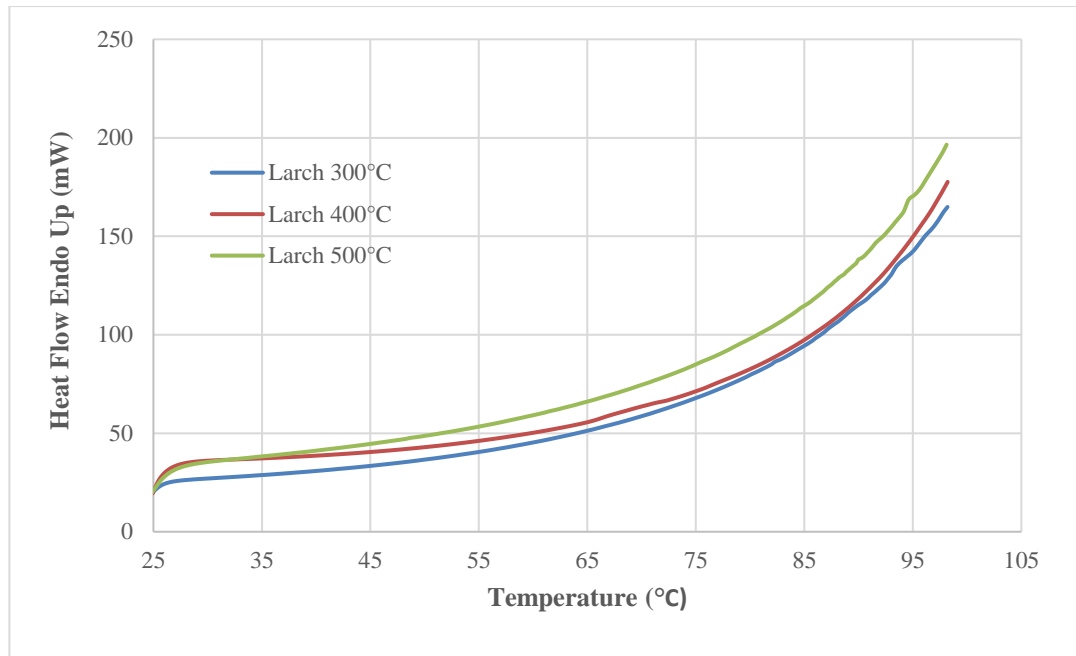


Figure 38. Heat flow of larch bio-oil

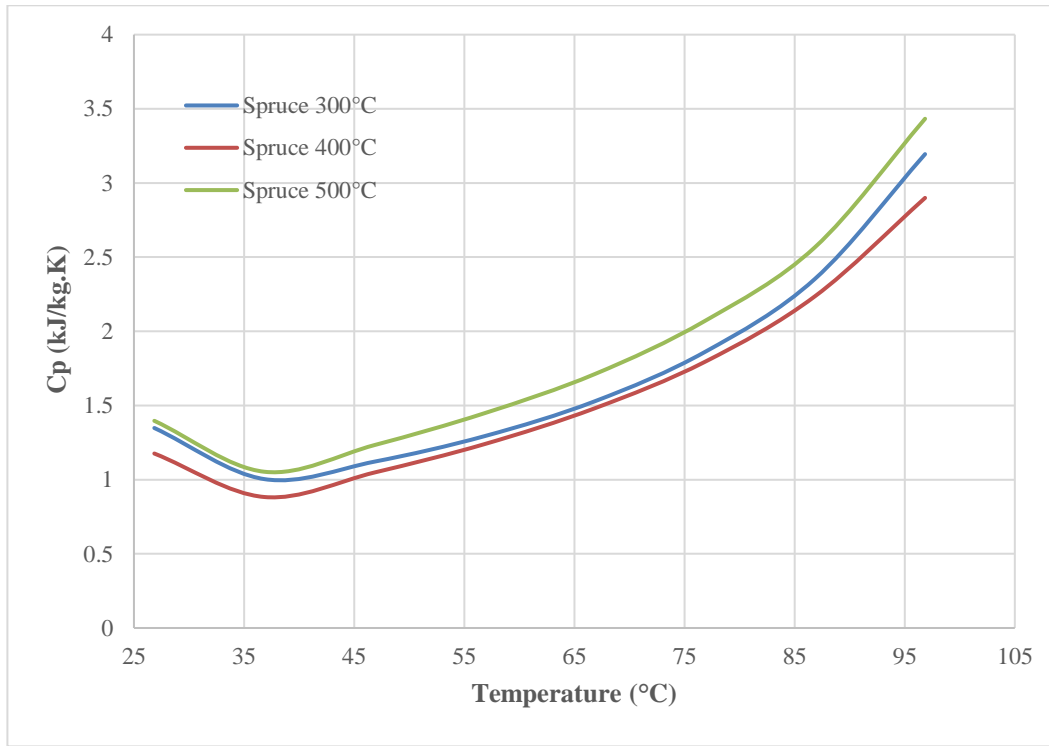


Figure 39. The Specific heat capacity of Spruce wood varying with temperature

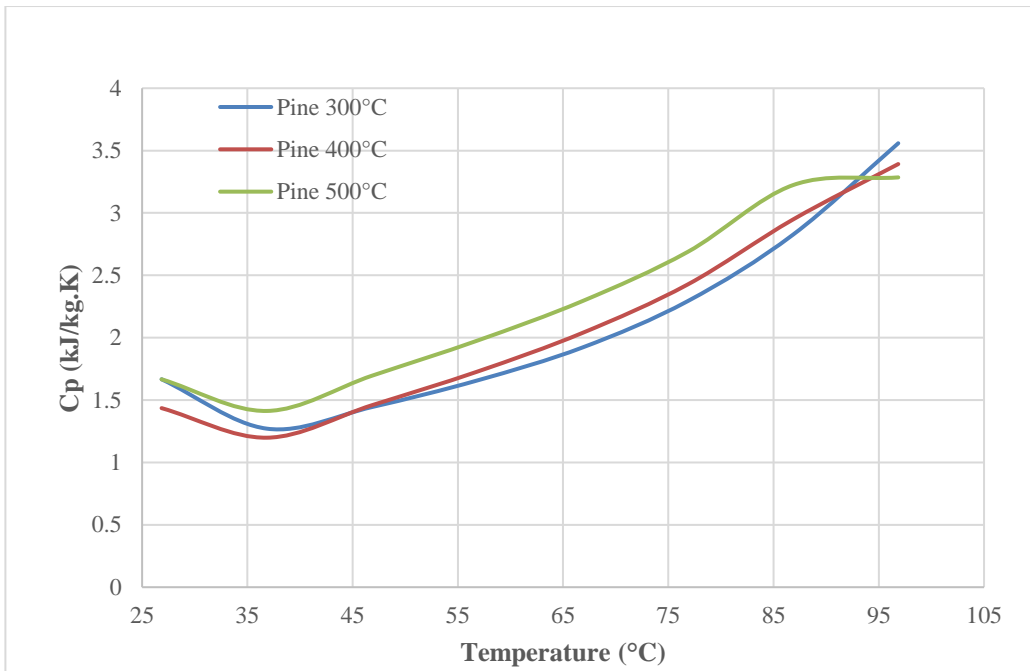


Figure 40. The Specific heat capacity of pine wood varying with temperature

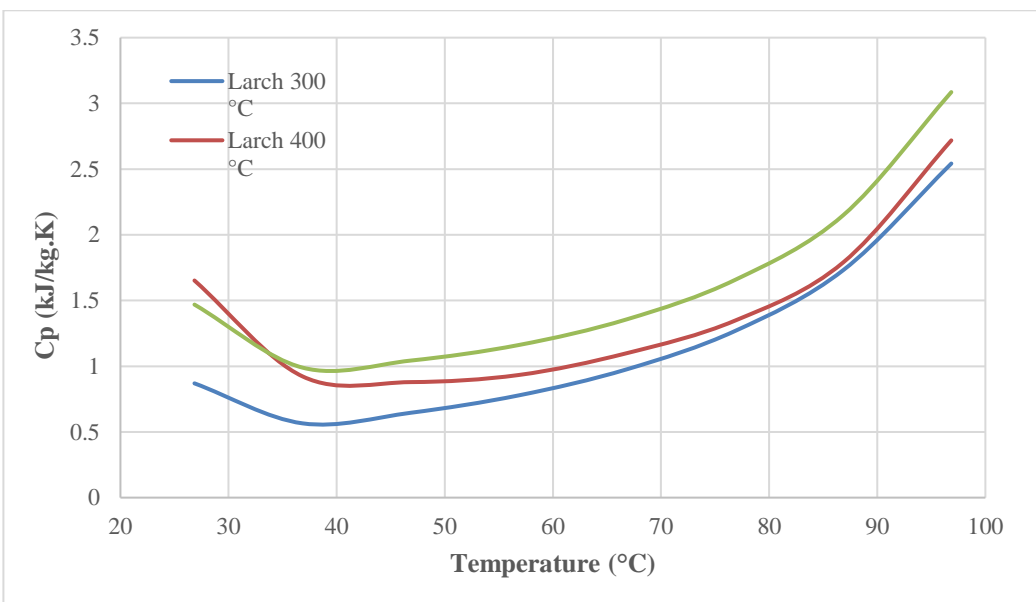


Figure 41. The Specific heat capacity of Larch wood varying with temperature

6.3.2.7. CHNSO Elemental analysis of the bio-oils

Vario MICRO cube (Elementar) was used for CHN determination. Around 2-4 mg oil sample was placed into tin capsules with the addition of Chromosorb W 30-60 Mesh for nitrogen determination. The sample was oxidised at 900°C, where combustion gas flow through GC-TPD column to determine the composition of organic element as a percentage of total weight (wt. %). The remaining composition such as oxygen (O) and sulphur (S) was computed by difference, where O+S = 100 - \sum carbon + hydrogen + nitrogen. The analysis was run in triplicate to ensure consistency. The procedure follows ASTM D3176, which is the Standard Practice for Ultimate Analysis of Coal and Coke.

$$O = 100 - \sum C + H + N$$

The measurement of the elements of the bio-oil were carried out for all bio-oil samples. The results are presented in Table 14:

Table 14: CHNSO Elemental Analysis of the Bio-oils

Biomass @ T		(wt.%)
Spruce@300C	C	54.18
	H	5.42
	N	0.39
	O+S	40.00
Spruce@400C	C	57.13
	H	5.75
	N	0.47
	O+S	36.64
Spruce@500C	C	68.04
	H	5.46
	N	0.45
	O+S	26.06
Pine@300C	C	46.97
	H	4.80
	N	0.45
	O+S	47.79
Pine@400C	C	56.29
	H	5.65
	N	0.62
	O+S	37.45
Pine@500C	C	52.81
	H	5.97
	N	0.48
	O+S	40.74
Larch@300C	C	53.14
	H	5.24
	N	0.54
	O+S	41.09
Larch@400C	C	51.42
	H	5.35
	N	0.53
	O+S	42.70
Larch@500C	C	49.15
	H	5.78
	N	0.46
	O+S	44.60
Bio-oil from wood [114]	C	54-58
	H	5.5-7
	N	0-0.2
	O+S	35-50

6.3.2.8. Determination of organic compounds in bio-oil (bio-oil composition)

Bio-oil characterisation could apply different techniques to determine the composition of the liquid biofuel. For this purpose, gas chromatography-mass spectrometry (GC/MS) is the most used technique to characterize the organic fraction of the bio-oil.

The GC/MS analysis was conducted by Nicholls-Colton Analytical for the determination of organic compounds in bio-oil. The equipment used is Shimadzu GCMS-QP2010.

The compositions of the bio-oil were carried out for all bio-oil samples. The results are presented in Table 15. As expected, large presence of phenolic compounds is reported in the bio-oil. The bio-oil obtained from these pyrolysis experiments cannot be used directly as biofuel in an engine or boiler, a next step is required to stabilise, improve the properties, and reduce oxygenated compounds present in the bio-oil

In Annex I, a complete analysis of the tars in the bio-oil is shown.

Table 15. Determinants detected in pyrolysis bio-oil (mg/kg)

Sample	Spruce			Pine			Larch		
Temperature (°C)	300	400	500	300	400	500	300	400	500
2,4-dimethylphenol	<100	<100	<100	112	111	135	97	196	<100
2-methylphenol	263	352	501	190	161	186	115	253	451
3/4-methylphenol	135	<100	147	389	325	402	282	527	<100
3-nitroaniline	<100	<100	<100	100	106	142	162	145	<100
4-chloro-3-methylphenol	<100	<100	<100	104	<20	98.5	58.8	221	<100
Phenol	2471	1993	3226	942	594	729	462	897	1760

6.3.2.9. Comparison of parameters with literature review

As the particle size exerts a negligible effect on the results and the highest bio-oil yields are reported at the lowest temperature (300C) due to the gasification reactions increasing at higher conditions, Table 16 shows a comparative study of the different biomasses' results with particle size A at 300C with a literature review.

Table 16. AgroCycle results comparison with literature review for bio-oil properties

Property	Typical value for bio-oil [115]	Typical value in fossil oil [116]	Pine @300 C	Larch C	@300	Spruce @300 C
Water content, %	15-30	-	29.84	28.62		20.58
Viscosity @40C, cSt	15-35	2-1,000	8.02	8.74		8.17
Density @25C, kg/dm ³	1.10-1.30	0.75-1	1.21	1.22		1.25
pH	2-3	As per the fuel	2.27	2.26		3.23
Other properties						
Ash, %	0.01-0.1	-	-	-		-
Suspended solids, %	<0.5	-	-	-		-
Flash point, C	40-110	-	-	-		-
LHV, MJ/kg	13-18	42	-	-		-

Bio-oils from forestry residues, especially pine, are reported to contain ca 28% water and a pH 3.0, as well as a low heating value (LHV) of 14 MJ/kg, and low presence of solids (below 0.05%) [117].

Pyrolysis from woody biomasses produce fragmentation of the original lignocellulosic polymers (cellulose, hemicellulose and lignin). The bio-oil from these feedstocks has a high oxygen content (between 45-50%) [118], as shown in the elemental analysis of the bio-oils. The oxygen is present in hundreds of compounds in the bio-oil, especially in phenolics and carboxylic acids. The relatively high presence of phenolics is due to the building blocks of lignin present in the biomass. The chemical composition and chemical properties of the bio-oils are possible to be manipulated by changing the temperature of the pyrolysis, as well as with the presence of a suitable catalyst as per the desired properties. The presence of a catalyst has not been considered in this study, as the objective is to test different forestry biomasses and study the properties of the biofuels, as well as to propose different solutions where appropriate to improve the future feasibility of the pyrolysis.

In contrast with the experiments, a review of the literature reveals different options. First, an upgrading and stabilisation of the bio-oil is necessary to use the pyrolysis oils as biofuels. It is necessary to reduce or transform the presence of oxygenated compounds in the bio-oil blend. This can be possible either during the pyrolysis process or by means of an upgrading processing after the pyrolysis reaction (as proposed in the next section of this report).

The molecular weight of the pyrolysis bio-oil blend can be controlled and reduced, and subsequently shifted to gases, by increasing the time/temperature ratio (cracking severity). When pyrolysis is developed at higher temperatures, an increase in the carbonisation and the production of larger polynuclear aromatics are reported. This also leads to the increase in the dehydrogenation reactions, hence a reduction of the phenolics and other oxygenated components is produced [119].

6.4. Other pyrolysis products – biochar and syngas

During this experimental programme for the AgroCycle project, only the liquid fraction from pyrolysis has been studied and characterised for energy applications. Bio-oils have reported a high potential to be used in engines and boilers, among others, for energy purposes. As detailed, additional stages are necessary to enhance the pyrolysis bio-oils, enhance their properties, and upgrade to an applicable biofuel.

On the other hand, other fractions are obtained during the pyrolysis of the forestry feedstocks: a gas fraction (mainly syngas), and a solid fraction (biochar). The gas fraction was released directly to the atmosphere during the pyrolysis process, due to the configuration and main purposes of the fixed bed reactor. Additional valorisation of the syngas fraction can be proposed for energetic and industrial applications.

Biochar was obtained in small quantities as the experiments were carried out at lab scale. All the biochar was used during the AgroCycle project in other activities with higher added value than the energetic applications as solid biofuel. Firstly, some biochar was proposed to be used in WP3 for soil enhancement applications, but finally was discarded due to insufficient quantities, logistics, and the definition of activities and schedules with the pyrolysis in WP3. Biochar was finally used in Task 2.5 (microbial fuel cell), as a catalyst for the anode – results and discussion of those experiments are reported in D2.7, and the remaining biochar was delivered and tested to IRIS partner for its testing in WP3 as an adsorbent in wastewater treatment

applications. For WP3 purposes, the remaining biomass from the pyrolysis experiments (a fraction of the biomass supplied by Harper Adams was pyrolysed for the experiments, whereas other fraction was stored in the event of repetition of experiments and for biomass analysis) was pyrolysed at 500C – in order to achieve the highest carbonisation level based on previous experiments and delivered along with the biochar samples. Results are shown in WP3's respective deliverables.

7. Simulations. Alternative process to upgrade bio-oil

Based on the aforementioned methods and results, a further virtual simulation is developed with the aim to propose a complete pyrolysis process for the most appropriate biomass, including an upgrading stage for the bio-oil product. The software used for this simulation is AspenOne suite v10, specifically Aspen Plus and Aspen HYSYS for the hydrocracking module.

Based on the previous experience at Exergy Ltd in modelling thermochemical process (gasification) for biomass valorisation purposes, mainly as biofuel, Aspen Plus software is selected as the most suitable for the modelling of the potential AgroCycle complete pyrolysis unit.

As mentioned, solid biomass from different sources can be turned into a range of useful energetic and chemical products for different industrial purposes: heat, power, biofuel, biochemicals, etc. Nevertheless, due to the complexity of the pyrolysis-bio-oil mixture and nature, which includes all types of organic compounds (acids, alcohols, ketones, aldehydes, esters, phenols, hydrocarbons, etc.), the properties of the potential biofuel are poor if it is not treated with an upgrading process: corrosion, instability, high oxygen content and immiscibility, among others.

There are several physical and chemical techniques which have been applied for the upgrading of the pyrolysis bio-oil from biomass. The techniques are listed as follows [120]:

- **Physical techniques:**

- A) *Emulsion.* Reduction of phenolic compounds and carboxylic acids.
- B) *Filtration.* Removal of particles, metals and char. Hot Vapor Filtration (HVF) is the physical upgrading method most commonly used.
- C) *Solvent addition.* Improvement of physical properties, such as viscosity and stability.
- D) *Distillation.* Separation of interesting mixtures based on the boiling point (gasoline, diesel and jet fuel – similar composition).

- **Chemical technologies.**

- E) *Hydrodeoxygenation or catalytic hydrogenation.* It is the removal of oxygen by means of hydrogen at high pressure and in the presence of a catalyst. A high quality oily product is upgraded with enhanced properties in terms of homogeneity, polity, heating value, viscosity and pH. The main issue related to this technology is the high rate of catalyst deactivation as well as the expensive costs of the hydrogen [121].
- F) *Catalytic cracking.* It is a similar process to the catalytic cracking applied in the oil refineries to reduce the large hydrocarbon molecules into shorter chains. Catalysed reactors are used to crack the bio-oil molecules into shorter ones as well as some pyrolysis reactors are designed to produce catalytic cracking during the pyrolysis reaction.
- G) *Steam reforming.* It is this reaction which turns hydrocarbons into syngas (mainly hydrogen) by means of the action of steam at high temperatures. It is a

reaction favoured by Le Chatelier's principle, it means that high temperatures and low pressures increases the CO/H₂ ratio.

Considering the results presented throughout this report, and especially the physical characteristics of the bio-oil with the values reported in other literature, the biomass selected for the pyrolysis simulation is larch and the conditions will be initially simulated at the lowest temperature, as it reports the maximum oil yield due to the low gasification rate.

The biomass feedstock is defined in Aspen Plus (part of the Aspen One Suite) as a non-conventional component. It cannot be defined as a conventional solid as biomass is a heterogeneous component, so it cannot be defined in terms of physical properties such as the molecular weight, chemical formula, vapor pressure or critical properties. Non-conventional solids or components are characterized from empirical factors which are called attributes. It is modelled from the ultimate and proximate analysis which has been carried out as initial step to characterise the biomass.

Due to the limitations in the GC/MS analysis for the determination of the components presented in the bio-oil, some of the components will be assumed in the component list.

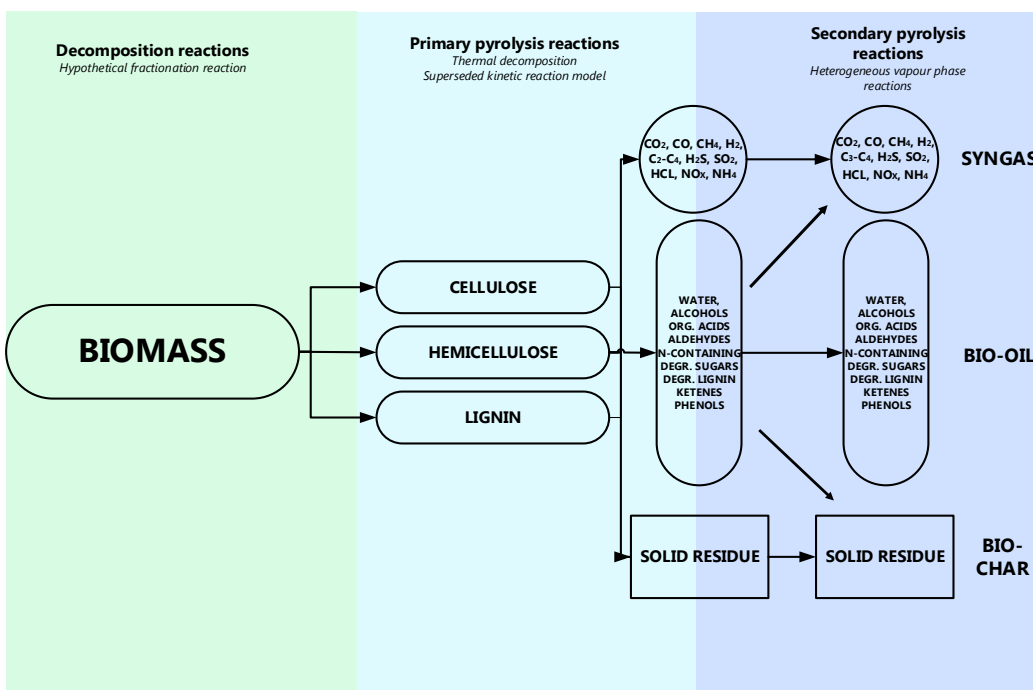


Figure 42. Pyrolysis stages when modelled [122]

7.1. Simulation specifications

The simulation has been defined by means of a new blank simulation in Aspen Plus software V10. Component list has been defined as a mixture of conventional, non-conventional and solid components as per the experimental results and some literature findings.

Table 17. Aspen simulation component list

Component ID	Type	Component name	Alias
CO	Conventional	CARBON-MONOXIDE	CO
H2	Conventional	HYDROGEN	H2
CH4	Conventional	METHANE	CH4
CO2	Conventional	CARBON-DIOXIDE	CO2
C2H6	Conventional	ETHANE	C2H6
C3H8	Conventional	PROPANE	C3H8
NH3	Conventional	AMMONIA	H3N
C2H4	Conventional	ETHYLENE	C2H4
C3H6	Conventional	PROPYLENE	C3H6-2
HYDRO-01	Conventional	HYDROGEN-SULFIDE	H2S
PHENO-01	Conventional	PHENOL	C6H6O
FORMI-01	Conventional	FORMIC-ACID	CH2O2
FORMA-01	Conventional	FORMALDEHYDE	CH2O
DEXTR-01	Conventional	DEXTROSE	C6H12O6
FLUOR-01	Conventional	FLUORANTHENE	C16H10-D1
WATER	Conventional	WATER	H2O
VANIL-01	Conventional	VANILLIN	C8H8O3-D1
2:4-X-01	Conventional	2,4-XYLENOL	C8H10O-6
O-CRE-01	Conventional	O-CRESOL	C7H8O-3
M-CRE-01	Conventional	M-CRESOL	C7H8O-4
P-CRE-01	Conventional	P-CRESOL	C7H8O-5
M-NIT-01	Conventional	M-NITROANILINE	C6H6N2O2-D1
ACETA-01	Conventional	ACETALDEHYDE	C2H4O-1
PROPI-01	Conventional	PROPIONIC-ACID	C3H6O2-1
BENZE-01	Conventional	BENZENE	C6H6
TOLUE-01	Conventional	TOLUENE	C7H8
BIOCHAR	Nonconventional		
ASH	Nonconventional		
BIOMASS	Nonconventional		
C	Solid	CARBON-GRAFITE	C
N2	Conventional	NITROGEN	N2

Initial assumptions:

- Lignin component is modelled as part of the composition of the biomass. It is modelled as “vanillin” component in the Aspen components’ list.
- Main solids are included as non-conventional and properties are set from experimental analysis (ultimate and proximate analyses).
- Thermodynamic selected method is UNIQUAC during the pyrolysis process.
- Biochar is modelled as a non-conventional component and properties are obtained from literature.

- Sulphur, nitrogen and chlorine containing based components have not been considered for this first approximation of the model by simulation.

7.2. Simulation Flowsheet

The pyrolysis simulated process consists of 4 sections. Three of them are simulated in Aspen Plus software, and the fourth one is simulated in Aspen HYSYS using conventional oil refining modules (hydrocracking).

- **S-10X. Pyrolysis section**

This first section is the pyrolysis itself. This part of the simulation is based on the data obtained from the experimental activities run by Exergy in the facilities of Harpur Hill Lab. (Sheffield Uni).

The flowsheet of this section is composed by:

- *U-101. Biomass dryer.* This equipment is used to reduce the humidity of the raw material (biomass) before pyrolysis. Pyrolysis yield decreases with the presence of water in the feedstock, and the energy requirements increase with this parameter.
- *R-101. Pyrolysis reactor.* In this equipment, the pyrolysis reaction is developed at the optimum conditions. It has been simulated by means of a RYIELD reaction in Aspen Plus.
- *U-102, U-103 and U-104. Cyclones.* The aim of this series of equipment is to clean up the pyrolysis products (gas state) from the biochar, ashes and non-reacted biomass (remaining biomass). Biochar will be valorised afterwards in S-30X to produce energy.
- *U-102. Mixer.* It is used to merge the different bottom streams coming from the cyclones and to have a single stream for the solids combustion.
- *E-101. Heat exchanger.* After drying, the stream coming from the dryer needs to be heated up to be pyrolyzed.

In Figure 43, the process developed in AspenPlus is represented.

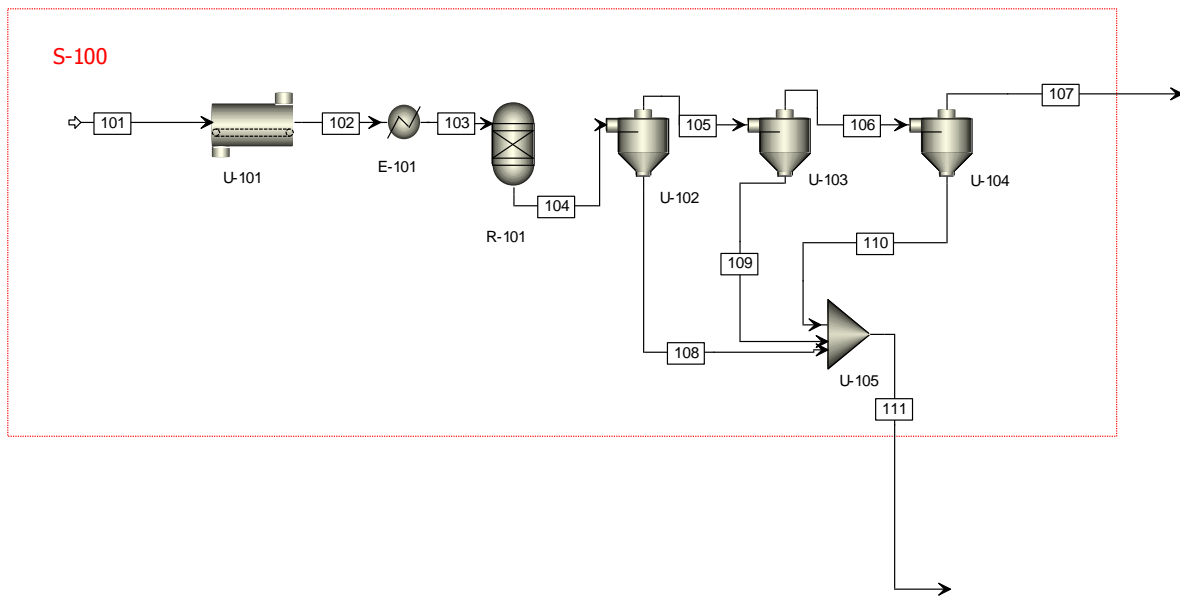


Figure 43. Pyrolysis section in Aspen

- **S-20X. Bio-oil separation section**

The main aim of this section is to separate the bio-oil from the non-condensable gases and to develop an initial refining and transformation of the phenolic and other organic components, in order to increase the energetic value of the bio-oil before the final refining by means of a later hydrocracking stage (S-40X).

This section is made up of:

- *V-101. Gas-Liquid separator vessel.* The objective is to separate the condensable from the non-condensable gases.
- *T-201 and T-202. Absorption and desorption columns.* The bio-oil is separated from the occluded gases which were not removed from the V-101 due to the energetic requirements.
- *R-201. Hydrodeoxygenation reactor.* The aim of this reactor is to upgrade the phenolic and other oxygenated components before the hydrocracking reactor. A RSTOIC module is used for this purpose in AspenPlus.
- *E-201, E-202, E-203, E-204 and E-205. Heat exchangers.* Heat exchangers are used to increase and to reduce the temperature of the different streams before the separations (flash vessels and absorption columns) and reactions.
- *U-201 and U-203. Mixer*
- *U-202. Splitter.*

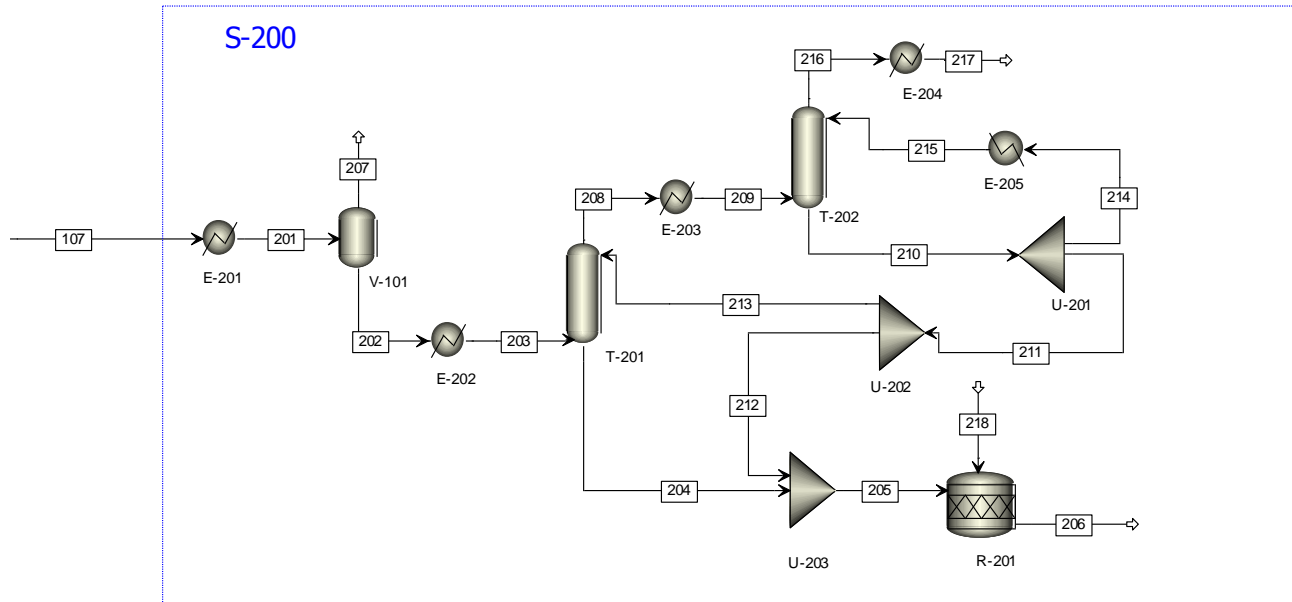


Figure 44. Bio-oil separation and upgrading

- **S-30X. Biochar valorisation**

This section is designed for the valorisation of the solids coming from the bottom of the cyclones in the S-10X. An energetic valorisation is proposed for the biochar, which is mixed with some ashes and non-reacted biomass.

- *R-301. Decomposition reactor.* It is the previous step (virtual) before the combustion of the solids in the R-302. It is simulated with a RYIELD module.
- *R-302. Combustion reactor.* The aim of this reactor is to turn the elemental solids and to reduce them by means of its combustion. It is simulated with a RGIBBS module in equilibrium.
- *U-301. Cyclone.* It is used to remove solids from the combustion gases (ashes), same as in S-10X.
- *C-301. Turbine.* Considering the energy from the combustion gases, this turbine produces work and electricity
- *P-301. Pump.* This pump uses the electricity generated by the turbine.
- *E-301 and E-302. Heat exchangers.* They are used to adjust the temperature to the process requirements and conditions.

This section has been simulated with energetic (for the decomposition and the combustion reactors, as in reality they represent the same operation) and work streams (from the energy generation by means of the turbine).

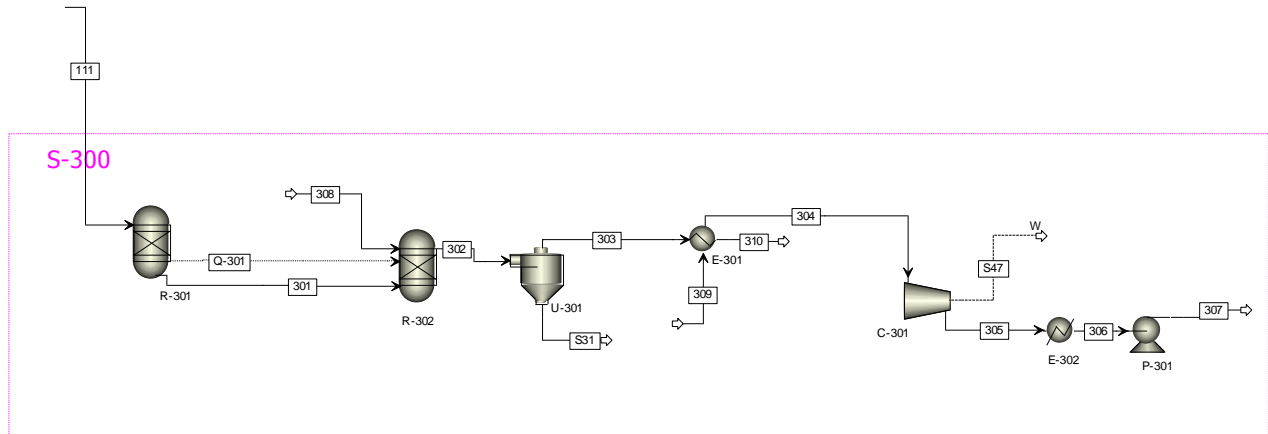


Figure 45. Biochar valorization

- **S-40X. Hydrocracking section**

This section simulated the final refining of the bio-oil into a drop-in-biofuel mixture. For this purpose, the following equipment are used:

- *R-401. Hydrocracking system.* It is used to break down the components into shorter molecules with the addition of hydrogen, temperature and catalyst. The product is a liquid hydrocarbon mixture.
- *T-401. Distillation tower.* The simulation operates in a similar way as a petroleum column. The distillation cuts are based on the ebullition points defined by the user.

Additionally, the following streams are created:

- *Stream 403.* It is an analogue of a naphtha stream (gasoline).
- *Stream 404.* It is a distillate stream (light diesel)
- *Stream 405.* It is an analogue of a diesel stream (heavy diesel).
- *Stream 406.* It is the bottom residue (heavy fuel). It might be further refined as waxes for other potential applications, such as asphalts.
- *Stream 407.* It is a purge of hydrogen. Hydrogen is introduced in stream 402 for the hydrocracking reaction.

There is a small recycle of bottom product to the hydrocracking system to optimise the working conditions in HYSYS.

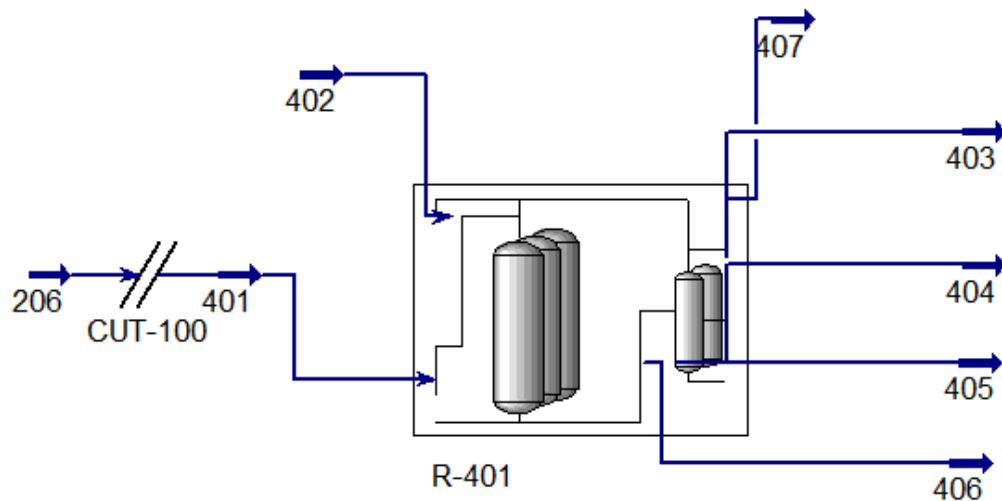


Figure 46. Hydrocracking system (Aspen HYSYS)

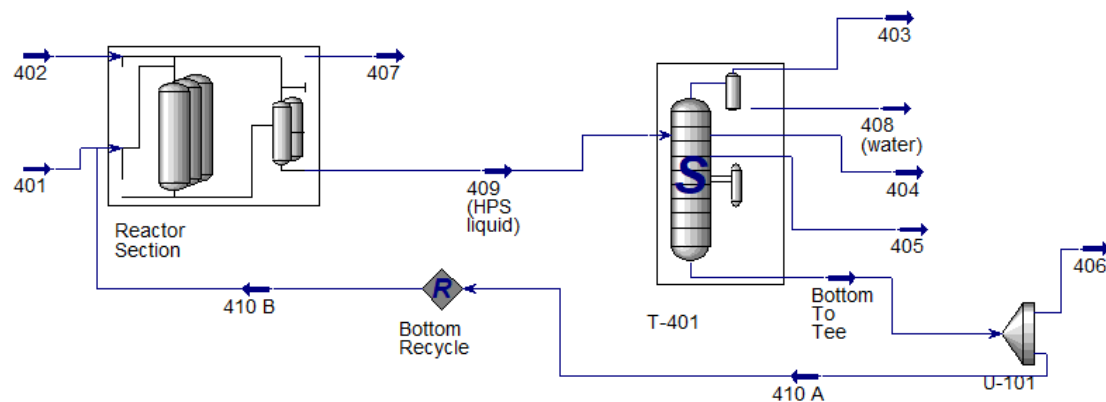


Figure 47. Detailed hydrocracking system environment

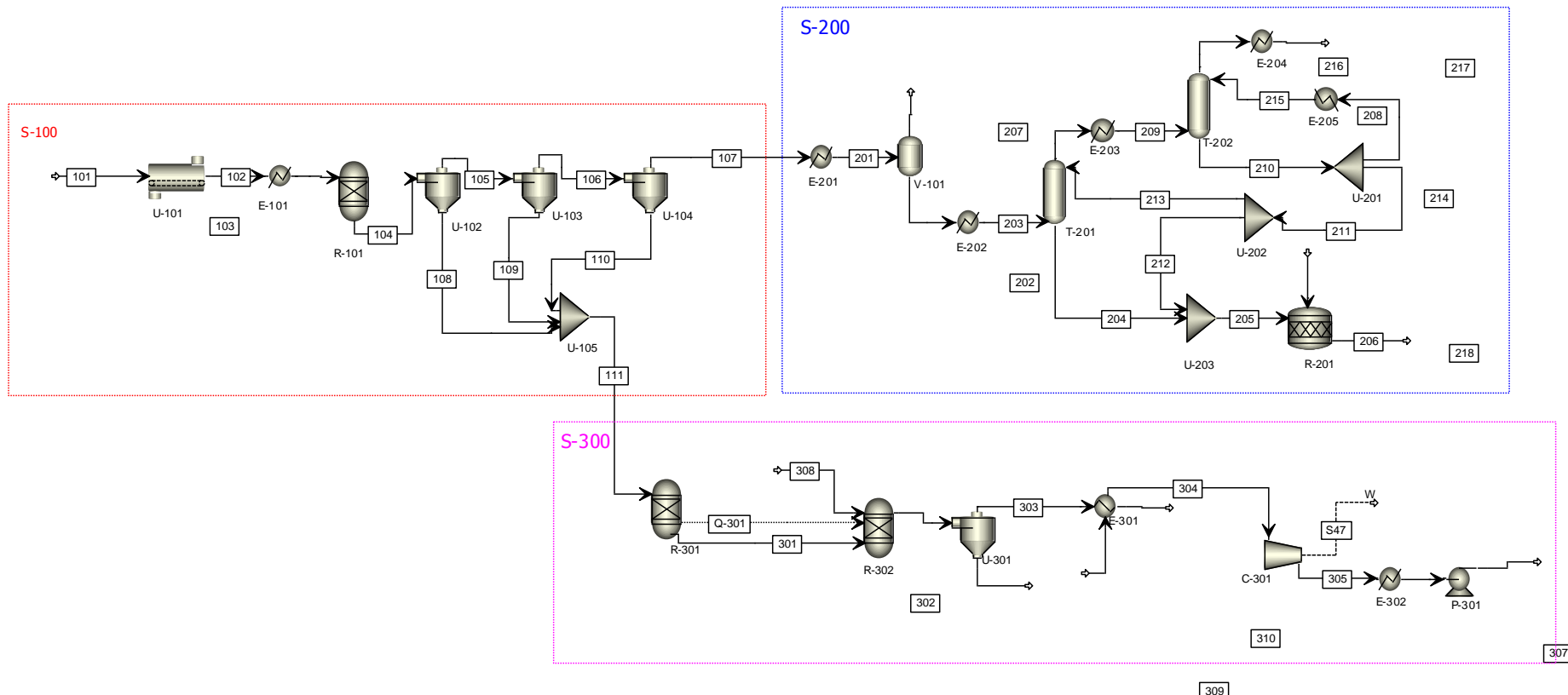


Figure 48. Aspen Flowsheet for the pyrolysis of larch

7.3. Section 10X. Pyrolysis

This section simulates the pyrolysis of the biomass. As larch showed slightly better results in the experimental activities, the composition and conditions for the larch biomass have been used in this simulation.

The feedstock, represented in the stream 101, has been modelled as a non-conventional solid. This is due to the nature of the biomass as a component itself, it cannot be modelled as a conventional solid. Conventional solids are pure materials which are specified using the solid component type in AspenPlus database. The area ideally used for simple stoichiometry or kinetic simulated reactions. They have characterised properties, which are: molecular weight, chemical formula, vapor pressure and critical properties. They can be used in the MIXED or CISOLID sub-streams in AspenPlus flowsheet.

However, biomass as well as pulp and paper and coal operations, cannot be modelled as conventional solids. These materials are characterised by empirical factors or component attributes. These component attributes represent the component composition by one or more of its constituents. These components are modelled as “non-conventional solids” and they do not participate in phase equilibrium. So, equilibrium reactors cannot be used for these purposes, but RStoic are appropriate to model the operations.

Biomass is modelled in the AspenPlus properties component list as a non-conventional component. Ultimate and proximate analysis from larch wood characterised by Sheffield University have been used for this purpose.

Biomass is modelled in Stream 101 (see Figure 43 above). The conditions are environment conditions, 25C and 1bar. One tonne of biomass (1,000 kg) per hour has been used as the basis for the simulation (in continuous), this biomass is containing 50kg of water (5% humidity).

In the tab NC solids, the proximate and ultimate analysis showed in previous sections of this report have been introduced to model the biomass composition. Ashes and chlorine have been not considered within these analyses.

The biomass is introduced into a dryer (U-101). In order to ease the simulation and obtain the final mass and energy analysis as the main target, the specifications for the simulations have been:

- Dryer type: shortcut
- Pressure: 1 bar
- Temperature: 140C (after sensitivity analysis).
- Moisture specification basis: WET
- Valid phases: vapor-liquid.

Ideally, the dryer uses an air stream to remove the humidity of the system. This air stream will drag the water from the biomass.

After leaving U-101, the outlet stream is going through a heat exchanger equipment, in order to reach the pyrolysis temperature. As shown in previous

results, the optimum temperature is the lowest, as the higher the temperature, the higher the gasification stage. The stream is heated up to 300C as in experimental activities. Then, the biomass stream with a reduced humidity and at reaction temperature, it is introduced in the pyrolysis reactor (R-101).

Pyrolysis reactor is modelled by means of a RYIELD module. The reaction conditions have been 300C and 1 bar, and the yield has been specified as the product distribution shown in this report, as well as literature complement where appropriate. The yield option selected has been component yield for the reaction and a mass basis. As part of the requirement, nitrogen as an inert component has been specified in the reactor. It is also important to mention that as part of the work with biomass as non-conventional component, as well as biochar and ashes, their compositions in the ultimate and proximate analyses are necessary to specify in the reactor. Databases from Aspen Plus have allowed to obtain the analyses for the ashes, whereas experiments from Sheffield University provide us the analyses for the biochar.

Once the reaction is finished, ideally there are four phases in three different streams (gaseous – syngas; liquid – biooil; aqueous – water; and solid – biochar). It is not possible to simulate the different phases in this reaction module in Aspen Plus, then a single stream as product is simulated and the different phases are separated after cyclones by means of different operations.

As mentioned, cyclones are simulated after the pyrolysis reaction in order to remove the solid phase from the gases and bio-oil. Three series of cyclones in series have been configured in order to reach the highest removal of particles from the gaseous product after the reaction.

The main characteristics for these cyclones are:

- Calculation method: Shepherd and Lapple
- Type: Barth 1- rectangular inlet

In order to increase the efficiency of the solid separation, the diameter of the cyclones have been reduced as much as possible for the simulations. The main parameters for these systems are as follows:

Table 18. Cyclones' parameters in pyrolysis section

Cyclone system	Diameter	Number of cyclones
U-102	0.25m	5
U-103	0.15m	1
U-104	0.19m	1

The gas stream from the last cyclone (stream 107) is going through S-20X with the aim to separate the bio-oil from the syngas and non-condensable components.

The bottom streams from all cyclones are collected in a mixer and are sent to S-30X with the aim to valorise the biochar (which contains some ashes and remaining biomass from the reaction) by means of a combustion.

7.4. Section 20X. Bio-oil separation and upgrading

The second section of the pyrolysis process consists of the upgrading of the bio-oil before the hydrocracking. As reported from the experimental activities, the content of oxygenated components is high, and due to this fact, the bio-oil cannot be used directly in biofuel applications. The steps which comprises this section are the flash separation, the absorption for the bio-oil and the hydrogenation of oxygenated compounds.

This section is parting from stream 107 from S-10X. The first operation unit is a flash vessel, which will separate the condensable gases and the bio-oil from the non-condensable gases (especially CO, CO₂, H₂ or syngas mixture). Small loses of condensable gases are reported, a balance has been reached between the minimum temperature achievable in the flash vessel and the desired separation. The parameters have been studied with a sensitivity analysis, and finally a temperature of 30C has been set. Hence, a cooler is cooling the temperature of the stream coming in S-10X (stream 111) down to 30C. The key component for the separation has been the ethane (C₂H₆), after developing a study of the thermodynamic separation factor (*k*) in the components involved in the process. The following figures present some sensitivity analyses carried out for the temperature selection.

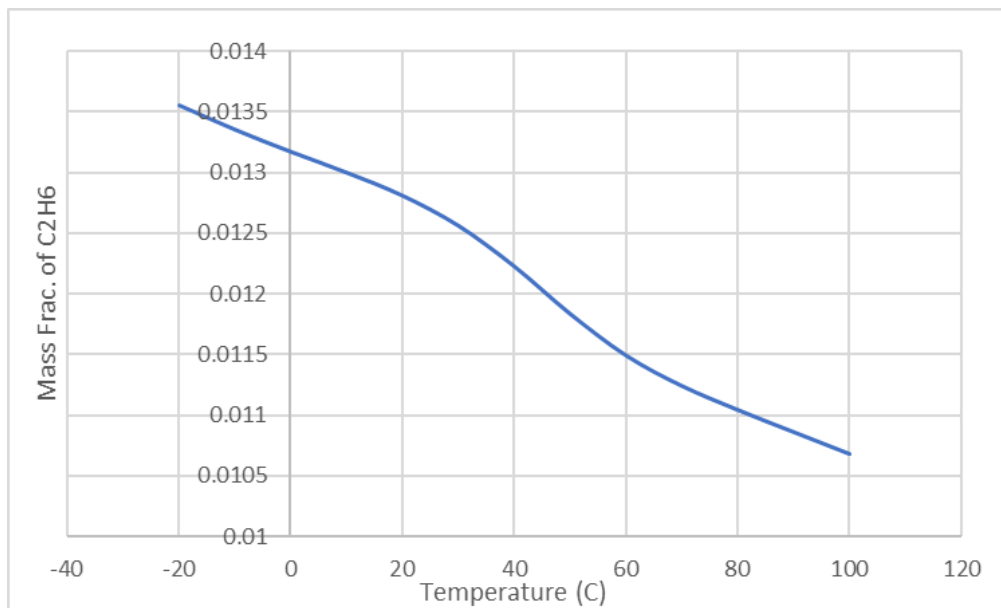


Figure 49. Mass fraction of ethene in stream 207 as function of temperature in flash vessel

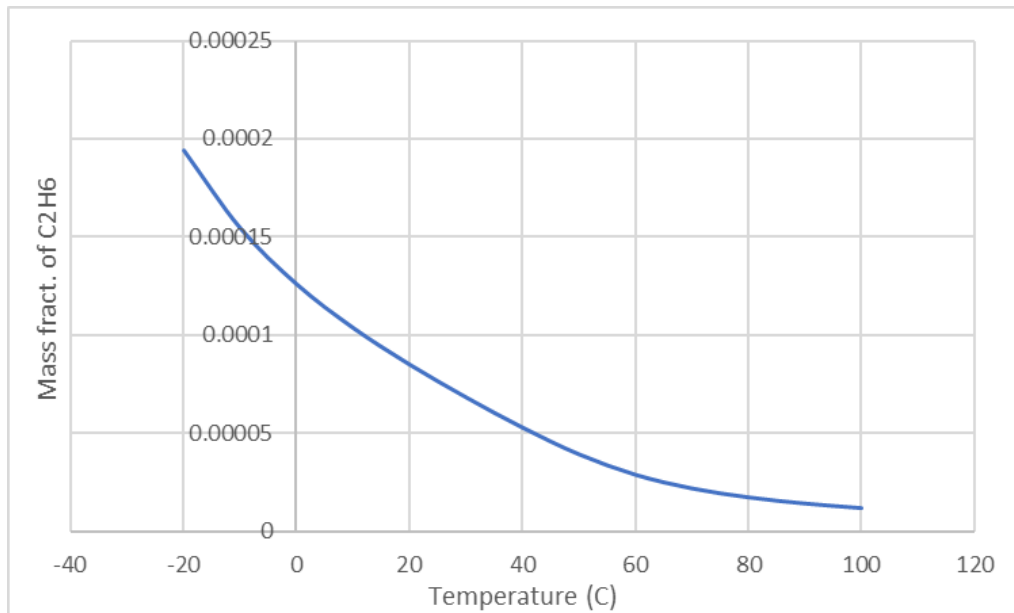


Figure 50. Mass fraction of ethene in stream 202 as function of temperature in flash vessel

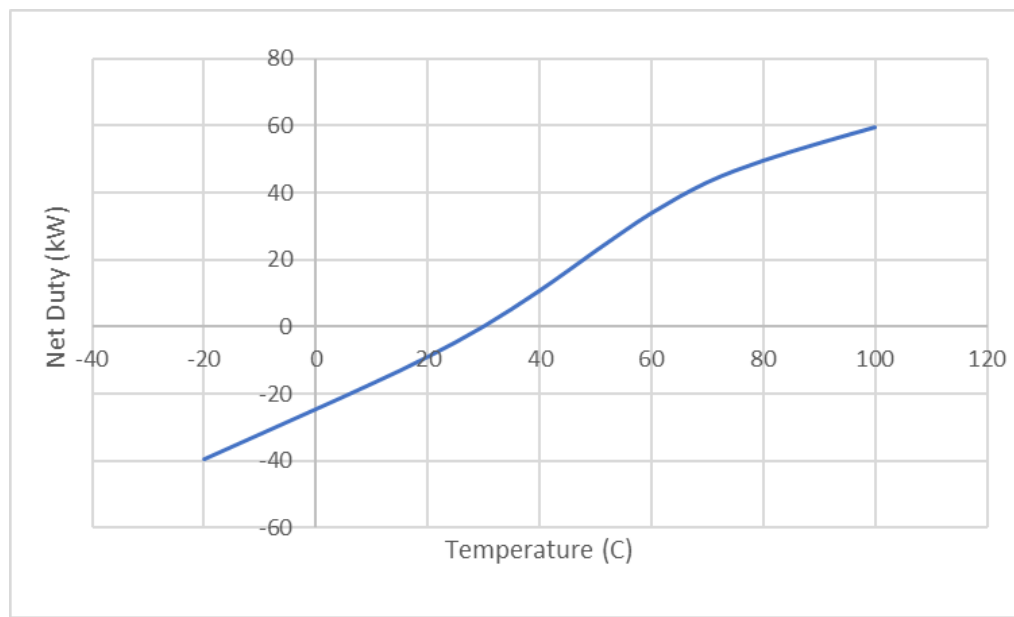


Figure 51. Net Duty of flash vessel (energy requirements) as per the temperature

The top stream (207) is made up of non-condensable gases, mainly syngas, along with small fractions of other condensable components. No further valorisation step has been proposed for this stream, although alternative processes can be developed in order to clean up the syngas and adjust the hydrogen ratio, and use it in subsequent industrial processes, including biofuel production.

Stream 202 contains the organic components, mainly all those of interest in as potential liquid biofuel. Some gases are still occluded within this stream (due to low inefficiency of flash operations when the components have similar separation factors). A further separation unit is proposed, by means of a series of absorption and desorption columns. The columns have been optimised

considering the removal of non-condensable gases, specially CO₂. Their main parameters are shown as follows:

Table 19. Absorption and desorption system in S-20X

Column	Number of stages	T of the condenser	T bottom	T top
T-201	14	43.3C	108.78C	101.206C
T-202	10	20C	41.7C	18C

Outlet streams are split to be returned to the absorption and desorption column in order to use the own gaseous streams as absorption gas. Finally, the bio-oil with a reduced amount of non-condensable gases is collected from both columns and mixed to be sent to refining stages.

Stream 205 is sent to a catalytic hydrogenation reactor, which works aiming at reducing the presence of oxygenated compounds. A series of reactions have been set in a RStoic reactor module (R-201). The conditions of the reactor have been established based on literature [123], which are 400C and 92 bar.

Different reactions have been specified in the RStoic module in order to turn the phenolic components into deoxygenated components. The ratio hydrogen/bio-oil has been optimised by means of sensitivity analysis in Aspen Plus.

The outlet stream (207) is sent to a final hydrocracking section (S-40X) for final refining. It is simulated by using Aspen HYSYS software.

7.5. S-30X. Biochar valorisation

This is the last section simulated with Aspen Plus software. The objective of this simulation is to demonstrate the energetic potential of the biochar after a combustion. The final outcome is the generation of electricity by means of a turbine.

All the biochar collected in the different cyclone systems in S-10X, it is mixed and sent to S-30X (stream 111). This stream will be transformed into other elements, such as water, N₂, O₂, CO, CO₂, H₂ and ashes in a combustion system with steam.

The enthalpy and density properties for the solids have been already defined when the properties of the non-conventional components have been established (used HCOALGEN and DCOALIGT). The process simulated in this section follows a similar process as to combust coal to obtain energy. This process, industrially, consists of burning coal or biomass into a furnace or boiler. Then, a stream of water is pumped through the pipeline system and turned into steam taking advantage of the heat produced in the process. This steam is then used to drive and run a turbine system connected with the shaft of generator, where magnet spin within wire coils to produce electricity. After this process, the steam is cold down into a condenser and then, used again in the process [124]. The process simulated into the Aspen Plus flowsheet is based on these foundations, but the simulation is slightly different due to the constraints of the software.

Firstly, the combustion reactor is simulated. In practise, it is a single reactor, but in the Aspen simulation, it has been split into two reactors to obtain the mass and energy balances. The first reactor is a RYIELD block (R-301) and it is used to split the biomass, ashes and biochar into their constituent elements (O₂, N₂, H₂, water, ASH, and C – solid). Sulphur composition has been considered negligible as their presence in the biomass was very small in comparison to the rest of elements. This reactor is necessary before the equilibrium reactor (RGIBBS) as the Gibbs module cannot operate with non-conventional components. Then, the Gibbs reactor (R-302) simulated the chemical equilibrium by minimising Gibbs free energy and models the combustion. It turns the elemental components into CO₂, NO₂, and water. This combustor is working with air, the optimum ratio of air has been also optimised by means of sensitivity analysis (it is not possible to establish a molar ratio as the biomass is modelled as non-conventional, so the molar flow is not available in the Aspen Plus results). From the RYield reactor (R-301) to the RGibbs reactor (R-302) a heat stream is transferred in order to take into consideration the decomposition heat in the reaction.

The conditions for the reactors are as follows:

Table 20. Biochar combustion reactors

Reactor	Type	Parameters
R-301	RYield	20C, 1 bar
R-302	RGibbs	Equilibrium reactor (phase and chemicals to be identified with the simulation) – identification on potential products in vapour and solid phases, Pressure drop 0 bar

The outlet stream from the reaction system (stream 302) is then cleaned by a cyclone system to remove the ashes. The parameters for this cyclone are as follows:

Table 21. Cyclone system before turbine

Cyclone system	Diameter	Number of cyclones
U-301	0.24m	4

After the cyclone, the hot gases will pass through a heat exchanger where a stream of water (stream 309) will be introduced in counter-current direction. Water is introduced at 10C and 1 bar pressure, and the pressure difference established in the heat exchanger is of 5 bar. The molar ratio water/combustion of gases is 0.58 after optimisation (with the work produced after the turbine).

The water stream as steam abandons the heat exchanger (S-304) at 151.9 C and 5 bar pressure. Combustion gases abandon the heat exchanger in stream 310, and a further treatment will be applied if necessary (not simulated in this project).

The steam passes then through a turbine C-301, where a work stream will be produced. The working parameters are 1 bar pressure at isentropic conditions. After the turbine, a work (electricity) stream is represented by W-301.

The steam will pass through a heat exchanger and a pump after the electricity generation and it will be cold down to liquid water again and reintroduced into the system.

7.6. S-40X. Hydrocracking

Firstly, to develop this section, some changes were made. A change in the used software (from Aspen Plus to Aspen HYSYS, as HYSYS includes a hydrocracking module among different petroleum units), as the feed stream is stream 206 (from Aspen Plus), and a change in the list of components and properties.

The list of components from the stream 206 in S-20X was introduced in HYSYS as a normal component list, which BWRS as thermodynamic model due to the characteristics of the components. As the module used is a petroleum operation, it is necessary a change in the component list to "HCRSRK" by means of a cutter.

The hydrocracker model needs to be calibrated with the properties and data of the stream to process. For this purpose, the ASTM curves of the stream have been obtained by means of a stream analysis in HYSYS and the info has been fed into the calibration model.

The curve selected the ASTM D86, and the curves are shown in Figure 52:

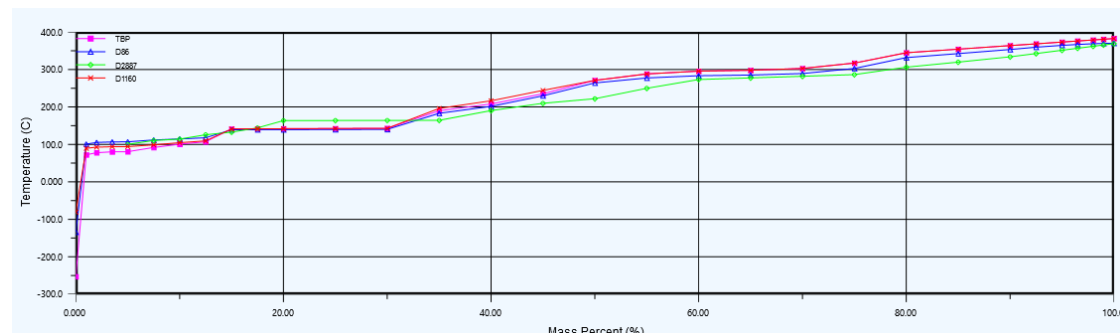


Figure 52. ASTM curve for bio-oil stream before final refining

The ASTM curve, along with some properties from the feed stream have been used for the calibration of the hydrocracker model in Aspen HYSYS. This step is key, as the hydrocracking, as well as other refining modules, only works when a previous model is created and calibrated.

The properties for the calibration model are one reactor, two beds, a fractionation column and a recycling of the bottoms. It is shown as follows:

Table 22. Hydrocracker calibrated model

Input	Value
Bed 1 diameter, m	1.50
Bed 2 diameter, m	1.50
Catalyst loading per bed, kg	900/500
Bed voidage (supposed)	0.5
Hydrocracker configuration	1 reactor, 2 beds, recycling. Hydrocracking blend (outlet stream) is distilled in a

Input	Value
	petroleum distillation column and bottoms are recycled to hydrocracker
Feed type	LVGO (Light Vacuum Gas Oil)
Feed mass flow, kg/h	207
Recycle mass flow, kg/h	77
Bed 1 inlet temperature, °C	360
Bed 2 inlet temperature, °C	380
H₂ temperature, °C	50
H₂ pressure, bar	70
Purge fraction	0.15

After creating a calibrated hydrocracker model, it is introduced in Aspen HYSYS flowsheet as shown in images above. The HYSYS HCR model uses its own component list with a specific thermodynamic model to work with lumped kinetics and to process all the reactions involved in the equipment operation. This thermodynamic model is called HCFSRK. It is necessary a transition by means of a cutter operation in HYSYS flowsheet to turn the original thermodynamic model (BWRS) to HCFSRK, which is based in hypos (boiling point ranges) for the components (stream 401). Then, the hydrocracking operations are running under the conditions fixed by the model (Table 22).

The properties for the final products (naphtha, distillate, diesel and a bottom residue) are shown below:

Table 23. Properties of hydrocracking products

Property	Naphtha	Distillate	Diesel	Bottoms
API gravity	55.10	29.08	36.45	26.13
Paraffins, %	74.23	35.62	61.48	0.005
Naphthalene's, %	4.19	12.92	10.30	27.07
Aromatics, %	21.57	51.46	28.22	72.92
RON	55.32	5.811	0	0
MON	51.21	4.99	0	0
Smoke point, mm	24.41	18.92	17.44	16.25
Freeze Point, C	-95.01	-17.30	137.2	344.6
Flash Point, C	-	115.2	150.4	171.7
Cetane Index	10.56	43.46	57.19	-6.79
Pour Point, C	55.32	5.81	0	0
Viscosity, cP @1000F	0.56	3.942	10.45	3387.14

7.7. Mass and energy balances. Electricity generated

In Table 24, the overall mass and energy balances from the different process streams are shown. It also includes the generation of electricity in the turbine, and a final summary of these balances and efficiency for the overall process.

From the overall energy balance, where all the energetic inputs and outputs from the equipment shown above have been considered, as well as the biomass and the main products and by-products (hydrogen, air and utilities

such as steam or water have not been considered for the energy balance), a 58.7% efficiency is reported. In these first calculations, a potential energy integration and optimisation (for instance, by means of a Pinch Analysis or by using Aspen Energy Analyzer) has not been developed. If developed and applied, important savings may be reported, which would also affect the overall life cycle assessment of the pyrolysis process, as the CO₂ emissions linked to the process will be also reduced.

Table 24. Mass and energy balance of overall pyrolysis simulation

Stream	T, C	P bar	Fraction	Mass Enthalpy J/kg	Enthalpy Flow kW	Biomass kg/h	Water kg/h	Hydrogen kg/h	Gases kg/h	Bio-oil kg/h	Ash kg/h	Biochar kg/h	Naphtha kg/h	Diesel kg/h	Bottoms kg/h
101	25	1	Solid	-6.86e+06	-2037.73	1,000	50	0	0	0	0	0	0	0	0
102	140	1	Solid (0.95)	-6.65e+06	-1094	1,000	50	0	0	0	0	0	0	0	0
103	300	1	Solid (0.95)	-6.30e+06	-1893	1,000	50	0	0	0	0	0	0	0	0
104	300	1	Vapor (0.599) solid (0.401)	-3.86e+06	-1127.26	174.75	42.04	21.91	304.61	282.54	1.47	244.65	0	0	0
105	300	0.97	Vapor (0.99) and solid (0.009)	-4.17e+06	-736.68	2.39	42.04	21.91	304.61	282.54	0.02	3.35	0	0	0
106	300	0.90	Vapor (0.998); solid (0.002)	-4.18e+06	-732.28	0.44	42.04	21.91	304.61	282.54	0.003	0.63	0	0	0
107	300	0.87	Vapor (0.999)	-4.18e+06	-731.58	0.40	42.04	21.91	304.61	282.54	0.001	0.19	0	0	0
108	300	0.97	Solid	-3.38e+06	-390.57	172.36	0	0	0	0	1.44	241.31	0	0	0
109	300	0.90	Solid	-3.38e+06	-4.40	1.94	0	0	0	0	0.02	2.72	0	0	0
110	300	0.87	Solid	-3.38e+06	-0.70	0.30	0	0	0	0	0.003	0.31	0	0	0
111	299. 99	0.87	Solid	-3.38e+06	-395.67	174.61	0	0	0	0	1.46	244.46	0	0	0
201	30	1	Vapor (0.68) liquid (0.32)	-5.00e+06	-875.41	0.40	42.04	21.91	304.61	282.54	0.001	0.19	0	0	0
202	30	1	Liquid (0.998) vapor (0.002)	-5.06e+06	-281.04	0.14	32.34	0	199.93	166.72	0.0011	0.19	0	0	0
203	110	1	Vapor (0.163) liquid (0.837)	-4.46e+06	-247.77	0.14	32.34	0	199.93	166.72	0.0011	0.19	0	0	0
204	108. 78	1	Liquid	-3.46e+06	-164.63	0.14	13.73	0	0.001	157.56	0.001	0.13	0	0	0
205	93.5 9	1	Liquid (0.990) vapor (0.009)	-4.77e+06	-264.29	0.14	32.34	0	0.06	166.44	0.001	0.13	0	0	0
206	400	92	Vapor (0.897)	-2.90e+06	-177.24	0.14	39.75	17.90	17.95	149.37	0.001	0.19	0	0	0

Stream	T, C	P bar	Fraction	Mass Enthalpy J/kg	Enthalpy Flow kW	Biomass kg/h	Water kg/h	Hydrogen kg/h	Gases kg/h	Bio-oil kg/h	Ash kg/h	Biochar kg/h	Naphtha kg/h	Diesel kg/h	Bottoms kg/h
			liquid (0.103)												
207	30	1	Vapor	-4.97e+06	-594.37	0	9.97	21.91	304.36	115.72	0	0	0	0	0
208	101. 21	1	Vapor	-1.07e+06	-94.22	0	20.67	0	0.03	1.05	0	0	0	0	0
209	43.3	1	Liquid (0.97) vapor (0.03)	-1.27e+06	-111.16	0	20.67	0	0.03	1.05	0	0	0	0	0
210	41.7 4	1	Liquid	-1.28e+06	-123.05	0	22.97	0	0.08	11.38	0	0	0	0	0
211	41.4 7	1	Liquid (0.997) vapor (0.003)	-1.28e+07	-110.74	0	20.67	0	0.07	10.24	0	0	0	0	0
212	41.4 8	1	Liquid (0.997) vapor (0.003)	-1.29e+06	-99.67	0	18.61	0	0.07	9.22	0	0	0	0	0
213	41.4 7	1	Liquid (0.997) vapor (0.003)	-1.28e+07	-11.07	0	2.06	0	0	1.02	0	0	0	0	0
214	41.4 7	1	Liquid (0.997) vapor (0.003)	-1.28e+07	-12.30	0	2.29	0	0	1.13	0	0	0	0	0
215	15.6	1	Liquid	-1.30e+07	-12.46	0	2.29	0	0	1.13	0	0	0	0	0
216	18.2 5	1	Vapor	-4.37e+06	-0.58	0	0.03	0	0.19	0.27	0	0	0	0	0
217	20	1	Vapor (0.934) liquid (0.066)	-4.40e+06	-0.58	0	0.03	0	0.19	0.27	0	0	0	0	0
218	25	1	Vapor	1.84e+09	1.03e-14	0	0	20.15	0	0	0	0	0	0	0
301	20	1	Solid	-3.23e+06	-378.341	C=42.05	84.10	84.10	N2=84 .10 O2=42 .05	0	84.10	0	0	0	0
302	208 7.87	1	Vapor (0.971) solid (0.029)	-420869	-399.889	C=14.55	835.76 1	0	CO2=100.76	0	84.10	0	0	0	0

Stream	T, C	P bar	Fraction	Mass Enthalpy J/kg	Enthalpy Flow kW	Biomass kg/h	Water kg/h	Hydrogen kg/h	Gases kg/h	Bio-oil kg/h	Ash kg/h	Biochar kg/h	Naphtha kg/h	Diesel kg/h	Bottoms kg/h
									N2=23 85.36						
303	208 7.87	1.96	Vapor (0.971) solid (0.029)	511934.27	-473.10	C=0.78	835.76 1	0	CO2= 100.76 N2=23 85.36	0	84.10	0	0	0	0
304	151. 92	5	Vapor – saturated (0.9999)Liqui id – 0.0001	-1.32e+07	-13414.1	0	3662.9	0	0	0	0	0	0	0	0
305	99.6 4	1	Vapor (0.9536) Liquid (0.0463)	-1.33e+07	-13621.6	0	3662.9	0	0	0	0	0	0	0	0
306	99.6 4	1	Liquid	-1.55427e+ 07	-6044.4	0	3662.9	0	0	0	0	0	0	0	0
307	101. 02	50	Liquid	-1.55365e+ 07	-6041.96	0	3662.9	0	0	0	0	0	0	0	0
308	20	2	Vapor	-5055.21	-4.21	0	0	0	N2=23 01.25 O2=69 8.751 Total air=30 00	0	0	0	0	0	0
309	10	1	Liquid	-1.59257e+ 07	-6196.34	0	3662.9	0	0	0	0	0	0	0	0
310	115. 83	5	Vapor (0.997) solid (0.003)	-3.52e+06	-3263.64		835.76		CO2= 100.76 N2=23 85.36	0	0	0	0	0	0
S31	208 7.87	1.96	Solid	2.82e+06	70.76	C=13.78	0	0	0	0	76.32	0	0	0	0
401	Same as stream 206 with a change in the thermodynamic model (HCRSRK) + change in component list (lump)														
402	100	70	Vapor	1.12e+06	-	0	0	192.24	0	0	0	0	0	0	0

Stream	T, C	P bar	Fraction	Mass Enthalpy J/kg	Enthalpy Flow kW	Biomass kg/h	Water kg/h	Hydrogen kg/h	Gases kg/h	Bio-oil kg/h	Ash kg/h	Biochar kg/h	Naphtha kg/h	Diesel kg/h	Bottoms kg/h
403	101. 6	1	Vapor	-1.61e+06	-	0	0	0	0	0	0	0	1.63	0	0
404	323	1	Vapor	-6.11e+05	-	0	0	0	0	0	0	0	15.59 (light distillate)	0	0
405	423. 3	1	Liquid	-6.53e+05	-	0	0	0	0	0	0	0	39.97 (heavy diesel)		0
406	601. 8	1	Liquid	-6.94e+05	-	0	0	0	0	0	0	0	0	0	23.17
407	50	70	Vapor	-7.94e+04	-	0	0	0	0	0	0	0	0	0	34.96
408	300	1	Liquid	-1.74e+06	-	0	0	0	0	0	0	0	0	0	77 (recycle stream)

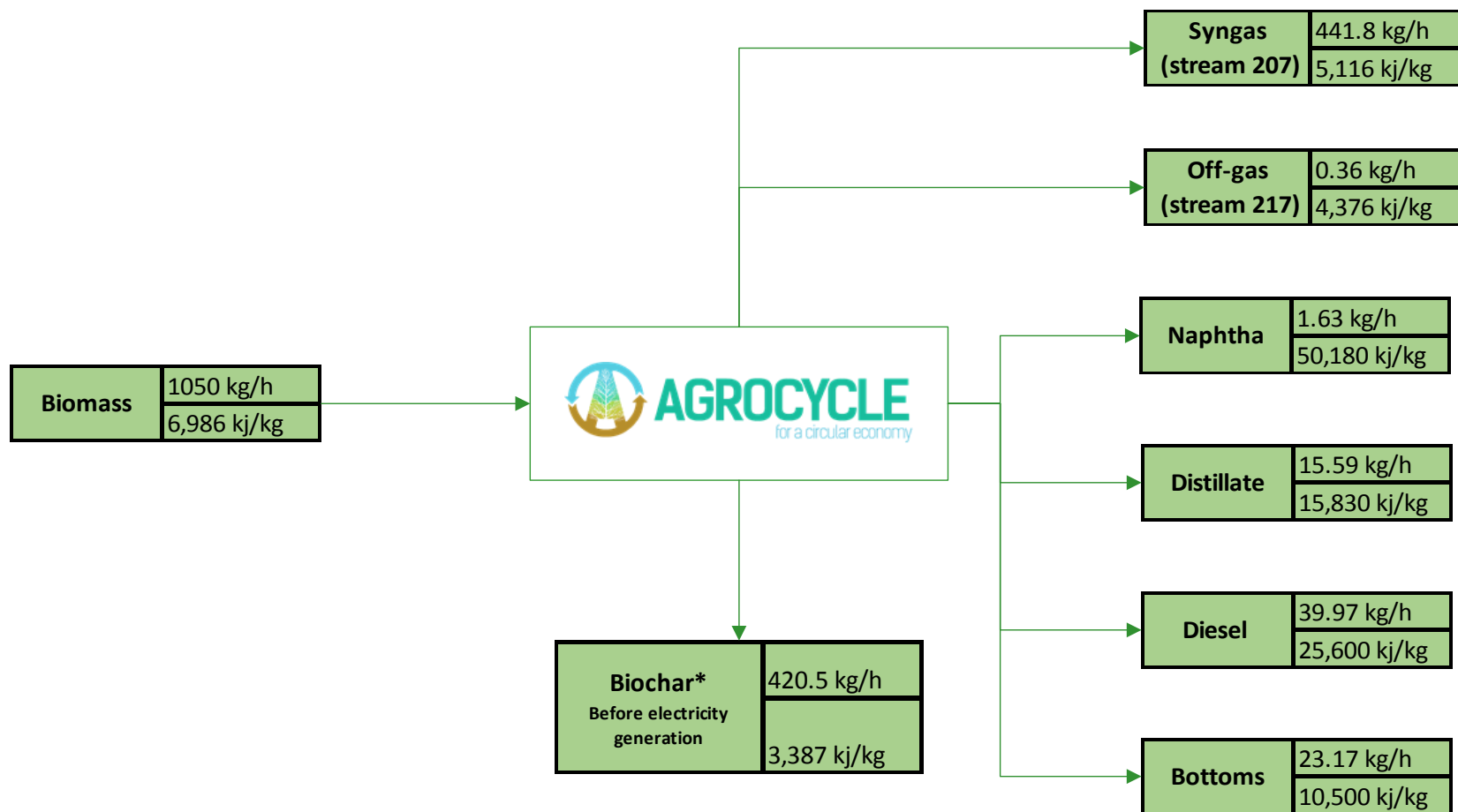


Figure 53. Pyrolysis simulation mass balance¹

¹ The image shows the main streams in (biomass) and out (products). It is not included the hydrogen and taken into account their reactions to produce new products, this accounts for loses of ca 50kg/h from the shown mass balance.

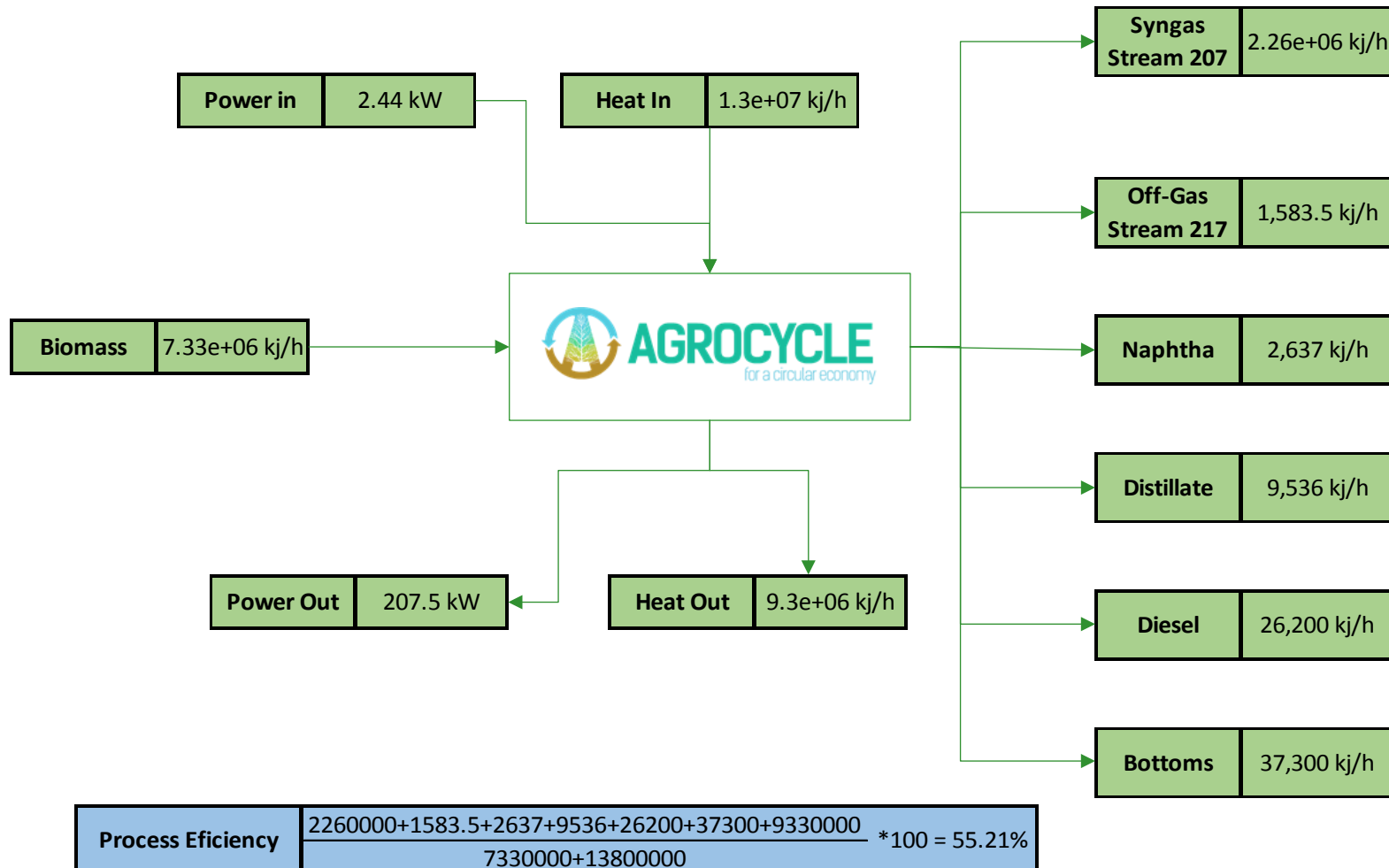


Figure 54. Pyrolysis simulation energy balance

7.8. Validation

Literature reports that bio-oil from lignocellulosic sources is lower in terms of heating value (HHV), since it is between 15-20 MJ/kg as per the feedstock used, which is up to 40-50% lower in comparison to conventional oil-based fuels or fossil fuels (42-45 MJ/kg) [125]. This is due to the high presence of oxygenated components, as shown in the tar composition (Annex I) and as modelled during the simulation. However, results from simulation show products with relatively good heating value (between 15 and 25 MJ/kg, as naphtha fraction is not considered due to an almost negligible production), whilst other properties (density, viscosity, flash point, cetane index, among others) must be analysed if the fuels are going to be used in conventional engines, and undoubtedly with the current legislation and parameters on biofuels if those are potentially used for commercialisation.

Due to the lignocellulosic structure of the pyrolysed biomasses, the phenolic components are reported as dominant in the bio-oil composition (and as obtained in the tar analysis shown in Annex I). This is mainly due to the phenolic structure of the lignin. Phenolic components can account for up to the 50% of the organic phase in the bio-oil according to literature data [126], which is less than for only lignin-based feedstocks, where the phenolic content can be up to 80% of the bio-oil [127].

As shown in experimental and simulated results, the content of water and phenolics is high, and this content is directly involved in the bio-oil quality. This results in lower heating values (HHV 16-19 MJ/kg) [114].

On the other hand, temperature is also a key factor to obtain a good quality bio-oil from a pyrolysis process. Usually, biomass pyrolysis process is reported to work in optimum conditions at a range between 550 and 650C, for the bio-oil yield. However, as observed in the experimental results, optimum oil yield was achieved at lower temperatures, whereas at 300C the maximum bio-oil yield was achieved.

This work has intended to develop a simplified model of a full biorefinery to turn forestry residues into biofuels (or potential building blocks for bioproducts). Some parameters have not been taken into account accurately due to the lack of information about the experimental parameters applied to this specific case (e.g. catalytic hydrodeoxygenation of the bio-oil, catalysts used for final hydrocracking), therefore, the main reactions and information about it have been used from literature without taking into account all the involved parameters (in hydrocracking, catalyst information – mandatory to calibrate and run the model, has been assumed as a typical hydrocracking catalysts based on Si-Al). This would need future validation in a pyrolysis plant by running experiments and comparing the final products characteristics with all those experiments gathered in the bibliography. However, this model can be used to study the techno-economics of the potential biorefinery plant (taking into consideration all the assumptions made and the conceptual engineering stage of the model), and thus compare the feasibility of the plant, at technical,

economic and logistical (considering the feedstocks availability and supply levels.

8. Potential bio-oil applications in the AgroCycle context

Bio-oils from pyrolysis of different renewable feedstocks, and especially from lignocellulosic (woody and forestry) biomasses, have been tested for different applications in the production of energy. Bio-oils are reported as different combustor fuels for electricity and heat production (for boilers, combustors, engines – diesel, turbines, and furnaces, among others) [128], in addition to being promising in other areas in the pharmaceutical, plastic, agriculture (fertilisers), and adhesive industries. They have shown a relatively good performance in diesel engines with a limited and short operation time, as long-term operation is unfeasible, due to the poor quality of the crude bio-oil (low volatility, high viscosity, instability, corrosiveness and potential for coking) [129].

After upgrading, the bio-oil enhances its properties as the oxygenated components are reduced and transformed. It means that the potential upgraded bio-oil can be used for energy applications, as transportation fuel or internal engines, turbines, furnaces and boilers. Apart from the energy applications, which are the main aim of WP2 in the AgroCycle project, the bio-oil and the gases produced during the entire process can be further valorised. The syngas produced during the pyrolysis (non-condensable gases) can be upgraded to produce biofuels or biochemicals. Phenolic components can be also separated and valorised in the chemical industry to produce chemicals, pharmaceuticals, additives and resins, among others.

The synthesis gas (syngas) produced during the pyrolysis of the biomass is rich in H₂. An additional stage can enhance the hydrogen production and the syngas ration for a synthetic biofuel production, such as Fischer-Tropsh [130]. It is important to consider that in this scenario, it will be necessary clean up the gases to remove the tars, nitrogen compounds, sulphur compounds, etc. The presence of these substances would reduce and poison the subsequent catalytic conversion of the syngas into valuable synthetic fuels.

Finally, as shown during the simulation, the biochar can act as a potential energy source to produce electricity after its combustion in a turbine. Apart from the energetic valorisation, biochar is very valuable as a plant nutrients and soil enhancer [131], apart from other uses such as a catalyst (after activation) and adsorbent, as tested in the AgroCycle project.

Considering the experimental results for the pyrolysis, as well as the simulation of the larch biomass, different options can be proposed for a potential biorefinery to valorise the lignocellulosic residues. The simulation model can be applied to different biomasses if the proximate and ultimate analyses are known as well as the behaviour of the feedstock during the process. The model can help in the decision-making stage as well as to predict the range of products. Preliminary economic results can also be generated from the simulation model. Parting from the results obtained from the larch after hydrocracking, it is possible to use the upgraded bio-oil (diesel fraction) in a diesel engine (after some modification and adaptation) as per the characteristics of the fuel streams in HYSYS. It is likely that some extra treatment is necessary to enhance the properties of the biofuel and the combustion, to comply with current EU Directives. Supplementary electricity can be also generated from a combustion

of the solid by product (biochar); the amount of electricity can vary from the biochar production and the turbine conditions. This electricity can be used in farming applications or in the running of the pyrolysis process itself.

9. Conclusions

From the observations of the experimental pyrolysis program, the experimental analysis of the bio-oils, and the simulations, it can be concluded that:

- Pyrolysis study was carried out using three biomass, Spruce, Pine and Larch in three particle ranges and at three pyrolysis temperatures, 300C, 400C and 500C. Those three biomasses have similar properties, Larch has slightly higher volatile matter.
- The production of bio-oil is primarily determined by the pyrolysis temperature. About 20 to 30% of the mass was converted to bio-oil during the pyrolysis. The highest oil production was at the temperature of 300C.
- Production of syngas has been reported between 38-60%, whereas biochar is between 20-35% and bio-oil 18-30% as per the conditions and the conifer biomass tested.
- Syngas has been released to the atmosphere during the pyrolysis process. This fraction has not been valorised, but potential applications may be proposed with an increase in the hydrogen production followed by an industrial process, such as Fischer-Tropsh.
- Particle size has no effect on the pyrolysis product yields.
- Bio-oil samples have high water content. The water content is about 20% at the pyrolysis temperature 300C, 30% at 400 C, and up to 60% at 500°C.
- Bio-oils have been characterised and compared to other reported bio-oils and with fossil fuels where appropriate.
- Bio-oils generally need further process such as the hydrogenation process to upgrade the phenols to higher value products.
- Improved quality of bio-oil is reported after the upgrading process and the hydrocracking of the bio-oil. Future work is necessary to validate the simulated work at plant level, and to test the biofuels in engines or boilers to validate their features.
- A full biorefinery based on pyrolysis (of the larch biomass) has been modelled in Aspen Plus. It has included the optimisation stages and the valorisation of biochar for electricity production within the energy context. The model is applicable to study the technoeconomic feasibility of the plant, and to test different biomasses at different scales as per the requirements.
- Bio-char produced in the pyrolysis has been used in other experimental activities in the AgroCycle project (as catalyst and as adsorbent). Bio-char may show potential applications in energy as solid biofuel (demonstrated in the Aspen Plus simulation), as well as in agriculture (fertilising applications).
- Bio-oil production from lignocellulosic materials remains a challenge when high quality standards are expected.

10. References

- [1] C. Di Blasi, "Modeling and simulation of combustion processes of charring and non-charring solid fuels," *Prog. Energy Combust. Sci.*, vol. 19, pp. 71-104, 1991.
- [2] D. C. Elliot, A. V. Beckman, J. P. Bridgwater, S. B. Diebold, S. B. Gevert and Y. Solantausta, "Developments in direct thermochemical liquefaction of biomass," *Energy Fuels*, vol. 5, pp. 339-419, 1999.
- [3] M. J. Antal, W. S. Mok, G. Varhegyi and T. Szekely, "Review of Methods for Improving the Yield of Charcoal from Biomass," *Energy and Fuels*, vol. 4, no. 3, 1990.
- [4] J. Lehmann, J. Gaunt and M. Rondon, "Biochar sequestration in terrestrial ecosystems - a review," *Mitig Adapt Strateg Global Change*, vol. 11, pp. 403-427, 2006.
- [5] K. Y. Chan, L. Zwieten, I. Meszaros, A. Downie and S. Joseph , "Agronomic values of green waste biochar as a soil amendment," *Aust J. Soil Res.*, vol. 45, pp. 629-634, 2007.
- [6] A. G. Buekens, A. V. Brigwater, G. L. Ferrero and K. Maniatis, Commercial and marketing aspects of gasifiers, Berling: Springer, 1990.
- [7] K. Maniatis, "Progress in biomass gasification: an overview," in *Progress in thermochemical biomass conversion*, Oxford, Blackwell Publishing Ltd, 2001.
- [8] C. Jazrawi, "Hydrotherman treatment of algal biomass: from batch to continuous pilot plants operations (Thesis)," University of Sydney, Sydney, Australia, 2014.
- [9] L. Garcia Alba, C. Torri, D. Samori van der Spek, S. R. Fabbri and D. W. Kersten , "Hydrothermal treatment (HTT) of microalgae: evaluation of the process as conversion method in an Agae Biorefinery Concept," *Energy Fuels*, vol. 26, pp. 642-657, 2012.
- [10] S. Bensaid, R. Conti and D. Fino , "Direct liquefaction of ligno-cellulosic residues for liquid fuel producion," *Fuel*, vol. 94, pp. 324-332, 2012.
- [11] F. Mermoud, S. Salvador, L. Van de Steene and F. Golfier, "Influence of the pyrolysis heating rate on the steam gasification rate of large wood char particles," *Fuel*, vol. 85, pp. 1473-1482, 2006.
- [12] C. Erlich, E. Bjornborn, D. Bolado, M. Giner and T. H. Fransson, "Pyrolysis and gasification of pellets from sugar cane bagasse and wood," *Fuel*, vol. 30, pp. 1535-1540, 2006.
- [13] V. M. Zubtsov, C. C. Pian and K. Yoshikawa, "Potential applications of high-temperature air/steam-blown gasification and pyrolysis systems," *Energy*, vol. 30, pp. 2229-2242, 2005.
- [14] A. Shikha Dahiya, J. Naresh Kumar, S. Shanthi , S. Chatterjee, O. Sakar and S. Venkata, "Food waste biorefinery: Sustainable strateg for circular bioeconomy," *Bioresource Technology*, vol. 248, pp. 2-12, 2018.

- [15] C. S. Lin, L. A. Pfaltzgraff, E. B. Herrero-Davila, E. B. Mubofu, S. Abderrahim, J. H. Clark, A. A. Koutinas, N. Kpsahelis, K. Stamatelatou and F. Dickson, "FW as a valuable resource for the production of chemicals, materials and fuels. Current situation and global perspective," *Energ Environ Sci*, vol. 6, pp. 426-446, 2013.
- [16] OECD, "Biomass and agriculture. Sustainability. Markets and policies," Paris, 2004.
- [17] H. Kahilouto, M. Kuisma, J. Havukainen, M. Luoranen, P. Karttunen, E. Lehtonen and M. Horttanainen , "Potential of agrifood wastes in mitigation of climate change and eutrophication - Two case regions," *Biomass and Bioenergy*, vol. 35, no. 5, pp. 1983-1994, 2011.
- [18] I. Deminal and S. Senoz, "Fixed-bed pyrolysis of hazelnut (*Corylus avellana L.*) bagasse: influence of pyrolysis parameters on products yields," *Energy sources, Part A: recovery, utilization and Environmental effects*, vol. 28, no. 12, pp. 1149-1158, 2006.
- [19] B. Wyrzykowska-Ceradini, B. K. Gullet, D. Tabor and A. Tourati, "Waste combustion as a source of ambient air polybrominated diphenylethers (PDBEs)," *Atms. Environ*, vol. 45, pp. 4008-4014, 2011.
- [20] D. Chen , L. Yin, H. Wang and P. He, "Pyrolysis technologies for municipal solid waste: a review," *Waste Manag*, vol. 34, pp. 2466-2486, 2014.
- [21] B. Biswal, S. Kumar and R. K. Singh, "Production of hydrocarbon liquid by thermal pyrolysis of paper cup waste," *J. Waste Manag*, vol. 34, pp. 2466-2486, 2014.
- [22] O. Masek, P. Brownsort, A. Cross and S. Sohi, "Influence of production conditions on the yield and environmental stability of biochar," *Fuel*, vol. 103, pp. 151-155, 2013.
- [23] M. P. McHenry, "Agricultural bio-char production, renewable energy generation and farm carbon sequestration in Western Australia: Certainty, uncertainty and risks," *Agriculture, Ecosystems & Environment*, vol. 129, no. 1, pp. 1-7, 2009.
- [24] A. Demirbas, "Effects of temperature and particle size on bio-char yield from pyrolysis of agricultural residues," *J. Anal Appl Pyrol*, vol. 78, pp. 243-248, 2004.
- [25] R. W. Nachenius, F. Ronsse, R. H. Venderbosch and W. Prins, "Biomass pyrolysis," *Chemical engineering for renewables conversion*, vol. 42, pp. 75-139, 2013.
- [26] Y. K. Park, M. L. Yoo, H. S. Heo, H. W. Lee, S. H. Park, S. C. Jung, S. S. Park and S. G. Seo, "Wild reed of suncheon bay: potential bio-energy source," *Renew Energy*, vol. 42, pp. 168-172, 2012.
- [27] V. Dhyani and T. Bhaskar, "A comprehensive review on the pyrolysis of lignocellulosic biomass," *Renewable Energy*, 2017.
- [28] P. Ahuja, P. C. Singh, S. N. Upadhyay and S. Kumar, "Kinetics of biomass and sewage sludge pyrolysis: thermogravimetric and sealed reactor studies," *Indian J Chem Tech*, vol. 3, pp. 306-312, 1996.

- [29] D. Savova, E. Apak, E. Ekinci, F. Yardim, N. Petrov and T. Budinova, "Biomass conversion to carbon adsorbents and gas," *Biomass Bioenergy*, vol. 21, pp. 133-142, 2001.
- [30] J. A. Caballero, J. A. Conesa, R. Font and A. Marcilla, "Pyrolysis kinetics of almond shells and olive stones considering their organic fractions," *J Anal App. Pyrol.*, vol. 62, pp. 93-109, 2002.
- [31] F. Suarez-Garcia, A. Martinez-Alonso and J. M. Tascon, "Pyrolysis of apple pulp: effect of operation conditions and chemical additives," *J Anal. Appl. Pyrol.*, vol. 62, pp. 93-109, 2002.
- [32] A. A. Zabaniotou, "Pyrolysis of forestry biomass by-products in Greece," *Energy Source*, vol. 21, pp. 395-493, 1999.
- [33] P. A. Della Rocca, E. G. Cerrella, P. R. Bonelli and A. L. Cukierman, "Pyrolysis of hardwood residues: on kinetics and chars characterisation," *Biomass Bioenergy*, vol. 16, pp. 79-88, 1999.
- [34] A. Ingermarsson, U. Nilsson, M. Nilsson, J. R. Pedersen and J. O. Olsson, "Slow pyrolysis of spruce and pine samples studied with GC/MS and GC/FTIR/FID," *Chemosphere*, vol. 36, pp. 2879-2889, 1998.
- [35] C. Di Blasi, E. G. Hernandez and A. Santoro, "Radioactive pyrolysis of single moist wood particles," *Ind Eng Chem Res*, vol. 39, pp. 873-882, 2000.
- [36] J. N. Murwanashyaka, H. Pakdel and C. Roy, "Step-wise and one-step vacuum pyrolysis of birch-derived biomass to monitor the evolution of phenols," *J. Anal. Appl. Pyrol.*, vol. 60, pp. 219-231, 2001.
- [37] V. Minkova, S. P. Marinov, R. Zanzi, E. Bjornborn, T. Budinova and M. Stefanova , "Thermochemical treatment of biomass in a flow of steam or in a mixture of steam and carbon dioxide," *Fuel Process. Technol.*, vol. 62, pp. 45-52, 2000.
- [38] H. J. Kim, I. Naruse, G. Q. Lu, K. Ohtake and M. Kamide, "Self denitrification behaviour of biobriquette added with pulp black liquor," *Kagaku Kogaku Ronbun*, vol. 24, pp. 779-783, 1998.
- [39] A. Caglar and A. Demirbas, "Conversion of cotton cocoon shell to hydrogen rich gaseous products by pyrolysis," *Energy Conv. Manage.*, vol. 43, pp. 489-497, 2002.
- [40] A. A. Zabaniotou, A. I. Roussos and C. J. Koroneos, "A laboratory study of cotton gin waste pyrolysis," *J. Anal. Appl. Pyrol.*, vol. 56, pp. 47-59, 2000.
- [41] A. E. Putun, "Biomass to bi-oil via fast pyrolysis of cotton straw and stalk," *Energy Sources*, vol. 24, pp. 275-285, 2002.
- [42] N. Ozbay, A. E. Putun and B. B. Uzun, "Biocrude from biomass: pyrolysis of cotton seed cake," *Renew. Energy*, vol. 24, pp. 615-625, 2001.
- [43] J. M. Encinar, J. F. Gonzalez and J. Gonzalez, "Steam gasification of *Cynara cardunculus* L: influence of variables," *Fuel Process. Technol.*, vol. 75, pp. 27-43, 2002.
- [44] J. D. Rocha, C. A. Luengo and C. E. Snape, "The scope of generating bio-oils with relatively low oxygen contents via hydropyrolysis," *Org Geochem*, vol. 30, pp. 1527-1534, 1999.

- [45] A. E. Putun, A. Ozcan, H. F. Gercel and E. Putun, "Production of biocrudes from biomass in a fixed-bed tubular reactor: product yields and compositions," *Fuel*, vol. 30, pp. 1371-1378, 2001.
- [46] J. Guo and A. C. Lua, "Kinetic study on pyrolysis of extracted oil palm fiber - Isothermal and non-isothermal conditions," *J. Therm. Anal. Calorim.*, vol. 59, pp. 763-774, 2000.
- [47] J. Reina, E. Velo and L. Puigjaner, "Thermogravimetric study of the pyrolysis of waste wood," *Thermochim. Acta*, vol. 320, pp. 161-167, 1998.
- [48] J. M. Encinar, F. J. Beltran, J. F. Gonzalez and M. J. Moreno, "Pyrolysis of maize, sunflower, grape and tobacco residues," *J. Chem. Techn. Biot.*, vol. 70, pp. 400-441, 1997.
- [49] C. Di Blasi, G. Signorelli, C. Di Russo and G. rea, "Product distribution from pyrolysis of wood and agricultural residues," *Ind. Eng. Chem. Res*, vol. 38, pp. 2216-2224, 1999.
- [50] J. Piskorz, P. Majerski, D. Radlein, D. S. Scott and A. V. Bridgwater, "Fast pyrolysis of sweet sorghum bagasse," *J. Anal. Appl. Pyrol.*, vol. 46, pp. 15-29, 1998.
- [51] K. Raveendran, A. Ganesh and K. C. Khilar, "Influence of mineral matter on biomass pyrolysis characteristics," *Fuel*, vol. 74, pp. 1812-1822, 1995.
- [52] K. Sipila, E. Kuoppala, L. Fagernas and A. Oasmaa, "Characterisation of biomass-based flash pyrolysis oil," *Biomass Bioenergy*, vol. 14, pp. 103-113, 1998.
- [53] E. Bjorkman and B. Stromberg, "Release of chlorine from biomass at pyrolysis and gasification conditions," *Energy Fuels*, vol. 11, pp. 1026-1032, 1997.
- [54] M. N. Islam, R. Zailani and F. N. Ani, "Pyrolytic oil from fluidised bed pyrolysis of oil palm shell and its characterization," *Renew. Energy*, vol. 17, pp. 73-84, 1999.
- [55] A. Demirbas, A. Caglar, F. Akdeniz and D. Gullu, "Conversion of olive husk to liquid fuel by pyrolysis and catalytic liquefaction," *Energy sources*, vol. 22, pp. 631-639, 2000.
- [56] J. A. Caballero, A. Marcilla and J. A. Conesa, "Thermogravimetric analysis of olive stones with sulphuric acid treatment," *J. Anal. Appl. Pyrol.*, vol. 44, pp. 75-88, 1997.
- [57] P. T. Williams and S. Besler, "The influence of temperature and heating rate on the pyrolysis of biomass," *Renew. Energy*, vol. 7, pp. 233-250, 1996.
- [58] L. Garcia, M. L. Salvador, J. Arauzo and R. Bilbao, "Catalytic steam gasification of pine sawdust. Effect on the catalyst weight/biomass flow rate and steam/biomass ratios on gas production and composition," *Energy Fuels*, vol. 13, pp. 851-859, 1999.
- [59] R. Aguado, M. Olazar, A. Barona and J. Bilbao, "Char formation kinetics in the pyrolysis of sawdust in a conical spouted reactor," *J. Chem. Techn. Biot.*, vol. 75, pp. 583-588, 2000.
- [60] M. Predel and W. Kamisnky, "Pyrolysis of rape-seed in a fluidised-bed reactor," *Biosource Technol*, vol. 66, pp. 113-117, 1998.

- [61] M. Predel and W. Kaminsky, "Pyrolysis of rape-seed in a fluidised-bed reactor," *Biosource technol.*, vol. 66, pp. 113-117, 1998.
- [62] S. H. Beis, O. Onay and O. M. Kockar, "Fixed bed pyrolysis of safflower seed: influence of pyrolysis parameters on product yields and compositions," *Renew. energy*, vol. 26, pp. 21-32, 2002.
- [63] C. Di Blasi, C. Branca, A. Santoro and E. G. Hernandez, "Pyrolytic behaviour and products of some wood varieties," *Combust Flame*, vol. 124, pp. 165-177, 2001.
- [64] F. Karaosmanoglu, A. Isigigur-Ergundenler and A. Sever, "Biochar from the straw-stalk of rapeseed plant," *Energy Fuels*, vol. 14, pp. 336-339, 2000.
- [65] M. J. Blesa, V. Fierro, J. L. Miranda, R. Moliner and J. M. Palacios, "Effect of the pyrolysis process on the physicochemical and mechanical properties of smokeless fuel briquettes," *Fuel Process. Technolo.*, vol. 74, pp. 1-17, 2001.
- [66] E. Karaosmanoglu and E. Tetik, "Fuel properties of pyrolytic oil of the straw and stalk of rape plant," *Renew. Energy*, vol. 16, pp. 1090-1032, 1999.
- [67] R. V. Pindoria, I. N. Chatzakis, J. Y. Lim, A. A. Herod, D. R. Dugwell and R. Kandiyoti, "Hydropyrolysis of sugar cane bagasse: effect of sample configuration on bio-oil yields and structures from two bench-scale reactors," *Fuel*, vol. 78, pp. 55-63, 1999.
- [68] S. Yorgun, S. Sensoz and O. M. Kockar, "Flash pyrolysis of sunflower oil cake for production of liquid fuels," *J. Anal. Appl. Pyrol.*, vol. 60, pp. 1-12, 2001.
- [69] M. Marquevich, R. Coll and D. Montane , "Steam reforming of sunflower oil for hydrogen production," *Ind. Eng. Chem. Res*, vol. 39, pp. 2140-2147, 2000.
- [70] R. K. Sharma, J. B. Wooten, V. L. Baliga, P. A. Martoglio-Smith and M. R. Hajaligol, "Characterization of char from the pyrolysis of tobacco," *J. Agr. Food Chem.*, vol. 50, pp. 771-783, 2002.
- [71] J. L. Valverde, C. Curbelo, O. Mayo and C. B. Molina, "Pyrolysis kinetics of tobacco dust," *Chem. Eng. Res. Des.*, vol. 78, pp. 921-924, 2000.
- [72] J. G. Olsson, U. Jaglid, J. B. Pettersson and P. Hald, "Alkali metal emission during pyrolysis of biomass," *Energy Fuels*, vol. 11, pp. 779-784, 1997.
- [73] L. Wang, J. Littlewood and R. J. Murphy, "Environmental sustainability of bioethanol production from weath straw in the UK," *Renewable and Sustainable Energy reviews*, vol. 28, pp. 715-725, 2013.
- [74] C. Wang, H. Machida, N. Nakagawa, T. Takarada and K. Kato, "Catalytic pyrolysis of plant - biomass in a powder particle fluidised bed," *Kagaku Kogaku Ronbun*, vol. 21, pp. 531-539, 1995.
- [75] R. Zanzi and K. Sjostr, "Rapid high-temperature pyrolysis of biomass in a free-fall reactor," *Fuel*, vol. 75, pp. 545-550, 1996.
- [76] E. E. Hood, P. Nelson and R. Powell, "Plant Biomass Conversion," 2011.

- [77] S. Haghghi Mood, A. Hossein Golfeshan, M. Tabatabaei, G. Salehi, G. H. Najafi and M. Gholami, "Lignocellulosic biomass to bioethanol, a comprehensive review with a focus on pretreatment," *Renew Sustain Energy Rev*, vol. 27, pp. 77-93, 2013.
- [78] C. Laine , "Structures of hemicellulose and pectins in wood and pulp," Helsinki University of Technology (PhD dissertation), Helsinki, 2005.
- [79] M. Carrier, A. Loppinet-serani and C. Aymonier, "Thermogavimetric analysis as a new method to determine the lignocellulosic composition of biomass," *Biomass Bioenergy*, vol. 35, pp. 28-307, 2011.
- [80] H. V. Lee, S. B. Hamid and S. K. Zain, "Conversion of lignocellulosic biomass to nanocellulose: structure and chemical process," *Sci. World J.*, 2014.
- [81] G. Caudullo, W. Tinner and D. de Rigo, "Picea abies in Europe: distribution, habitat, usage and threats," in *European Atlas of Forest Tree Species*, Luxembourg, Office of the European Union, 2016, pp. 114-116.
- [82] J. E. Eckenwalder, *Conifers of the World: The complete reference*, Timber Press, 2009.
- [83] The wood data base, [Online]. Available: <http://www.wood-database.com/norway-spruce/>. [Accessed March 2018].
- [84] A. Farjon, *A handbook of the world's conifers*, Leiden: Koninklijke Brill, 2010.
- [85] IUCRN Red List, "Larix decidua," [Online]. Available: <http://www.iucnredlist.org/details/42309/0> . [Accessed March 2018].
- [86] PFAF, "Lariz decidua Mill," 2014. [Online]. Available: <http://www.pfaf.org/user/Plant.aspx?LatinName=Larix+decidua>. [Accessed March 2018].
- [87] Forestry Commission England, "Distribution of native and plantation species across Europe," [Online]. Available: <https://www.forestry.gov.uk/forestry/infid-8qnk35>. [Accessed March 2018].
- [88] EU Science Hub, "Scots Pine," [Online]. Available: <https://ec.europa.eu/jrc/en/research-topic/forestry/qr-tree-project/scots-pine> . [Accessed March 2018].
- [89] Y. Zhou and K. Qui, "A new technology for recycling materials from waste printed circuit boards," *J. Hazard. Mater.*, vol. 175, pp. 823-828, 2010.
- [90] H. Jouhara, T. K. Nannou, L. Anguilano, H. Ghazal and N. Spencer , "Heat pipe based municipal waste treatment unit for home energy recovery," *Energy*, 2017.
- [91] D. Chen, L. Yin, H. Wang and P. He, "Pyrolysis technologies for municipal solid waste: a review," *Waste Manag*, vol. 34, pp. 2466-2486, 2014.
- [92] A. J. Marshall, "Commercial application of pyrolysis technology in agriculture," [Online]. Available: www.ofa.on.ca/uploads/userfiles/files/pyrolysis%20report%20final.pdf. [Accessed 20 September 2017].

- [93] S. D. Anuar, F. Abnisa, W. M. A. Wan Daud and M. K. Aroua, "A review on pyrolysis of plastic wastes," *Energy Convers Manag*, vol. 115, pp. 308-326, 2016.
- [94] P. Brassard, S. Godbout and V. Raghavan, "Pyrolysis in auger reactors for biochar and bio-oil production: A review," *Biosystem Engineering*, vol. 161, pp. 80-92, 2017.
- [95] D. Czajczynska, L. Anguilano, H. Ghazal , R. Krzyzynska, A. J. Reynolds, N. Spencer and H. Jouhara, "Potential of pyrolysis Processes in the Waste Management Sector," *Thermal Science and Engineering Progress*, 2017.
- [96] S. Q. Li, J. H. Yan, R. D. Li , Y. Chi and K. F. Cen, "Axial transport and residence time of MSW in rotatory kilns - Part I," *Experimental Powder Technol/*, vol. 126, pp. 217-227, 2002.
- [97] M. Trninic, D. Stojijkovic, A. Jovovic and G. Janke , "Biomass gasification technology: The state of the art overview," in *Environment Freindly Energies and Applications (EFEA). 4th International Symposium* , 2016.
- [98] K. M. Holland, "Apparatus for waste pyrolysis". US Patent 5,387,321, 7 February 1995.
- [99] L. S. Shiung and H. A. Chase, "A review on Waste to Energy Processes Using Microwave Pyrolysis," *Energies*, vol. 5, no. 10, pp. 4209-4232, 2012.
- [100] Y. F. Huang, P. T. Chiueh and S. L. Lo, "A review on microwave pyrolysis of lignocellulosic biomass," *Sustainable Environmental research*, vol. 26, no. 3, pp. 103-109, 2016.
- [101] D. Benegaso, T. Monti, E. T. Kostas and J. Robinson, "Microwave pyrolysis of biomass for bio-oil production: Scalable processing concepts," *Chemical Engineering Journal*, vol. 316, pp. 481-498, 2017.
- [102] V. L. Budarin, P. S. Shuttleworth, J. R. Dodson, A. J. Hunt, B. Lanigan, R. Marriot, K. J. Mikowski, A. J. Wilson, S. W. Breeden, J. Fan, E. H. Sin and J. H. Clark, "Use of green chemical technologies in an integrated biorefinery," *Energy Envuron. Sci.*, vol. 4, pp. 471-479, 2011.
- [103] G. Luo, D. S. Chandler and L. C. Anjos, "Pyrolysis of whole wood chips and rods in a novel ablative reactor," *Fuel*, vol. 194, pp. 229-238, 2017.
- [104] IEA Bioenergy, "Direct Thermochemical Liquefaction," [Online]. Available: <http://www.pyne.co.uk> . [Accessed September 2017].
- [105] Z. Wang, J. Cao and J. Wang, "Pyrolytic characteristics of pine wood in a slowly heating and gas sweeping fixed-bed reactor," *J. Anal Appl. Pyrolysis*, vol. 84, pp. 179-184, 2009.
- [106] J. Lehmann, J. Gaunt and M. Rondon, "Biochar sequestration in terrestrial ecosystems," *Mit. Adapt. Strat. Glob. Change*, vol. 11, pp. 395-419, 2006.
- [107] M. J. Antal and M. Gronli, "The art, science and technology of charcoal production," *J. Am. Chem. Soc*, vol. 42, pp. 1619-1640, 2003.
- [108] F. Abnisa and W. M. Daud, "A review of co-pyrolysis of biomass: an optional technique to obtain a high-grade pyrolysis oil.," *Energy Conversion and Management*, vol. 87, pp. 71-85, 2014.

- [109] V. Dhyani and T. Bhaskar, "A comprehensive review on the pyrolysis of lignocellulosic biomass," *Renewable Energy*, 2017.
- [110] H. Li, Q. Xu, H. Xue and Y. Yan, "Catalytic reforming of the aqueous phase derived from fast pyrolysis of biomass," *Renew Energy*, vol. 24, pp. 2872-2877, 2009.
- [111] S. Cxernik, D. K. Johnson and S. Black, "Stability of wood fast pyrolysis oil," *Biomass Bioenergy*, vol. 7, pp. 187-192, 1994.
- [112] Y. K. Park, M. L. Yoo, H. S. Heo, S. H. Lee, S. C. Park, S. S. Jung and S. G. Park, "Wild reed of suncheon bay: potential bio-energy source," *Renew. Energy*, vol. 42, pp. 168-172, 2012.
- [113] H. S. Heo, H. J. Park, Y. K. Park, C. Ryu, D. J. Suh, Y. W. Suh, J. H. Yim and S. S. Kim, "Bio-oil production from fast pyrolysis of waste furniture sawdust in a fluidized bed," *Bioresourc. Technol*, vol. 101, pp. 91-96, 2010.
- [114] Q. Zhang, J. Chang, T. Wang and Y. Xu, "Review of biomass pyrolysis oil properties and upgrading research," *Energy Convers. Manag*, vol. 48, pp. 87-92, 2007.
- [115] D. Vaibhav and T. Bhaskar, "A comprehensive review on the pyrolysis of lignocellulosic biomass," *Renewable Energy*, 2017 - Article in Press.
- [116] X. Miao, Q. Wu and C. Yang, *Jounal Anal. Appl. Pyrolysis*, vol. 71, pp. 855-863, 2004.
- [117] A. Oasmaa, E. Kuoppala, E. Gust and Y. Solantausta, *Energy Fuels*, vol. 1, pp. 1-12, 2003.
- [118] A. Oasmaa and S. Czernik, *Energy Fuels*, vol. 13, pp. 914-921, 1999.
- [119] D. Mohan, C. U. Pittman and P. H. Steele, "Pyrolysis of Wood/Biomass for Bio-Oil: A critical review," *Energy & Fuels*, vol. 20, pp. 848-889, 2006.
- [120] Y. Huijun , "Overview of upgrading of pyrolysis of oil of biomass," in *The 6th International Conference on Applied Energy - ICAE2014*, 2014.
- [121] E. Furimsky, "Catalytic hydrodeoxygenation," *Appl. Catal. A Gen*, vol. 199, pp. 147-190, 2000.
- [122] J. F. Peters, D. Iribarren and J. Dufour, "Predictive pyrolysisprocess modelling in Aspen Plus," in *21st European Biomass Conference and Exhiition*, Copenhagen, Denmark, 2013.
- [123] D. Abhijit, S. Asad and E. Tan, "Process Design and Economics for the Conversion of Lignocellulosic Biomass to Hydrocarbons Fuels. Thermochemical Research Pathways with In Situ and Ex Situ Upgrading of Fast Pyrolysis Vapors," NREL, 2015.
- [124] AspenTech Support, [Online]. Available: <https://esupport.aspentechn.com/>.
- [125] A. Demirbas, "The influcnce of temperature on the yields of compounds existing in bio-oils obtained from biomass samples via pyrolysis," *Fuel Process Technol.*, vol. 88, pp. 591-597, 2007.
- [126] C. Borges, Z. Du, Q. Xie, J. O. Trierweiler, Y. Cheng, Y. Wan, Y. Liu, R. Zhu, X. Lin, P. Chen and R. Ruan, "Fast microwave assisted pyrolysis of biomass using microwave absorbent," *Bioseour. Technol.*, vol. 156, pp. 267-274, 2014.

- [127] L. Fan, P. Chen, Y. Zhang, S. Liu, Y. Wang, L. Dai and R. Ruan, "Fast microwave-assisted catalytic co-pyrolysis of lignin and low-density polyethylene with HZSM-5 and MgO for improved bio-oil yield and quality," *Bioresour. Technol.*, vol. 225, pp. 199-205, 2017.
- [128] A. P. Crayford, P. J. Bowen, P. J. Kay and H. Laget, "Comparison of gas-oil and bio-oil spray performance for use in a gas turbine," in *Proceedings of the ASME Turbo Expo*, 2010.
- [129] A. V. Bridgwater, "Principles and practice of biomass fast pyrolysis processes for liquids," *J. Anal. Appl. Pyrol.*, vol. 51, pp. 3-22, 1999.
- [130] Q. L. Hao, C. Wang, D. Q. Lu, D. Li and G. J. Li, "Production of hydrogen-rich gas from plant biomass by catalytic pyrolysis at low temperature," *Int J Hydrog Energy*, vol. 35, pp. 8884-8890, 2010.
- [131] M. K. Hossain, V. Strezov, K. Y. Chan, A. Ziolkowski and P. F. Nelson, "Influence of pyrolysis temperature on production and nutrient properties of wastewater sludge biochar," *J Environ Manag*, vol. 92, pp. 223-228, 2011.

11. Annex I. Tar composition

Table A 1. Analytical results SVOC

Determinant		Pine @ 300C	Pine @ 400C	Pine @ 500 C	Larc h @ 300C	Larc h @ 400C	Larc h @ 500C	Spruce @ 300C
Benzene	mg/kg	<9.70	<9.83	<9.66	<9.72	<9.97	<9.95	<9.80
Toluene	mg/kg	<9.70	<9.83	<9.66	<9.72	<9.97	<9.95	<9.80
Ethylbenzene	mg/kg	<9.70	<9.83	<9.66	<9.72	<9.97	<9.95	<9.80
m&p Xylene	mg/kg	<9.70	<9.83	<9.66	<9.72	<9.97	<9.95	<9.80
o-Xylene	mg/kg	<9.70	<9.83	<9.66	<9.72	<9.97	<9.95	<9.80
Dichlorodifluoromethane	mg/kg	<9.70	<9.83	<9.66	<9.72	<9.97	<9.95	<9.80
Chloromethane	mg/kg	<9.70	<9.83	<9.66	<9.72	<9.97	<9.95	<9.80
Vinyl Chloride	mg/kg	<9.70	<9.83	<9.66	<9.72	<9.97	<9.95	<9.80
Bromomethane	mg/kg	<9.70	<9.83	<9.66	<9.72	<9.97	<9.95	<9.80
Chloroethane	mg/kg	<9.70	<9.83	<9.66	<9.72	<9.97	<9.95	<9.80
Trichlorofluoromethane	mg/kg	<9.70	<9.83	<9.66	<9.72	<9.97	<9.95	<9.80
1,1-Dich chloroethylene	mg/kg	<9.70	<9.83	<9.66	<9.72	<9.97	<9.95	<9.80
Dichloromethane	mg/kg	<9.70	<9.83	<9.66	<9.72	<9.97	<9.95	<9.80
MTBE	mg/kg	<9.70	<9.83	<9.66	<9.72	<9.97	<9.95	<9.80
trans-1,2,-d dichloroethylene	mg/kg	<9.70	<9.83	<9.66	<9.72	<9.97	<9.95	<9.80
1,1-Dich chloroethane	mg/kg	<9.70	<9.83	<9.66	<9.72	<9.97	<9.95	<9.80
2,2-Dich chloropropane	mg/kg	<9.70	<9.83	<9.66	<9.72	<9.97	<9.95	<9.80
cis--1,2,-dichloroethylene	mg/kg	<9.70	<9.83	<9.66	<9.72	<9.97	<9.95	<9.80
Bromochloromethane	mg/kg	<9.70	<9.83	<9.66	<9.72	<9.97	<9.95	<9.80
Chloroform	mg/kg	<9.70	<9.83	<9.66	<9.72	<9.97	<9.95	<9.80
1,1,1-Triehloroethane	mg/kg	<9.70	<9.83	<9.66	<9.72	<9.97	<9.95	<9.80
1,1-Dichloropropene	mg/kg	<9.70	<9.83	<9.66	<9.72	<9.97	<9.95	<9.80
Carbon Tetrachloride	mg/kg	<9.70	<9.83	<9.66	<9.72	<9.97	<9.95	<9.80
1,2-dichloroethane	mg/kg	<9.70	<9.83	<9.66	<9.72	<9.97	<9.95	<9.80
Trichloroethylene	mg/kg	<9.70	<9.83	<9.66	<9.72	<9.97	<9.95	<9.80
1,2-Dichloropropane	mg/kg	<9.70	<9.83	<9.66	<9.72	<9.97	<9.95	<9.80
Dibromoethane	mg/kg	<9.70	<9.83	<9.66	<9.72	<9.97	<9.95	<9.80
Bromodichloromethane	mg/kg	<9.70	<9.83	<9.66	<9.72	<9.97	<9.95	<9.80
cis-1,2-dichloropropylene	mg/kg	<9.70	<9.83	<9.66	<9.72	<9.97	<9.95	<9.80
trans-1,3-dichloropropylene	mg/kg	<9.70	<9.83	<9.66	<9.72	<9.97	<9.95	<9.80
1,1,2-Triehloroethane	mg/kg	<9.70	<9.83	<9.66	<9.72	<9.97	<9.95	<9.80
1,3-Dichloropropane	mg/kg	<9.70	<9.83	<9.66	<9.72	<9.97	<9.95	<9.80
Tetrachloroethylene	mg/kg	<9.70	<9.83	<9.66	<9.72	<9.97	<9.95	<9.80
Chlorodibromomethane	mg/kg	<9.70	<9.83	<9.66	<9.72	<9.97	<9.95	<9.80
1,2-Dibromoethane	mg/kg	<9.70	<9.83	<9.66	<9.72	<9.97	<9.95	<9.80
Chlorobenzene	mg/kg	<9.70	<9.83	<9.66	<9.72	<9.97	<9.95	<9.80
1,1,1,2-tetrachloroethane	mg/kg	<9.70	<9.83	<9.66	<9.72	<9.97	<9.95	<9.80
Styrene	mg/kg	<9.70	<9.83	<9.66	<9.72	<9.97	<9.95	<9.80
Isopropylbenzene	mg/kg	<9.70	<9.83	<9.66	<9.72	<9.97	<9.95	<9.80
Bromoform	mg/kg	<9.70	<9.83	<9.66	<9.72	<9.97	<9.95	<9.80
1,1,2,2-Tetrachloroethane	mg/kg	<9.70	<9.83	<9.66	<9.72	<9.97	<9.95	<9.80
1,2,3-Triehloropropane	mg/kg	<9.70	<9.83	<9.66	<9.72	<9.97	<9.95	<9.80
n-Propyl benzene	mg/kg	<9.70	<9.83	<9.66	<9.72	<9.97	<9.95	<9.80
Bromobenzene	mg/kg	<9.70	<9.83	<9.66	<9.72	<9.97	<9.95	<9.80
1,3,5-Tri methylbenzene	mg/kg	<9.70	<9.83	<9.66	<9.72	<9.97	<9.95	<9.80
2-chlorotoluene	mg/kg	<9.70	<9.83	<9.66	<9.72	<9.97	<9.95	<9.80
4-chlorotoluene	mg/kg	<9.70	<9.83	<9.66	<9.72	<9.97	<9.95	<9.80
tert-butylbenzene	mg/kg	<9.70	<9.83	<9.66	<9.72	<9.97	<9.95	<9.80
1,2,4-trimethylbenzene	mg/kg	<9.70	<9.83	<9.66	<9.72	<9.97	<9.95	<9.80
sec-Butyl benzene	mg/kg	<9.70	<9.83	<9.66	<9.72	<9.97	<9.95	<9.80

Determinant		Pine @ 300C	Pine @ 400C	Pine @ 500 C	Larc h @ 300C	Larc h @ 400C	Larc h @ 500C	Spruce @ 300C
4-Isopropyltoluene (P-Cymene)	mg/kg	<9.70	<9.83	<9.66	<9.72	<9.97	<9.95	<9.80
1,3-Dichlorobenzene	mg/kg	<9.70	<9.83	<9.66	<9.72	<9.97	<9.95	<9.80
1,4-Dichlorobenzene	mg/kg	<9.70	<9.83	<9.66	<9.72	<9.97	<9.95	<9.80
n-Butylbenzene	mg/kg	<9.70	<9.83	<9.66	<9.72	<9.97	<9.95	<9.80
1,2-Dichlorobenzene	mg/kg	<9.70	<9.83	<9.66	<9.72	<9.97	<9.95	<9.80
1,2-Dibromo-3-chloropropane	mg/kg	<9.70	<9.83	<9.66	<9.72	<9.97	<9.95	<9.80
1,2,4-Trienchlorobenzene	mg/kg	<9.70	<9.83	<9.66	<9.72	<9.97	<9.95	<9.80
Hexachlorobutadiene	mg/kg	<9.70	<9.83	<9.66	<9.72	<9.97	<9.95	<9.80
Naphthalene	mg/kg	<9.70	<9.83	<9.66	<9.72	<9.97	<9.95	<9.80
1,2,3-Trienchlorobenzene	mg/kg	<9.70	<9.83	<9.66	<9.72	<9.97	<9.95	<9.80

Table A 2. Analytical results SVOC

Determinant	Units	Spruce @ 400C	Spruce @ 500C
Benzene	(mg/kg)	<9.93	<9.70
Toluene	(mg/kg)	<9.93	<9.70
Ethylbenzene	(mg/kg)	<9.93	<9.70
m&p Xylene	(mg/kg)	<9.93	<9.70
o-Xylene	(mg/kg)	<9.93	<9.70
Dichlorodifluoromethane	(mg/kg)	<9.93	<9.70
Chloromethane	(mg/kg)	<9.93	<9.70
Vinyl Chloride	(mg/kg)	<9.93	<9.70
Bromomethane	(mg/kg)	<9.93	<9.70
Chloroethane	(mg/kg)	<9.93	<9.70
Trichlorofluoromethane	(mg/kg)	<9.93	<9.70
1,1-Dichloroethylene	(mg/kg)	<9.93	<9.70
Dichloromethane	(mg/kg)	<9.93	<9.70
MTBE	(mg/kg)	<9.93	<9.70
trans-1,2, -dichloroethylene	(mg/kg)	<9.93	<9.70
1,1-Dichloroethane	(mg/kg)	<9.93	<9.70
2,2-Dichloropropane	(mg/kg)	<9.93	<9.70
cis--1,2,-dichloroethylene	(mg/kg)	<9.93	<9.70
Bromochloromethane	(mg/kg)	<9.93	<9.70
Chloroform	(mg/kg)	<9.93	<9.70
1,1,1-Triehloroethane	(mg/kg)	<9.93	<9.70
1,1-Dichloropropene	(mg/kg)	<9.93	<9.70
Carbon Tetrachloride	(mg/kg)	<9.93	<9.70
1,2-dichloroethane	(mg/kg)	<9.93	<9.70
Trichloroethylene	(mg/kg)	<9.93	<9.70
1,2-Dichloropropane	(mg/kg)	<9.93	<9.70
Dibromoethane	(mg/kg)	<9.93	<9.70
Bromodichloromethane	(mg/kg)	<9.93	<9.70
cis-1,2-dichloropropylene	(mg/kg)	<9.93	<9.70
trans-1,3-diehloropropylene	(mg/kg)	<9.93	<9.70
1,1,2-Triehloroethane	(mg/kg)	<9.93	<9.70
1,3-Diehloropropane	(mg/kg)	<9.93	<9.70
Tetrachloroethylene	(mg/kg)	<9.93	<9.70
Chlorodibromomethane	(mg/kg)	<9.93	<9.70
1,2-Dibromoethane	(mg/kg)	<9.93	<9.70
Chlorobenzene	(mg/kg)	<9.93	<9.70
1,1,1,2-tetraehloroethane	(mg/kg)	<9.93	<9.70
Styrene	(mg/kg)	<9.93	<9.70
Isopropylbenzene	(mg/kg)	<9.93	<9.70
Bromoform	(mg/kg)	<9.93	<9.70
1,1,2,2-Tetraeh loroethane	(mg/kg)	<9.93	<9.70
1,2,3-Triehloropropane	(mg/kg)	<9.93	<9.70
n-Propyl benzene	(mg/kg)	<9.93	<9.70
Bromobenzene	(mg/kg)	<9.93	<9.70
1,3,5-Tri methylbenzene	(mg/kg)	<9.93	<9.70
2-ehlorotoluene	(mg/kg)	<9.93	<9.70
4-ehlorotoluene	(mg/kg)	<9.93	<9.70
tert-butylbenzene	(mg/kg)	<9.93	<9.70
1,2,4-trimethylbenzene	(mg/kg)	<9.93	<9.70
see-Butyl benzene	(mg/kg)	<9.93	<9.70
4-Isopropyltoluene (P-Cymene)	(mg/kg)	<9.93	<9.70
1,3-Diehlorobenzene	(mg/kg)	<9.93	<9.70
1,4-Diehlorobenzene	(mg/kg)	<9.93	<9.70
n-Butylbenzene	(mg/kg)	<9.93	<9.70

1,2-Diechlorobenzene	(mg/kg)	<9.93	<9.70
1,2-Dibromo-3-ehloropropane	(mg/kg)	<9.93	<9.70
1,2,4-Triehlorobenzene	(mg/kg)	<9.93	<9.70
Hexachlorobutadiene	(mg/kg)	<9.93	<9.70
Naphthalene	(mg/kg)	<9.93	<9.70
1,2,3-Triechlorobenzene	(mg/kg)	<9.93	<9.70

Table A 3. Analytical results SVOC

Determinant	Units	Pine @ 300C	Pine @ 400C	Pine @ 500C	Larch @ 300C	Larch @ 400C	Larch @ 500C
1,2,4-trichlorobenzene,	mg/kg	<20	<20	<20	<20	<20	<100
1,3-dichlorobenzene,	mg/kg	<20	<20	<20	<20	<20	<100
1,4-dichlorobenzene,	mg/kg	<20	<20	<20	<20	<20	<100
1-chloronaphthalene,	mg/kg	<20	<20	<20	<20	<20	<100
2,3,4,6-tetrachlorophenol al	mg/kg	<20	<20	<20	<20	<20	<100
2,4,5-trichlorophenol	mg/kg	<20	<20	<20	<20	<20	<100
2,4,6-trichlorophenol	mg/kg	<20	<20	<20	<20	<20	<100
2,4-Dichorophenol	mg/kg	<20	<20	<20	<20	<20	<100
2,4-dimethylphenol	mg/kg	112	111	135	97.0	196	<100
2,4-Dinitrophenol,	mg/kg	<20	<20	<20	<20	<20	<100
2,6-Dichorophenol	mg/kg	<20	<20	<20	<20	<20	<100
2,6-Dinitrotoluene	mg/kg	<20	<20	<20	<20	<20	<100
2-chlorophenol,	mg/kg	<20	<20	<20	<20	<20	<100
2-Methyl naphthalene	mg/kg	<20	<20	<20	<20	<20	<100
2-methylphenol,	mg/kg	190	161	186	115	253	451
2-Nitroaniline	mg/kg	<20	<20	<20	<20	<20	<100
2-Nitrophenol	mg/kg	<20	<20	<20	<20	<20	<100
3,3-Dichlorobenzidine	mg/kg	<20	<20	<20	<20	<20	<100
3/4-methylphenol,	mg/kg	389	325	402	282	527	<100
3-Nitroaniline	mg/kg	100	106	142	162	145	<100
4 Chlorophenyl phenyl ether	mg/kg	<20	<20	<20	<20	<20	<100
4,6-Di nitro-2-methyl phenol	mg/kg	<20	<20	<20	<20	<20	<100
4-bromophenyl phenyl ether	mg/kg	<20	<20	<20	<20	<20	<100
4-chloro-3-methyl phenol,	mg/kg	104	<20	98.5	58.8	221	<100
4-Chloroaniline	mg/kg	<20	<20	<20	<20	23.6	<100
4-Nitroaniline	mg/kg	<20	<20	<20	<20	<20	<100
4-nitrophenol,	mg/kg	<20	<20	<20	<20	<20	<100
Acenaphthene	mg/kg	<20	<20	<20	<20	<20	<100
Acenaphthylene	mg/kg	<20	<20	<20	<20	<20	<100
Aniline	mg/kg	<20	<20	<20	<20	<20	<100
Anthracene	mg/kg	<20	<20	<20	<20	<20	<100
Azobenzene	mg/kg	<20	<20	<20	<20	<20	<100
Benz[a]anthracene	mg/kg	<20	<20	<20	<20	<20	<100
Benzene, 1,2-dichloro-	mg/kg	<20	<20	<20	<20	<20	<100
Benzo{ghi}perylene	mg/kg	<20	<20	<20	<20	<20	<100
Benzo[a]pyrene	mg/kg	<20	<20	<20	<20	<20	<100
Benzo[b] fluoranthene	mg/kg	<20	<20	<20	<20	<20	<100
Benzo[k] fluoranthene	mg/kg	<20	<20	<20	<20	<20	<100
Benzyl Alcohol	mg/kg	<20	26.4	20.7	<20	<20	<100
Benzyl butyl phthalate	mg/kg	<20	<20	<20	<20	<20	<100
Bis{2-chloroethoxy)methane	mg/kg	<20	<20	<20	<20	<20	<100
Bis{2-chloroethyl)ether	mg/kg	<20	<20	<20	<20	<20	<100
Bis{2-chloroisopropyl)ether	mg/kg	<20	<20	<20	<20	<20	<100
Bis{2-ethylhexyl) phthalate	mg/kg	<20	<20	<20	<20	<20	<100
Chrysene	mg/kg	<20	<20	<20	<20	<20	<100
Dibenz (a,h)anthracene	mg/kg	<20	<20	<20	<20	<20	<100
Dibenzofuran	mg/kg	<20	<20	<20	<20	<20	<100
Dibutyl phthalate	mg/kg	<20	<20	<20	<20	<20	<100
Diethyl Phthalate	mg/kg	<20	<20	<20	<20	<20	<100

Dimethyl phthalate	mg/kg	<20	<20	<20	<20	<20	<100
Di-n-octyl phthalate	mg/kg	<20	<20	<20	<20	<20	<100
Diphenylamine	mg/kg	<20	<20	<20	<20	<20	<100
Fluoranthene	mg/kg	<20	<20	<20	<20	<20	<100
Fluorene	mg/kg	<20	<20	<20	<20	<20	<100
Hexachlorobenzene	mg/kg	<20	<20	<20	<20	<20	<100
Hexachlorobutadiene	mg/kg	<20	<20	<20	<20	<20	<100
Hexaehlorocyclopentadiene	mg/kg	<20	<20	<20	<20	<20	<100
Hexachloroethane,	mg/kg	<20	<20	<20	<20	<20	<100
Indeno[1,2,3-cd] pyrene	mg/kg	<20	<20	<20	<20	<20	<100
Isophorone	mg/kg	<20	<20	<20	<20	<20	<100
Methyl-Methane sulfonate	mg/kg	<20	<20	<20	<20	<20	<100
Naphthalene	mg/kg	<20	<20	<20	<20	<20	<100
Nitrobenzene	mg/kg	<20	<20	<20	<20	<20	<100
N-Nitroso dimethylamine	mg/kg	<20	<20	<20	<20	<20	<100
Pentachlorophenol	mg/kg	<20	<20	<20	<20	<20	<100
Phenanthrene	mg/kg	<20	<20	<20	<20	<20	<100
Phenol	mg/kg	942	594	729	462	897	1760
Pyrene	mg/kg	<20	<20	<20	<20	<20	<100

Table A 4. Analytical results SVOC

Determinant	Units	Spruce @ 300C	Spruce @ 400C	Spruce @ 500C
1,2,4-trichlorobenzene,	{mg/kg}	<100	<100	<100
1,3-dichlorobenzene,	{mg/kg}	<100	<100	<100
1,4-dichlorobenzene, 1-chloronaphthalene,	{mg/kg}	<100	<100	<100
2,3,4,6-tetrachlorophenol	{mg/kg}	<100	<100	<100
2,4,5-trichlorophenol	{mg/kg}	<100	<100	<100
2,4,6-trichlorophenol	{mg/kg}	<100	<100	<100
2,4-Dichorophenol	{mg/kg}	<100	<100	<100
2,4-dimethyphenol	{mg/kg}	<100	<100	<100
2,4-Dinitrophenol,	{mg/kg}	<100	<100	<100
2,6-Dichorophenol	{mg/kg}	<100	<100	<100
2,6-Dinitrotoluene	{mg/kg}	<100	<100	<100
2-chlorophenol,	{mg/kg}	<100	<100	<100
2-Methyl naphthalene	{mg/kg}	<100	<100	<100
2-methylphenol,	{mg/kg}	263	352	501
2-Nitroaniline	{mg/kg}	<100	<100	<100
2-Nitrophenol	{mg/kg}	<100	<100	<100
3,3-Dichlorobenzidine	{mg/kg}	<100	<100	<100
3/4-methylphenol,	{mg/kg}	135	<100	147
3-Nitroaniline	{mg/kg}	<100	<100	<100
4 Chlorophenyl phenyl ether	{mg/kg}	<100	<100	<100
4,6-Di nitro-2-methyl phenol	{mg/kg}	<100	<100	<100
4-bromophenyl phenyl ether	{mg/kg}	<100	<100	<100
4-chloro-3-methyl phenol,	{mg/kg}	<100	<100	<100
4-Chloroaniline	{mg/kg}	<100	<100	<100
4-Nitroaniline	{mg/kg}	<100	<100	<100
4-nitrophenol,	{mg/kg}	<100	<100	<100
Acenaphthene	{mg/kg}	<100	<100	<100
Acenaphthylene	{mg/kg}	<100	<100	<100
Aniline	{mg/kg}	<100	<100	<100
Anthracene	{mg/kg}	<100	<100	<100
Azobenzene	{mg/kg}	<100	<100	<100
Benz[a]anthracene	{mg/kg}	<100	<100	<100
Benzene, 1,2-dichloro-	{mg/kg}	<100	<100	<100
Benzo[ghi]perylene	{mg/kg}	<100	<100	<100
Benzo[a]pyrene	{mg/kg}	<100	<100	<100
Benzo[fluoranthene	{mg/kg}	<100	<100	<100
Benzo[k]fluoranthene	{mg/kg}	<100	<100	<100
Benzyl Alcohol	{mg/kg}	<100	<100	<100
Benzyl butyl phthalate	{mg/kg}	<100	<100	<100
Bis(2-chloroethoxy)methane	{mg/kg}	<100	<100	<100
Bis(2-chloroethyl)ether	{mg/kg}	<100	<100	<100
Bis(2-chloroisopropyl)ether	{mg/kg}	<100	<100	<100
Bis(2-ethylheKYI)phthalate	{mg/kg}	<100	<100	<100
Chrysene	{mg/kg}	<100	<100	<100
Dibenz{a,h}anthracene	{mg/kg}	<100	<100	<100
Dibenzofuran	{mg/kg}	<100	<100	<100
Dibutyl phthalate	{mg/kg}	<100	<100	<100
Diethyl Phthalate	{mg/kg}	<100	<100	<100
Dimethyl phthalate	{mg/kg}	<100	<100	<100
Di-n-octyl phthalate	{mg/kg}	<100	<100	<100
Diphenylamine	{mg/kg}	<100	<100	<100
Fluoranthene	{mg/kg}	<100	<100	<100

Fluorene	{mg/kg}	<100	<100	<100
Hexachlorobenzene	{mg/kg}	<100	<100	<100
Hexachlorobutadiene	{mg/kg}	<100	<100	<100
Hexaethylcyclopentadiene	{mg/kg}	<100	<100	<100
Hexachloroethane,	{mg/kg}	<100	<100	<100
Indeno[1,2,3-cd] pyrene	{mg/kg}	<100	<100	<100
Isophorone	{mg/kg}	<100	<100	<100
Methyl-Methanesulfonate	{mg/kg}	<100	<100	<100
Naphthalene	{mg/kg}	<100	<100	<100
NitroBenzene	{mg/kg}	<100	<100	<100
N-Nitrosodimethylamine	{mg/kg}	<100	<100	<100
Pentachlorophenol	{mg/kg}	<100	<100	<100
Phenanthrene	{mg/kg}	<100	<100	<100
Phenol	{mg/kg}	2471	1993	3226
Pyrene	{mg/kg}	<100	<100	<100